Determining the water use and growth of forest plantations through GIS-based integration of remote sensing and field data in the 3-PG model

Report to the Water Research Commission

by

P. Dye[1], R. Megown[2], S. Jacobs[2], D. Drew[2], K. Megown[2], M. Dicks[2],

S. Mthembu[2] and C. Pretorius[3]

Environmentek, CSIR

[1]Pietermaritzburg, [2]Durban, [3]Pretoria

November 2002

WRC Project No. 1194/1/02
ISBN No. 1-86845-950-0

Table of Contents

Executive Summary

1. Introduction

It is widely recognized in South Africa that water resources are severely limited, and therefore need to be managed efficiently in order to meet the rising demand for water by the agricultural, urban and industrial sectors. One of the important factors to consider in optimising water resources is the pattern of land use in the high-rainfall, source areas of our rivers. Most of these areas were originally covered by seasonally dormant grasslands and Fynbos, but have increasingly been converted to forest plantations to meet growing demand for wood products. Over a century of experience has shown that such afforestation may result in major reductions in catchment water yields (van der Zel, 1995). The reason for this effect has much to do with the length of time that the vegetation remains physiologically active through the year. Non-riparian grasslands and Fynbos become dormant during the dry season, and hence their annual evapotranspiration (ET) is much less than that of perennial forests that are able to remain green and transpire throughout the year. Differences in annual ET between grass/Fynbos and forests may exceed 400 mm (Versfeld, 1994). Catchment Management Agencies will be tasked with managing land use and water resource allocations to ensure optimal benefits for the water management region. Decisions will need to be based on sound and credible scientific information. While much information on forest hydrology is available from past research, it remains difficult to predict spatial and temporal patterns of ET in South African plantation forests, since they are influenced by a very wide range of site factors, forest characteristics and management actions.

A recently developed “process-based” model (3-PG; **P**hysiological **P**rinciples in **P**redicting **G**rowth) shows great promise in practically predicting both growth and water use in forest stands (Landsberg and Waring, 1997). It is based on a simplified treatment of the major physiological processes governing growth and water use in stands of even-aged trees. Tree growth predictions have been validated in a number of of forestry species from widely different climate and site conditions (Coops, *et al*., 1998; Coops, 1999a; Morris, 2000; Waring, 2000). Successful validation on several South African forestry plantations has also taken place (Gush, 1999; Dye, 2001). Overall, results suggests that 3-PG yields realistic results for a wide range of forest stands, and that it has great potential for providing improved, site-specific predictions of forest growth and water use. It is timely, therefore, to consider the practicality of running 3-PG spatially on an operational scale.

Several studies have been directed at investigating the potential use of remote sensing data in spatial applications of 3-PG. Coops *et al*., 1998, and Coops and Waring (2001c) reported the first example of using a modified version of 3-PG to integrate with satellite remote sensing data. A subsequent version of 3-PG (3-PG-SPATIAL) was developed to enhance the spatial use of the model through the use of GIS techniques and spatial coverages of such model inputs as topography, soils, and climatic inputs such as radiation, temperature, precipitation and humidity (Keenan *et al*., 2000). These studies have shown the potential benefits of integrating remote-sensing data with spatial information of climate and site conditions, through the use of GIS. The purpose of this study was to explore this potential further, and ascertain its usefulness in obtaining spatial estimates of the impacts of forest plantations on surface water resources in South Africa.

2. Project Objectives

The project objectives were defined as follows:

- Determine if the 3-PG model predicts plantation water use and growth to acceptable accuracy and spatial resolution.
- Demonstrate the potential application of 3-PGs as a tool for quantifying streamflow reducing impacts of forests.
- Develop a generic methodology, based on the integration of remote sensing, GIS and process-based models, which can be applied to evaluate streamflow-reducing activities of different crops in the context of catchment management.

3. Research strategy and methods

A research strategy was designed to provide a rigorous test of the practicality of modelling diverse assemblages of forest stands with the spatial versions of 3-PG. We selected a group of 12 stands of *Eucalyptus grandis X camaldulensis* clones situated in the Bushlands and Kwambonambi districts of Zululand. These stands varied in age and represented a wide range of site growth potential. Detailed measurements of biomass components, leaf area index, sap flow rates, xylem pressure potential, litterfall and weather conditions were performed over a 12-month monitoring period. Using these data, 3-PG was set up for each stand to run for the same 12-month period. Two important site variables (maximum soil water storage and soil fertility index) are acknowledged by modellers to be very difficult to quantify. Soil water storage was estimated to be consistent with the degree and timing of stress as reflected in pre-dawn xylem pressure potential readings. Site fertility index was estimated by assuming it to be correlated to site index, and to vary over a range of 0.2 to 1.0. The latter assumption was based on a similar study of *Eucalyptus globulus* in Australia (Landsberg, 2000).

4. Results

Realistic simulations were achieved for 11 of the 12 stands (Figure a). One stand exhibited an exceptionally high annual growth increment, and this was under-simulated by the model. The trees in this stand were shown to have access to a shallow water table, and this is believed to have resulted in physiological adaptations not recognized in 3-PG. Overall, simulated transpiration by trees in months associated with high soil water availability were realistic when compared to measured sap flow rates. In months of low soil water availability, however, simulated transpiration was too low. This is attributed to the trees using sinker roots to access deep soil water reserves below the principle rooting depth, thus avoiding severe physiological stress. We nevertheless conclude that the 3-PG model appears to be capable of describing the physiological state of trees growing in a wide range of conditions, and believe that improved predictions of growth and water use at a compartment scale are possible.

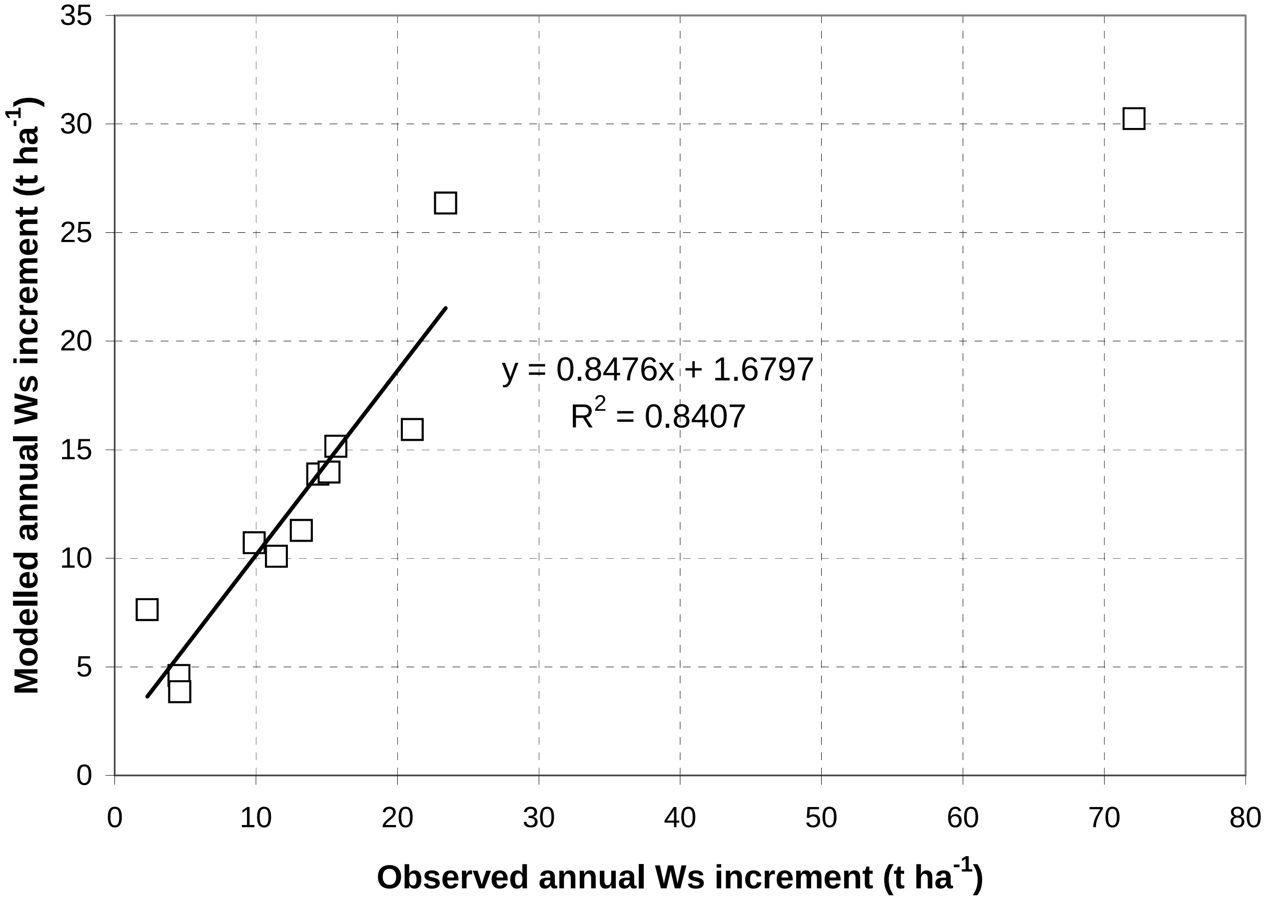

Figure a. Comparison of simulated and observed annual Ws growth increment for the 12 study sites using 3-PG. The outlier data point was excluded from the regression analysis.

5. The use of remote sensing data in spatial model applications

Assessment of the usefulness of remote sensing in spatial applications of the 3-PG model proved to be a complex task. We reviewed the recent literature on the application of remote sensing data to forest studies, as a means of highlighting the various possibilities and limitations. Major limitations that restrict the usefulness of current satellite imagery to operational forestry applications include insufficient resolution, poor image quality (especially resulting from cloud cover), high costs, inappropriate satellite pass-over times, the need for atmospheric corrections, and problems in separating tree canopy reflectances from ground and understorey reflectances. Of the various spatial inputs required by the model, only those linked to the quantity of green leaf in the canopies (absorbed photosynthetically-active radiation (APAR), leaf area index (LAI)) were considered feasible from affordable LANDSAT imagery, and therefore worth investigating in this project.

In a practical assessment of problems of combining remote-sensing (RS) data into spatial models using GIS techniques, we first examined correlations between four RS vegetation indices and two ground-based estimates of LAI. These were disappointingly poor, with highest correlation ($r^2 = 0.61$) shown between NDVI and LAI based on destructive tree sampling. Since leaf area is a critical feature of tree stands that greatly affects rates of growth and water use, we accordingly chose the option of running the spatial version of 3-PG without input of remotely sensed data.

The model was set up for a sample area in the Kwambonambi and Bushlands districts. Spatial coverages of soils and long-term average climate parameters were obtained for this purpose. Simulations over an assumed eight-year rotation produced realistic final yields. The spatial patterns of these modelled yields closely followed soil patterns, indicating that the 3-PG soil parameters are important determinants of tree growth in the Zululand area. Model outputs clearly reflect the scale of the soils data. Successful simulation of tree growth at the compartment scale will require more detailed soils coverages that reflect local variations in soil characteristics.

6. Conclusions and recommendations

The following main conclusions and recommendations arose from this project:

- A one-year field study of critical structural and physiological features of trees in 12 *Eucalyptus* stands representing a wide range of age and site quality was sufficient to produce a 3-PG parameterisation that yielded realistic and useful predictions of growth and water use. A practical procedure allowing further refinement of model parameters during real-time simulations of forest compartments is recommended and briefly described.

- This study has identified several areas in which the 3-PG model requires improvement.
    a. Soil water uptake during dry conditions. Sap flow data indicate that transpiration rates by trees during periods of low soil water content are higher than predicted by 3-PG. This is believed to result from difficulty in adequately defining the rooting zone of the trees. While most roots are commonly restricted to a well-defined depth of soil, a feature of many *Eucalyptus* species is their ability to send relatively few sinker roots to very great depths in order to access further soil/subsoil water reserves (Knight, 1999). This supply is sufficient to prevent excessive water stress in the trees, which could lead to long-lasting physiological damage.
    b. Physiological changes brought about by continuous access to ground water. Exceptionally high growth and sap flow rates were recorded in a stand of trees known to have continuous access to a shallow water table. Such conditions are believed to be capable of altering some of the physiological characteristics of the trees (e.g. canopy conductance, leaf dynamics, wood density) that are assumed in the model to be invariant for the species.
    c. The need to quantify a soil fertility index. This remains a problem to all 3-PG modellers. There is also considerable scope to improve the estimation procedure used for producing a spatial coverage of soil fertility.
    d. The need to estimate the maximum storage capacity for soil available water. The timing and intensity of water stress has a large effect on temporal patterns of growth and water use, and is very sensitive to the capacity of a soil to store soil water. Direct field measurement of this capacity is extremely difficult, and impractical in studies involving large numbers of stands. Techniques to monitor xylem water potential of trees are becoming available, and offer a practical means of

determining the onset of stress. This information is useful in gauging whether the assumed soil water storage capacity at a site is reasonably correct, too high or too low.

e. Detailed physiological studies on the major South African forest species are required to investigate such physiologically important features as carbon allocation patterns, canopy conductances, leaf dynamics and rooting patterns. Such "hard to measure" features are currently simulated on the basis of data obtained overseas for different species. Local data are required to improve the physiological foundation of 3-PG simulations in South Africa.

- The potential usefulness of remote-sensing data in spatial applications of 3-PG is unquestioned. However, a range of limitations (principally cost and image resolution) prevents significant use of current satellite-derived data for operational use on forestry estates. Recent developments in hyperspectral remote sensing from aircraft appear to show better prospects for characterising forest stands and providing some of the spatial data required in forestry models (Coops, pers. comm.). LIDAR has also been shown to exhibit great potential in characterising forest plantations, especially structural attributes required for growth assessments. This is an active research field, and developments need to be closely monitored.

- Efforts should also be directed towards developing practical and low-cost ground-based solutions to providing some of the critical physiological and structural inputs required by the model. Monitoring xylem water potential to detect water stress has already been mentioned. Such instruments as dendrometers and canopy analysers can provide valuable and low cost information on tree growth, standing biomass and leaf area index.

- There are insufficient sources of weather data in many forestry regions on which to base 3-PG simulations. Rainfall and ambient humidity data are particularly scarce, yet important inputs required by 3-PG. Automatic weather stations offer the best prospect for cost-effective, long-term collection of high quality weather data.

- This project has represented an important step in the process of developing and evaluating process-based models for the South African forestry industry. It followed several earlier studies in South Africa that demonstrated the potential usefulness of 3-PG on a limited selection of *Eucalyptus* and pine stands. It is now to be followed by a three-year Innovation Fund project in which parameter values for all major forestry species will be developed for the entire national forestry estate, and where the eventual goal will be the development of model products suited for use by both small-scale growers and forestry companies. Experience gained in this project will significantly enhance the chance of success of the new project.

- There appears to be no reason why the 3-PG/remote sensing data/GIS approach to predicting growth and water use by forests cannot be broadened to include all land use options in a given catchment. A variety of crop-specific models are readily available, and GIS skills are becoming more available in many agricultural, forestry and hydrological organizations. The greatest limitation remains in accessing cost-effective remote-sensing imagery and determining how it may best be analysed to provide the necessary spatial input into the model.

7. Capacity building

This project was planned to make a significant contribution towards building research skills in a number of younger researchers. Mr Sibusiso Mthembu in particular was earmarked for intensive training in remote sensing and GIS modelling. This project contributed to the costs of his MSc degree in the Centre for Environment and Development, University of Natal, and he benefited considerably from interactions with Bekee Megown. With his departure, the main skills transfer effort was re-directed to Shayne Jacobs. Following a sudden loss of remote sensing skills in the CSIR, the project supported a one-week visit by Shayne to Pretoria in order to receive training within the CSIR remote-sensing group. The project also funded a one-week visit to the project team by Nicholas Coops from the CSIRO in Australia. Ms Cindy Pretorius from the Pretoria remote-sensing group was invited to the Durban office during this visit, to gain experience from Dr Coops in using remote-sensing data for spatial application of 3-PG. This project supported her costs in this regard. David Drew, and two CSIR interns (Darren Naidoo and Frank Venter) gained valuable experience in various ecophysiological techniques during the course of this project. David has drawn on this experience in planning his MSc degree in the University of Natal.

Acknowledgements

The research in this report emanated from a project funded by the Water Research Commission and entitled:

DETERMINING THE WATER USE AND GROWTH OF FOREST PLANTATIONS THROUGH GIS-BASED INTEGRATION OF REMOTE SENSING AND FIELD DATA IN THE 3-PG MODEL

The steering committee responsible for this project consisted of the following members:

Mr H. Maaren	Water Research Commission (Chairman)
Dr S. Mkhize	Water Research Commission (Co-chairman)
Dr G. Green	Water Research Commission
Professor PJT Roberts	Forestry South Africa
Mr T. Newby	ISCW, ARC
Dr R. Harris	GEODATECT
Dr G. Jewitt	BEEH, University of Natal

The financing of the project by the Water Research Commission, and the contributions of the members of the Steering Committee are gratefully acknowledged.

The authors wish to thank the following people and organizations for supporting the aims and implementation of the project:

Dr C. Smith	ICFR, Pietermaritzburg
Dr N. Coops	CSIRO Division of Forestry and Forest Products, Clayton South, Victoria, Australia
Dr J. Landsberg	Landsberg Consulting, Canberra, Australia
Dr M. Thompson	Geospace International, Pretoria, South Africa

Mr A. Loughead	CSIRO Division of Forestry and Forest Products, Kingston, ACT, Australia
Mr Anders Siggins	CSIRO Division of Forestry and Forest Products, Kingston, ACT, Australia
Mondi Forests	

List of Figures

List of Tables

List of abbreviations (excluding equation variables)

AVHRR	Advanced Very High Resolution Radiometer
AVIRIS	Airborne Visible/Infrared Imaging Spectrometer
AWS	Automatic weather station
Ca	Calcium
CASI	Compact airborne Spectrographic Imager
DBH	Diameter at breast height
ET	Evapotranspiration
fPAR	Fraction of absorbed photosynthetically active radiation
FR	Fertility rating
GIS	Geographic Information system
GPP	Gross primary production
H	Height
K	Potassium
LAI	Leaf area index
MAI	Mean annual increment
MAXASW	Maximum available soil water
MODIS	Moderate Resolution Imaging Spectroradiometer
N	Nitrogen
NDTI	Normalized difference temperature index
NDVI	Normalized difference vegetation index
NDVIc	Corrected normalized difference vegetation index
NOAA	National Oceanographic and Atmospheric Administration
NPP	Net primary production
P	Potassium
PAI	Plant area index
PAR	Photosynthetically active radiation
Pg	Gross primary production
PVI	Perpendicular vegetation index
RS	Remote sensing
S	Sulphur
SAC	Satellite Applications Centre
SAVI	Soil adjusted vegetation index
SI	Site Index
SLA	Specific leaf area
SPH	Stems per hectare
SR	Solar radiation
SWIR	Short wave infrared
Tmax	Maximum temperatuire
Tmin	Minimum temperature
TSAVI	Transformed soil adjusted vegetation index
VI	Vegetation index
VPD	Vapour pressure deficit
Wf	Foliage biomass
Wr	Root biomass
Ws	Stem and branch biomass
XPP	Xylem pressure potential

1. INTRODUCTION

It is widely recognized in South Africa that water resources are severely limited, and therefore need to be managed efficiently in order to meet the rising demand for water by the agricultural, urban and industrial sectors. One of the important factors to consider in optimising water resources is the pattern of land use in the high-rainfall, source areas of our rivers. Most of these areas were originally covered by seasonally dormant grasslands and Fynbos, but have increasingly been converted to forest plantations to meet growing demand for wood products. Over a century of experience has shown that forest plantations result in potentially major declines in catchment water yields (van der Zel, 1995). The reason for this effect has much to do with the length of time that the vegetation remains physiologically active through the year. Non-riparian grasslands and Fynbos become dormant during the dry season, and hence their annual evapotranspiration (ET) is much less than that of perennial forests that are able to remain green and transpire throughout the year. Differences in annual ET between grass/Fynbos and forests may exceed 400 mm (Versfeld, 1994), and have a major influence on the amount and timing of downstream flows. This effect has generated concerns over many years (Malherbe, 1968), and led to the introduction of an afforestation permit system to limit the extent of afforestation permitted in catchments. The declaration of forestry as a streamflow reducing activity is the latest legislative action designed to control the extent of afforestation in areas where water supply is in short supply. Catchment Management Agencies will be tasked with managing land use and water resource allocations to ensure optimal benefits for the water management region. Decisions will need to be based on sound and credible scientific information. While much information on forest hydrology is available from past research, it remains difficult to predict spatial and temporal patterns of ET in South African plantation forests, since they are influenced by a very wide range of site factors, forest characteristics and management actions.

Currently two types of model are commonly used to estimate forest impacts on catchment water yields:

- Empirical models based on streamflow reduction trends recorded in high-rainfall research catchments (Nänni 1970; van der Zel,1995; Scott and Smith, 1997). These trends are linked to tree age, and describe flow reductions observed in high-rainfall catchments originally covered by indigenous grassland or Fynbos. They have been used to estimate streamflow reduction for quaternary catchments and magisterial districts over the entire national forestry estate (Scott *et al*., 1998).

- Physical and/or conceptual catchment models based on the major hydrological processes. Examples include the Pitman, ACRU, HSPF and SWAT models. They are more complex than the trend models, and the latter three in particular allow greater flexibility in assessing land-use change scenarios involving a wide range of crops and natural vegetation types. Examples of model studies of afforested catchments have been reported (Schulze and George, 1987; Jewitt and Schulze, 1993; Gush *et al.*, 2001).

What all these models lack is a suitably detailed and proven capacity to model forest growth as well as ET. Efficiency of water use is becoming an important land use consideration. Plantation forests are grown on a very wide variety of sites. Site quality is highly variable, causing mean annual growth increments of eucalypts to range from about 10 (the economically viable limit) to 35 t ha^{-1} (Economics Advisory Committee, 1991). ET is very likely to also vary strongly in relation to site quality (Dye, 2000), since adaption by the trees to drier conditions results in lower leaf area index (Specht, 1972; Specht and Specht, 1989) and stomatal conductance (Dye, *et al.*, 1997a), both of which control the rate of ET. In order to assess the WUE of forest plantations in a given catchment, estimates of both growth and ET need to be specific to local site conditions.

Forest owners are also sensitive to the overall hydrological impacts of their plantations, and commonly plan their estates to minimize streamflow reduction through such measures as excluding trees from riparian zones. There remains much scope for further optimisation of timber production and catchment water yield if improved predictions of growth and ET can be made at the compartment scale.

A recently developed "process-based" model (3-PG; **P**hysiological **P**rinciples in **P**redicting **G**rowth) shows great promise in practically predicting both growth and water use in forest stands (Landsberg and Waring, 1997). It is based on a simplified treatment of the major physiological processes governing growth and water use in stands of even-aged trees. Tree growth predictions have been validated in a number of forestry species from widely different climate and site conditions (Coops, *et al*., 1998; Coops, 1999a; Morris, 2000; Waring, 2000). Successful validation on several South African forestry plantations has also taken place (Gush, 1999; Dye, 2001). Overall, results suggests that 3-PG yields realistic results for a wide range of forest stands, and that it has great potential for providing improved, site-specific predictions of forest growth and water use. It is timely, therefore, to consider the practicality of running 3-PG spatially at an operational scale. Three important questions need to be answered:

- How can a large number of forest compartments be parameterised and initialised quickly and at minimum cost?
- What practical measures can be used to check model predictions during the course of the rotation?
- With what resolution can 3-PG predict increments of growth and water use?

Such questions have spurred several studies of the potential use of remote sensing data. Coops *et al*. (1998) reported the first example of using a modified version of 3-PG to integrate with satellite remote sensing data. A subsequent version of 3-PG (3-PG SPATIAL) was developed to enhance the spatial use of the model through the use of GIS techniques and spatial coverages of such model inputs as topography, soils, and climatic inputs such as radiation, temperature, precipitation and humidity (Keenan *et al*., 2000). These studies have shown the potential benefits of integrating remote-sensing data with spatial information of climate and site conditions, through the use of GIS. The purpose of this study was to explore this potential further, and ascertain its usefulness in obtaining spatial estimates of the impacts of forest plantations on surface water resources in South Africa.

Against this background, the project objectives were set as follows:

1. To determine if the 3-PG model predicts plantation water use and growth to acceptable accuracy and spatial resolution.
2. To demonstrate the potential application of 3-PGs as a tool for quantifying streamflow reducing impacts of forests.
3. Develop a generic methodology, based on the integration of remote sensing, GIS and process-based models, which can be applied to evaluate streamflow-reducing activities of different crops in the context of catchment management.

2. 3-PG LITERATURE AND SOFTWARE REVIEW

2.1 3-PG

The 3-PG model was initially developed by Landsberg and Waring (1997) in a quest to produce a process-based model of forest growth and water use that is simple enough to use in an operational forestry environment. It was designed to incorporate a number of simplifications in the modelling of physiological processes, the feasibility of which have become apparent from recent forest physiological studies around the world. Subsequent model testing by researchers in many countries has confirmed the usefulness of the model when applied to a wide variety of forest species (Waring, 2000, **Sitka Spruce**; White *et al*., 2000, **various New Zealand trees and shrubs**; Dye, 2001, ***Pinus patula***; Morris, 2000, ***E. grandis*** and ***E. globulus***; Gush, 1999, ***E. grandis***; Sands and Landsberg, 2001, ***E. globulus***), and interest is beginning to be shown by forest companies (Almeida, 2000).

Figure 1 represents a flow diagram of the model that illustrates the principle processes modelled and the sequence of calculations. The model itself is well described in the literature (Landsberg and Waring, 1997), and so a detailed description is not presented here. A user-friendly, Excel-based version of the model (Sands, 2000) has become the standard version for non-spatial (“point”) simulations of forest stands, and may be currently downloaded, together with a manual, through the web site www.ffp.csiro.au/software.

2.2 3-PGs

This version of 3-PG is described by Coops *et al*. (1998), and was the first to link remote sensing imagery to 3-PG. The basic model structure of 3-PGs (satellite) is outlined in Figure 2. Absorbed photosynthetically active radiation (APAR) is a crucial calculation in the simulation of tree growth, and was estimated in a two-step procedure:

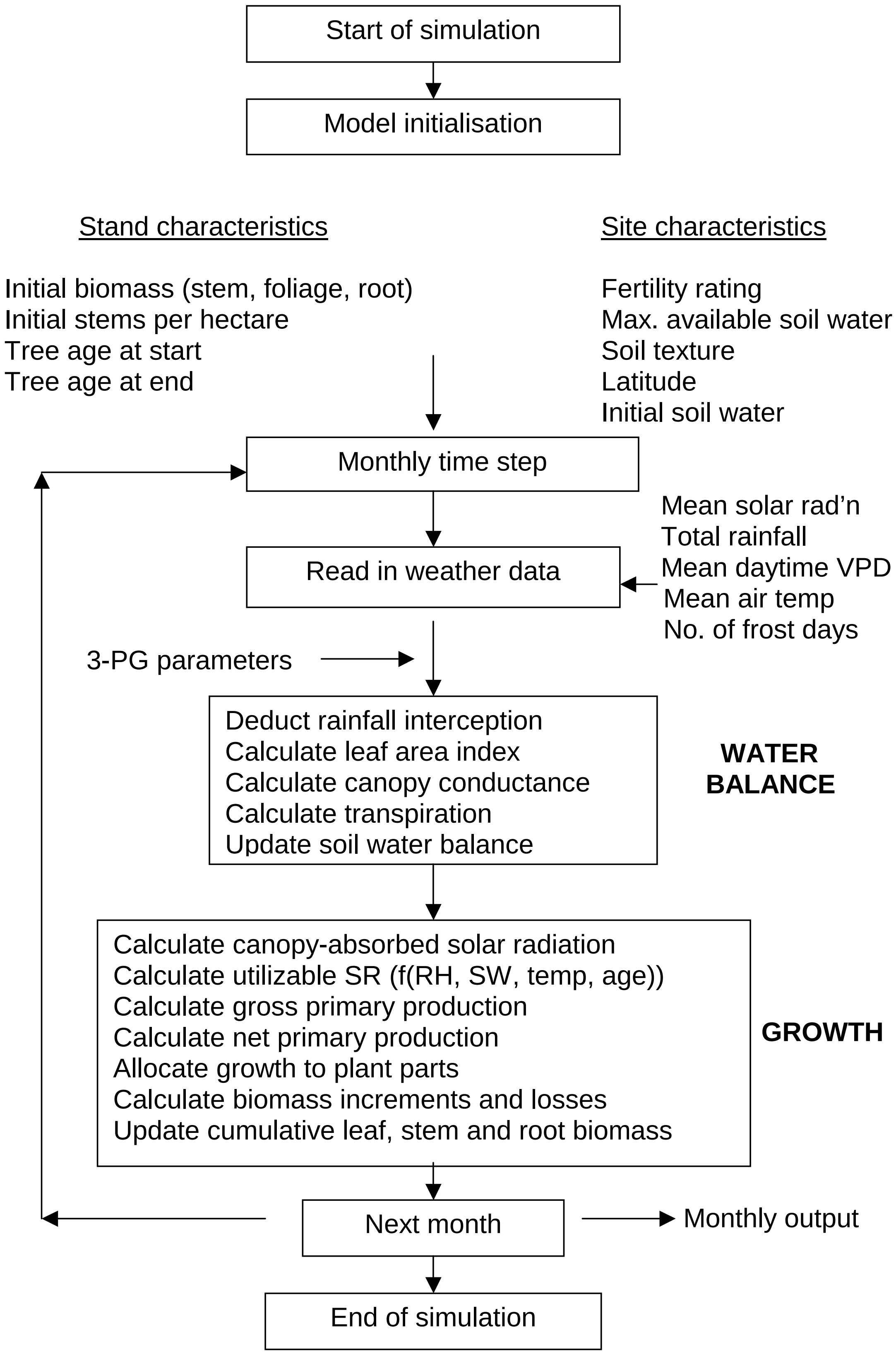

Figure 1. A flow diagram of 3-PG.

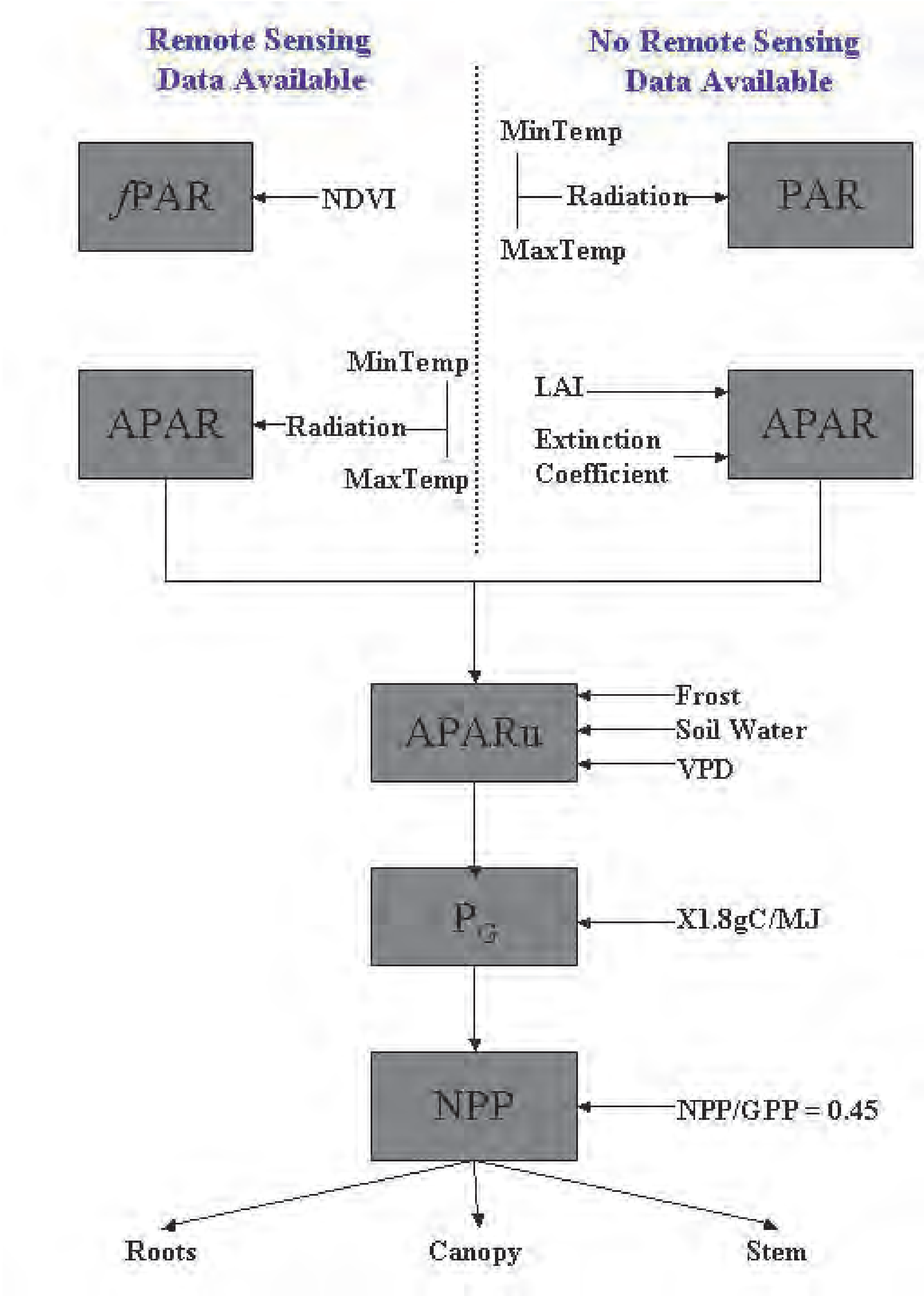

Figure 2. Diagrammatic flow of components of the 3-PGs model with and without remote sensing data. *f*PAR = fraction of absorbed photosynthetically active radiation; APAR = Absorbed PAR; APARu = Utilizable APAR; P_G = Gross Primary Production; NPP = Net Primary Production; NDVI = Normalized Difference Vegetation Index.

- Global solar radiation was estimated using an established empirical relationship based on average maximum and minimum temperatures recorded on the ground.

- The fraction of PAR absorbed by the vegetation was estimated from the satellite-derived normalised difference vegetation index (NDVI). This index is based on reflectances measured in the near-infrared and red wavelengths, and has been shown, both empirically and theoretically, to be related to the fraction of PAR absorbed in vegetation canopies (Kumar and Monteith, 1982; Sellers, 1985, 1987).

The NDVI was calculated from data recorded by the Advanced Very High Resolution Radiometer (AVHRR) sensor carried by the National Oceanographic and Atmospheric Administration (NOAA) weather satellite. The coarse spatial resolution of the AVHRR imagery (8 X 8 km) limited the model to regional-scale applications.

In a subsequent paper, Coops (1999b) used LANDSAT MSS imagery in conjunction with AVHRR data. In this way, NDVI interpretation was improved by the added ability to discriminate different forest age classes. This approach is more suited to studies at the plantation forestry scale. Further examples of the use of 3-PGs have been reported by Coops *et al*., 1998; Coops and Waring, 2001a; Coops and Waring, 2001b).

2.3 3-PG SPATIAL

This version of the model was developed to provide a common framework for the 3-PG and 3-PGs versions of the model, and operates in a Geographic Information System (GIS) environment using the ESRI^{tm} suite of software. The core model remains very similar to the original version. However, a spatial modelling framework allows the use of spatial database coverages of site, land cover and climate, that are now widely available for most forestry regions, and generates output coverages that are compatible with the input data. This version of the model can also use satellite data to provide estimates of leaf area index and APAR, crucial variables governing the rate of growth and transpiration.

Tickle *et al.*, (2000; 2001a; 2001b) report on their use of 3-PG SPATIAL to predict growth over several thousands of hectares of natural eucalypt forest in Australia. An alternate methodology for determining APAR using modelled temperature, LAI and the extinction coefficient (Coops, 1999b) was used in the absence of remote sensing information (Figure 2). Inadequate information on soil water holding capacity and soil properties was recognized as placing a severe constraint on the predictive capabilities of the model. 3-PG SPATIAL nevertheless outperformed conventional empirical models in predictions of volume, DBH and stand density.

3. RESEARCH STRATEGY AND METHODS

3.1 Research strategy

The research strategy was designed to provide a rigorous test of the practicality of modelling diverse groups of forest stands with the spatial versions of 3-PG. Three aspects of model application were seen as being vital to demonstrate:

- the practicality of parameterising the model for a diverse selection of forest stands
- the accuracy with which 3-PG can predict growth and water use over a wide range of site conditions
- the degree to which remote sensing data may be useful in running spatial versions of 3-PG.

The strategy adopted was to select a group of stands exhibiting a wide range of standing biomass, and representing a diverse range of soil and climatic conditions. 3-PG would be set up for each stand, and run for a period of 12 months. Intensive field measurements would be undertaken to quantify the annual growth increments, and a range of processes useful in parameterising the model and validating output. These would include sap flow rates, leaf area index, litterfall rates, allometric ratios, climate inputs and temporal patterns in leaf water potential. Comparison of observed and simulated growth would provide an indication of the model success in describing growth and water use over a diverse range of forest stands. This process was deemed to be a practical one likely to be followed in deriving an initial set of model parameters for a range of forestry compartments. Subsequent “real time” comparisons of model output to observed growth rates would serve as an independent check on parameter estimates, and offer the opportunity for model fine-tuning.

The field data would also provide the ground truth data required to test the use of remote sensing data in providing some of the spatial input required by 3-PG.

3.2 Site selection

Twelve sample compartments were selected in the Zululand forestry region for the following reasons:

- Easily accessible from Durban and Pietermaritzburg where the project team was based.
- Established links between the project team and Zululand foresters
- Flat topography, minimal shadow problem in satellite imagery
- Very uniform clonal *Eucalyptus* stands, little understorey vegetation
- Sufficient diversity in site growth potential
- A distinct rainfall gradient over the forestry region
- Existing automatic weather stations

After investigating a large number of forest compartments, and paying particular attention to the issue of security of personnel and equipment, 12 sites were chosen to represent the range of tree age and site growth potential in the KwaMbonambi and Bushlands districts (see Figures 3 and 4, and Table 1). All sites were planted to *Eucalyptus grandis* / *camaldulensis* hybrid clones, which occur extensively over a wide range of rainfall and site quality.

Table 1. A summary of major site characteristics.

	Bushlands						Kwambonambi					
	Low site index			High site index			Low site index			High site index		
Stand age	**early**	**mid**	**late**	**early**	**mid**	**late**	**early**	**mid**	**late**	**early**	**mid**	**late**
Compt No.	**A04c**	**B04**	**F05**	**A10b**	**A05a**	**A05c**	**NP23**	**RG20b**	**NH01**	**NA24b**	**NK25**	**NP20b**
Compt. Area (ha)	6.4	12.4	7	9	14.7	20	4.9	4.1	4.2	4.7	4.7	5
Co-ordinates	28^{o}07’38’S 32^{o}17’10’E	28^{o}06’21’S 32^{o}17’51’E	28^{o}04’56’S 32^{o}19’16’E	28^{o}07’23’S 32^{o}17’27’E	28^{o}07’14’S 32^{o}17’09’E	28^{o}07’08”S 32^{o}16’45”E	28^{o}54’05’S 31^{o}57’27’E	28^{o}35’08’S 32^{o}03’29’E	28^{o}42’09’S 32^{o}00’56’E	28^{o}41’36’S 32^{o}01’08’E	28^{o}41’11’S 32^{o}03’30’E	28^{o}44’54”S 31^{o}57’26”E
Estate	Bushlands						Nseleni	Rattray	Nseleni	Nseleni	Nseleni	Nseleni
Hybrid	E. grandis / camuldulensis						E. grandis / camuldulensis					
Clone	HGC747	HGC540	HGCmix	HGC121	HGCmix	HGCmix	HGC962	HGC550	HGC550	HGC785	HGC505	HGC550
Planting date	May 97	Jul 95	May 93	Nov 98	Apr 95	Sep 94	Apr 97	May 94	Apr 93	Mar 97	Sep 95	Jun 93
Age at start (yrs)	3.08	4.92	7.08	1.58	5.17	5.75	3.17	6.08	7.14	3.25	4.75	7.00
Age at end (yrs)	4.08	5.92	8.08	2.58	6.17	6.75	4.17	7.08	8.14	4.25	5.75	8.00

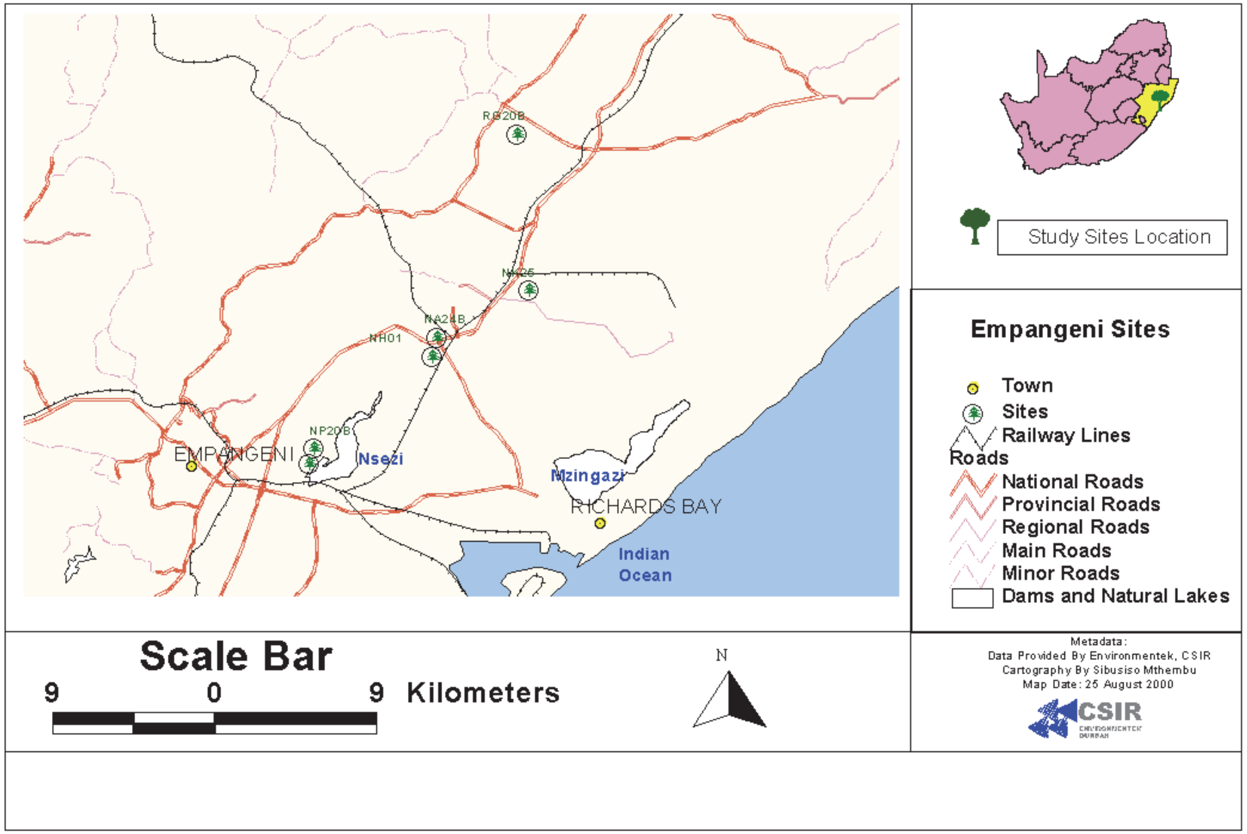

Figure 3. Location of sites in the Kwambonambi district.

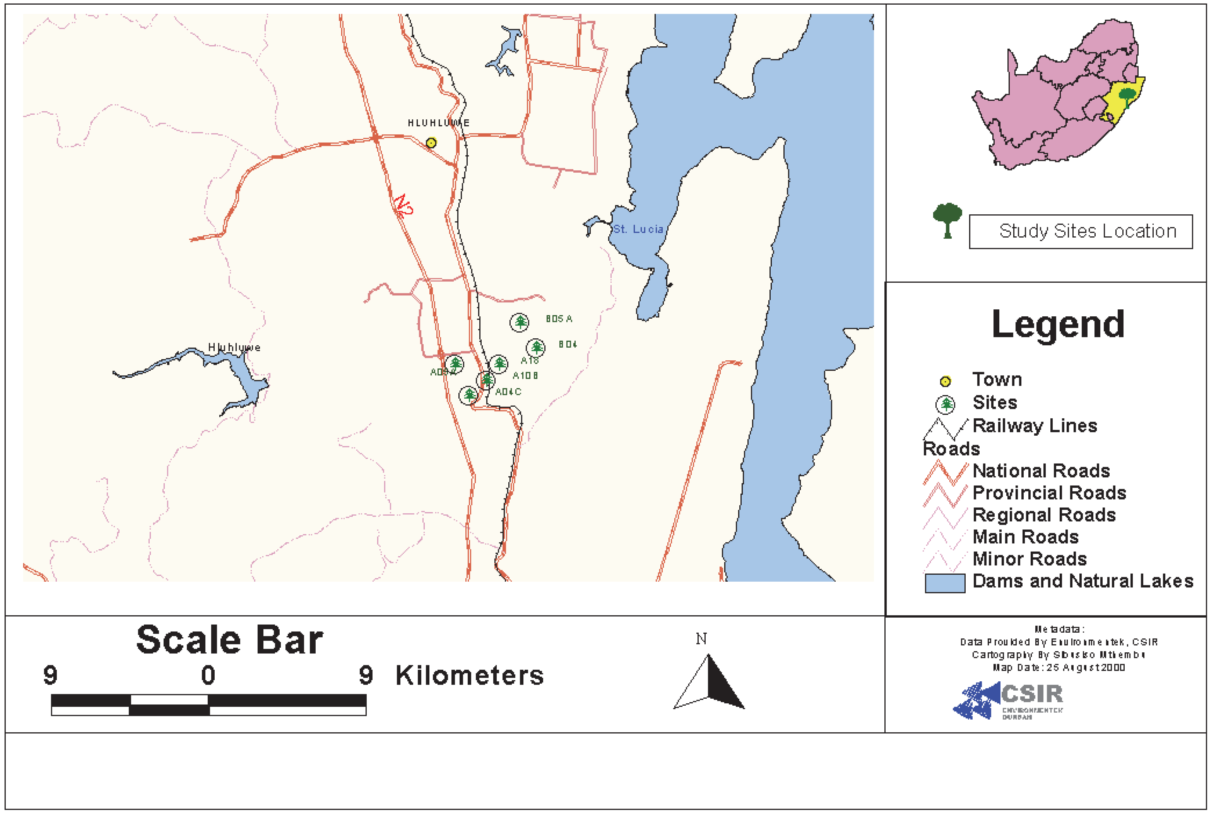

Figure 4. Location of sites in the Bushlands district.

3.3 Weather data

The 3-PG model requires monthly values of total rainfall, mean daily solar radiation, mean daily temperature, number of frost days, and mean daylight vapour pressure deficit. Months were defined as starting on the 15th and ending on the 14th, to coincide with the timing of field visits to the sites.

3.3.1 Rainfall

A tipping bucket rain gauge recorded rainfall at an automatic weather station (AWS) situated close to the Bushlands sites (28^{o} 8.232’ S; 32^{o} 16.331’ E). Data were downloaded at intervals using a cellphone link. A gap in the data record occurred from 11 October 2000 to 27 November 2000 due to a persistent data logger problem. This gap was patched using daily rainfall data recorded at a gauge situated at Bonamanzi (28^{o} 4.042’ S; 32^{o} 18.198’ E), a distance of 8 km from the Bushlands AWS. The Kwambonambi sites were more dispersed than the Bushlands sites, and two gauges were used. Rainfall recorded at the Kwambonambi Fire Protection Service gauge (28^{o}35’45’’S; 32^{o}05’23’’E) was applied to RG20b, NK25, NA24b and NH01, while rainfall recorded in a monthly gauge designated Hugo’s house (28^{o} 43’ 40’’ S, 31^{o} 56’ 55’’ E) was applied to NP20b and NP23. This gauge consisted of a standard 8 “ (203.2 mm) rim fitted to a large plastic container. The monthly catch was measured in millilitres and converted to an equivalent depth of water, assuming that 1 ml = 0.0308 mm.

3.3.2 Temperature and vapour pressure deficit.

A hobo temperature and humidity sensor (Onset Computer Corporation, P.O. Box 3450, Pocasset, MA 02559-3450, USA) was attached to a tree stem in compartments A04c (Bushlands) and NP23 (Kwambonambi). These sensors were protected from rain by a plastic shelter that allowed free movement of air, and were programmed to provide hourly mean temperature and relative humidity. Hourly temperature values were averaged from 01h00 to 24h00 and daily means averaged over each month. Hourly temperature and relative humidity data were used to calculate saturated vapour pressures, actual vapour pressures and vapour pressure deficits. VPD was averaged over each day from 06h00 to 18h00, and used in the calculation of monthly means. Finally, the absence of frost days at the sites was confirmed from inspection of daily minimum temperatures.

3.3.3 Solar radiation.

Hourly solar radiation data were available from LI-COR (LI-COR, Inc., P.O. Box 4425, Lincoln, NE 68504, USA) pyradiometers recorded at the automatic weather stations at Bushlands and Heatonville (31^o 45$^/$ 40$^{//}$ S; 28^o 45$^/$ 30$^{//}$ E). Mean hourly SR in units of W m^{-2} were converted to MJ m^{-2} day^{-1}, and then used to calculate mean daily SR from 06h00 to 18h00. Mean daily SR was averaged over each month. A comparison of mean monthly SR recorded at the two stations showed only minor differences. Consequently, Heatonville data were used to patch the missing data in the Bushlands AWS data record.

3.4 Forest stand descriptors

The following stand descriptors were recorded in each of the 12 test sites:

3.4.1 Stem and branch mass (Ws), tree density

Measurements of tree diameter at breast height (DBH), tree height and tree density took place from 3 July until 18 August 2000 in sample plots at each of the 12 test sites. The number of sample trees per plot varied from 58 to 80, depending on initial planting espacements, plot size and tree mortality. The surveys of the Kwambonambi sites took place from 3-7 July 2000, while those of the Bushlands sites took place from 15-18 August 2000. A final survey of compartment F05 occurred from 18-20 September 2000. Tree diameters were measured with callipers, while the heights of approximately 20 trees were measured using a Suunto clinometer (Suunto Oy, Valimotie 7, FIN-01510 Vantaa, Finland). The heights of the remaining trees in the sample plots were estimated from their diameter using a regression equation based on the 20 measured trees. Plot means of DBH and height were calculated. A second survey of trees within the same sample plots took place at the end of the 12-month measurement period. This time, all tree heights were measured with a Vertex 3 hypsometer (Haglöf Sweden AB, Box 28, Klockargatan 8, S-88221 Langsele, Sweden).

Calculation of individual stem volumes was based on the Schumacher and Hall individual tree volume equation:

$$\ln(V) = b0 + b1 \ln(DBH + f) + b2 \ln(H) \quad (1)$$

where V is utilizable volume (m^3), DBH is diameter at breast height (1.3 m) (cm over bark), H is tree height (m) and f is a correction factor. Coefficients used for this equation for *Eucalyptus grandis X camuldulensis* were those obtained by DuPlessis (1996), published in the South African Forestry Handbook (Bredenkamp, 2000). The volume of each measured tree was calculated, and then summed for each sample plot. Allowance was made for the loss of three trees destructively sampled for biomass measurement (see 3.4.2). The calculated volume per hectare was thus based on the total standing volume in each plot of known area.

Problems were experienced in measuring stand volumes in compartment A04c at the end of the 12-month monitoring period. The tops of eight trees were found to have snapped off as a result of strong winds. Final tree heights had to be estimated from DBH using a DBH-height relationship determined from the undamaged trees.

The dry mass of stems was calculated by assuming a mean wood density of 500 kg per m^3 volume of wood (Malan *et al*., 1994). Biomass data (see 3.4.2) were used to estimate an additional mass of branches, to calculate Ws.

3.4.2 Allometric relation between DBH and Ws, Wf

These relationships are required by the model to ensure that allocation of new growth to foliage and stem proceeds in a balanced fashion as the trees grow. Biomass data were recorded to derive the necessary equation coefficients describing the relation of tree DBH to dry mass of stems and branches. In each compartment, three sample trees (representing small medium and large size classes of tree) were destructively sampled over the period 16-22 October 2000. Total fresh mass of stem, branches and leaves were recorded in the field. Sub-samples were returned to the laboratory where fresh and oven-dried mass was recorded. These ratios were used to estimate total dry mass of stem, branches and leaves.

At the end of the 12 month measurement period, a further sample of three trees was felled in each plot to record only foliage mass. The purpose was to obtain an accurate estimate of Wf at the end of the simulation period, providing further opportunity for testing the usefulness of LANDSAT imagery for spatial estimation of LAI.

3.4.3 Leaf area index, specific leaf area

The leaf area index of stands is a crucial measure of the ability of the trees to transpire and to intercept solar radiation for photosynthesis. It was estimated through destructive sampling of trees described above, as well as from regular monthly readings taken with a LI-COR LAI-2000 Canopy Analyzer.

3.4.3.1 Estimates based on destructive sampling

The biomass sampling procedure is described under 3.4.2. Leaves of all sample trees were stripped off and their fresh mass recorded in the field. Dry mass was calculated on the basis of sub-sample ratios of fresh to oven-dry mass recorded in the laboratory. Total sub-sample leaf area of the fresh leaves was measured with a LI-COR LI-3100 Area Meter, and used to calculate specific leaf area (area of leaves per unit dry mass; m^2 kg^{-1}). Total leaf area of each sample tree was then used to estimate the stand LAI, assuming that each tree represented one third of the total number of trees.

3.4.3.2 Estimates based on Canopy Analyzer measurements

A LI-COR LAI-2000 Canopy Analyzer was used to record monthly LAI at all sites. The purpose was to independently check the estimates based on destructive sampling, and also to look for possible seasonal trends in LAI. The procedure adopted was as follows: Readings were timed, as far as possible, for early morning and late afternoon to reduce the likelihood of light reflection through the canopy. A 90^o mask was fitted over the sensor to exclude the shadow of the instrument operator. At each compartment, a first above-canopy reading was taken in the nearest open space. Eight below-canopy readings followed as quickly as possible, and were taken at random positions in the stand. As stems and branches also intercept sunlight, a correction applicable to *Eucalyptus* trees was used to estimate the true LAI of the canopy alone. The correction (Battaglia *et al*., 1998) takes the following form:

$$LAI\ (true) = 1.54 * PAI\ (canopy\ analyzer) – 0.11 \qquad r^2 = 0.997 \qquad (2)$$

where PAI represents the entire plant area index sensed by the instrument. Limited data from SA supports this correction factor for *E. grandis* (Dye, 1998).

3.4.4 Fertility rating

3-PG requires a fertility rating (0-1) describing the soil fertility in the rooting zone. This is extremely difficult to estimate for trees with well-developed roots that explore deep soil profiles, as is the case in the Zululand sites. The fertility of the upper 1m of soil is often extremely low, and may bear little relation to site productivity. As deep soil excavation is problematic in loose sands, we assumed that the FR is correlated to the growth potential of the site. One measure of this is the site index. This was calculated for each stand using a modified Clutter and Jones difference form equation (Clutter and Jones, 1980):

$$SI = \exp\{[(\ln(H) – b2/Age-b3)(\exp(b1(1/Age_{SI}-1/Age)))]+b2/Age_{SI} – b3\} \qquad (3)$$

where SI is site index (m), H is dominant height at current age (m), Age_{SI} is site index base age (taken to be 5 years) and Age is current stand age. The equation was originally published using base age for site index as 25 years, but in the form given above it allows the specification of the base age. This was taken to be five (5) years for all calculations. Coefficients for this equation were obtained by permission from Mondi Ltd. for their *Eucalyptus grandis X camuldulensis* plantations in coastal Zululand.

3.4.5 Sap flow

3-PG predicts the rate of transpiration from stands of trees, and some observed sap flow data were considered desirable to determine if model-predicted rates were realistic. Our strategy was to obtain limited sap flow data according to the sampling strategy shown in Table 2. In any particular month, hourly sap flow data were recorded in a single sample tree from the higher growth potential Kwambonambi sites and the lower growth potential Bushlands sites. Data from early, mid and late rotation stands were sampled sequentially through the year.

Four sets of heat pulse probes were implanted in each sample tree, each set sampling a different sapwood depth. Three vertically aligned holes were drilled radially into the sapwood at four positions around the trunk, using a 1.85 mm drill bit. Use of a 20 mm-thick drill jig ensured that the holes were exactly parallel to each other. A line heater was inserted into the central hole, while temperature-sensing probes were implanted 10 mm above and 5 mm below the heater. The line heater consisted of a steel tube with an outside diameter of 1.8 mm. Temperature probes consisted of a single thermistor sealed within a Teflon tube of similar diameter. Each sensor probe pair thus gave a point estimate of sapwood temperature. Each thermistor pair was connected in a Wheatstone bridge configuration and automatically zeroed before each heat pulse initiation. The logger was programmed to apply a current of 30 amps lasting 0.8 s to each heater probe. Heat pulse velocity (u) was measured for each probe set using the compensation technique (Huber and Schmidt, 1937; Swanson, 1974). The temperature rise was measured at distances X_u upstream and X_d downstream from the heater, and u was calculated as follows:

Table 2. A summary of the sap flow sampling procedure adopted in this study.

				Months from start											
	SI	Compt	Age	1	2	3	4	5	6	7	8	9	10	11	12
Kwambonambi	High site index	NP23	Early	X			X			X			X		
Kwambonambi		NK25	Mid		X			X			X			X	
Kwambonambi		NP20b	Late			X			X			X			X
Bushlands	Low site index	A04c	Early	X			X			X			X		
Bushlands		B04	Mid		X			X			X			X	
Bushlands		F05	Late			X			X			X			X

$$u = (X_u + X_d) / 2t \qquad (4)$$

where t is the time delay for the temperatures at points X_u and X_d to become equal. The heat pulse velocity is calculated from the time taken for the pulse to travel the distance of 2.5 mm, i.e. the distance between the heater and a point midway between the thermistors.

Heat pulse velocities were corrected for sapwood wounding caused during the drilling procedure. Swanson and Whitfield's (1981) wound correction coefficients were used to derive corrected heat pulse velocities (u'). The correction takes the form:

$$u' = p + qu + r(u)^2 \qquad (5)$$

where p, q and r are the correction coefficients appropriate to the measured wound size, diameter of Teflon probes, and probe separation distances, respectively.

The corrected heat pulse velocities were converted to sap flux (v) using the following equation (Marshall, 1958):

$$v = \rho_b (m_c + c_{dw})\, u' \quad (6)$$

where ρ_b is dry wood density, m_c is the moisture fraction of sapwood, and c_{dw} is the specific heat of dry wood, assumed constant at 0.33 (Dunlap, 1912). Total sap flow was then calculated as the product of mean sap flux density and sapwood area.

At the conclusion of each monthly sampling period, trunk segments containing the drilled holes were removed to the laboratory to measure the sapwood properties required to calculate sap flow from null-balance times. The four sections of the tree trunk containing the probe implantation holes were excised and re-cut longitudinally at the particular radial depth below the cambium where the thermistor was originally positioned. The exposed, fresh face was shaved smooth using a microtome to allow precise measurement of probe separation distances and wound widths. These were typically -5 mm between the heater probe and the lower thermistor, and 10 mm between the heater probe and the upper thermistor probe, yielding a X_u-X_d/2 = 2.5 mm. Measurements of wound widths were taken midway between the line heater position and both the upper and lower thermistors. An average width was applied to the probe set.

Additional samples of sapwood were excised from each trunk sample. A portable electronic scale was used to record fresh mass of each sapwood sample immediately after its removal from the trunk. The immersed weights of the samples were also required. A small container of water of a size sufficient to hold the sapwood samples was placed on the balance. A laboratory clamp stand was set up next to the balance, and a sharp pointed seeker was clamped to position its point 2-3 mm below the water surface. The balance was then zeroed. The seeker was unclamped and impaled into the sapwood sample, and then replaced to completely immerse the sapwood sample under water. No part of the sample was allowed to touch the sides or bottom of the water container. A new weight was immediately recorded, and using Archimedes' principle, taken to be equivalent to the weight of water displaced. Assuming a specific gravity of water of 1000 kg m^{-3}, the immersed weight in grams was assumed equal to the sample volume in cubic centimetres. The sapwood samples were subsequently brought back to the laboratory, where they were oven-dried to constant weight, before their dry mass was recorded. Moisture fraction was calculated as (fresh weight - dry weight) / dry weight, while basic wood density was calculated as dry weight / volume of the freshly excised section of wood.

Depths are measured from the cambium inwards, and therefore exclude the bark. Previous experience has shown that sapwood is mostly 30 to 40 mm thick in all ages of *E. grandis* trees. Implantation depths were therefore chosen to sample this region of the trunk. Four probe sets were implanted into each sample tree. Thermistors were implanted to depths of approximately 4, 9, 16 and 24 mm below the cambium. This sampling arrangement has been shown to result in good estimates of sap flow in *E. grandis* (Olbrich, 1991).

HPV data loggers were programmed to record null balance times every hour between 04h30 and 21h30 over the year.

The following data analysis procedure took place. The raw data were first examined using a custom-developed Visual Basic analysis programme to identify probes with missing or faulty data, those with long null-balance times, and those exhibiting poor correlation with other probe sets. Missing or poor quality data were patched using simultaneous data from another probe set with which it is most highly correlated. Long null-balance times that indicate slow sap flow rates were sometimes recorded by the deepest probes, indicating close proximity to heartwood. These probes were excluded where the number of missing data was high. Patched files were then saved and subsequently read again during the calculation of sap flow. The analysis programme calculated hourly sap flow for the tree, and saved the output in three files containing the hourly sap flow rates, daily total sap flow, and the parameters used in the calculations. The daily data files were then concatenated, and partial days at the start and end of files were joined appropriately. These files were checked as follows:

- The whole-year pattern was examined to check for unusually high and low values, and marked discontinuities across the original files.

- Broadly similar patterns of daily sap flow were expected in both sample trees at any given time.

- Readings taken at times when transpiration rates were not reduced by soil water deficits were plotted against mean daily vapour pressure deficit (VPD). High correlations are typical under these conditions, and suspect logger data are immediately apparent.

Where suspect data were identified, they were removed and replaced with patched data.

3.4.6 Litterfall

An accurate assessment of the rate of litterfall is especially crucial in 3-PG to ensure that the simulated tree canopy remains at a realistic size. Five litter traps were installed at each test site, and catches were recorded at monthly intervals. Each trap consisted of a wire frame suspending a catch bag made of shade cloth and collecting over an area of 0.332 m^2. The catch bags were emptied at each monthly visit. Leaves were separated from twigs, and then oven-dried before weighing. The mean leaf mass from all catch bags was multiplied by 30120.5 to scale up to a hectare. A significant number of litter traps were stolen, causing gaps in the data record and periodic reduced sampling intensity.

3.4.7 Pre-dawn xylem pressure potential (XPP)

Information on the degree of drought stress experienced by the trees during the dry season is a very important requirement for 3-PG modelling. Such stress periods have a significant effect on rates of transpiration and growth. Pre-dawn XPP readings were performed during the 2000 and 2001 dry seasons. A maximum of five leaf samples were obtained by shooting stones into the canopy with a catapult. These were swiftly inserted into a PMS pressure chamber and a minimum counter pressure applied to the chamber to bring the sap to the surface of the cut petiole. This xylem pressure potential was then recorded.

4. RESULTS

4.1 Weather data

Tables 3 and 4 summarise the monthly weather data used in the simulations of the Bushlands and Kwambonambi sites. Comparison of available solar radiation data from the Bushlands and Heatonville AWS showed sufficient similarity of monthly means (slope = 0.82; intercept = 1.88; R^2 = 0.92) to permit the use of the Heatonville data to patch the gap in the Bushlands data record. The whole-year pattern of daily solar radiation is shown in Figure 5.

Figure 6 shows the hourly range of temperature through the year as recorded at the Bushlands AWS, and illustrates the absence of frost in the area. Similarly, the range and seasonal pattern of mean daytime VPD, as recorded by a Hobo sensor at A04c, is illustrated in Figure 7. Gaps in the data record were patched using the data from the Hobo sensor in NP23 (November) or estimated as the mean of January and March (February).

Table 3. Weather data applicable to the Bushlands sites.

	2000					2001							
Month beginning	**Aug**	**Sep**	**Oct**	**Nov**	**Dec**	**Jan**	**Feb**	**Mar**	**Apr**	**May**	**Jun**	**Jul**	**Aug**
SR (MJ m^{-2} day^{-1})	15.7	12.5	13.3	14.5	21.1	18.5	16.2	16.3	13.0	9.4	6.4	10.7	10.8
Rain (mm) AWS	1.0	68.5*	90.5*	289.8*	72.9	64.4	49.7	74.7*	3.4	8.0	19.3	21.3	73.7
VPD (kPa)	1.40	1.06	1.21”	0.88”	1.23”	1.48	1.14^	0.80	0.98	0.98	0.93	1.08	1.14
Frost days	0	0	0	0	0	0	0	0	0	0	0	0	0
Temp (^{o}C)	19.6	20.0	20.5	22.1	23.9	24.1	24.2	23.2	20.6	19.3	17.1	16.9	19.3
Tmax (^{o}C)	25.9	21.9	21.8	24.9	25.0	22.5	24.9	24.1	24.7	26.1	22.5	22.0	24.9
Tmin (^{o}C)	13.4	16.0	16.4	15.8	16.7	17.0	15.0	15.0	14.4	13.5	10.2	10.2	13.9

- * Patched using Bonamanzi rain gauge
- ^ Average of January and March
- “ Patched using NP23 data

Table 4. Weather data applicable to the Kwambonambi sites.

	2000						2001						
Month beginning	**Jul**	**Aug**	**Sep**	**Oct**	**Nov**	**Dec**	**Jan**	**Feb**	**Mar**	**Apr**	**May**	**Jun**	**Jul**
SR (MJ m^{-2} day^{-1})	12.0	15.7	10.0	13.3	14.2	19.8	16.9	15.8	13.6	12.2	8.4	7.9	12.0
Rain (Hugo) (mm)	16.0*	4.0*	74.0	404.0	98.7	195.0	83.3	49.3	107.9	20.0	7.7	6.2	34.1
Rain Kwambo FPS (mm)	16.0	4.0	110.0	123.9	363.0	134.0	151.0	45.8	113.7	23.0	14.0	9.0	44.0
VPD (kPa)	0.84	1.22	0.99	1.05	1.27	1.34	1.13	1.14	0.80	0.98	0.84	0.85	1.06
Frost days	0	0	0	0	0	0	0	0	0	0	0	0	0
Temp (^{o}C)	17.6	19.6	15.7	19.5	18.3	22.8	22.3	23.0	20.8	16.0	13.9	15.3	17.6
Tmax (^{o}C)	23.4	25.9	21.9	21.8	24.9	25.0	22.5	24.9	24.1	24.7	26.1	22.5	22.0
Tmin (^{o}C)	9.1	13.4	16.0	16.4	15.8	16.7	17.0	15.0	15.0	14.4	13.5	10.2	10.2

- * Data recorded at the Kwambo FPS site

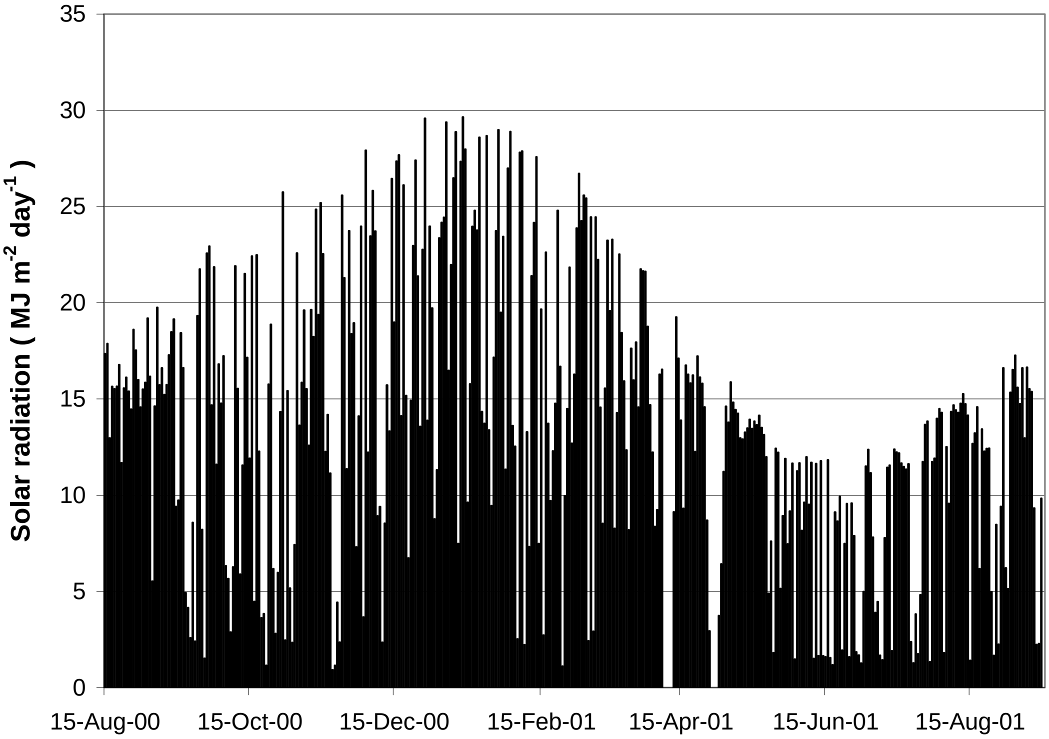

Figure 5. The annual pattern of solar radiation recorded at the Bushlands AWS.

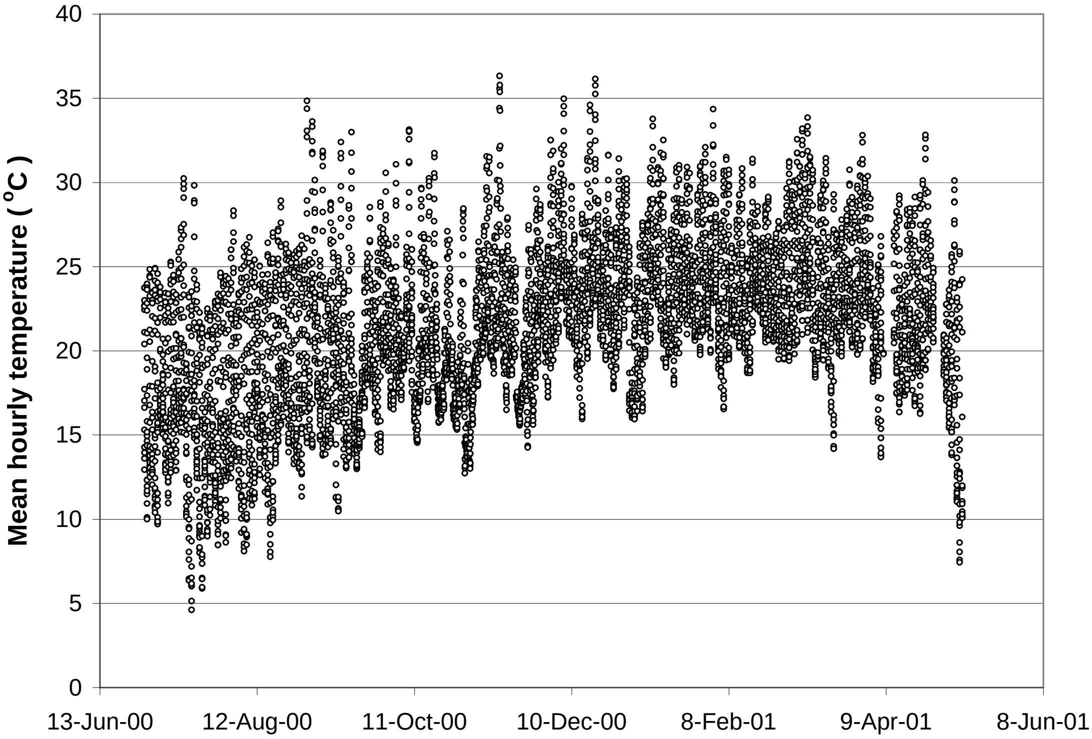

Figure 6. The annual pattern of hourly temperature recorded at the Bushlands AWS.

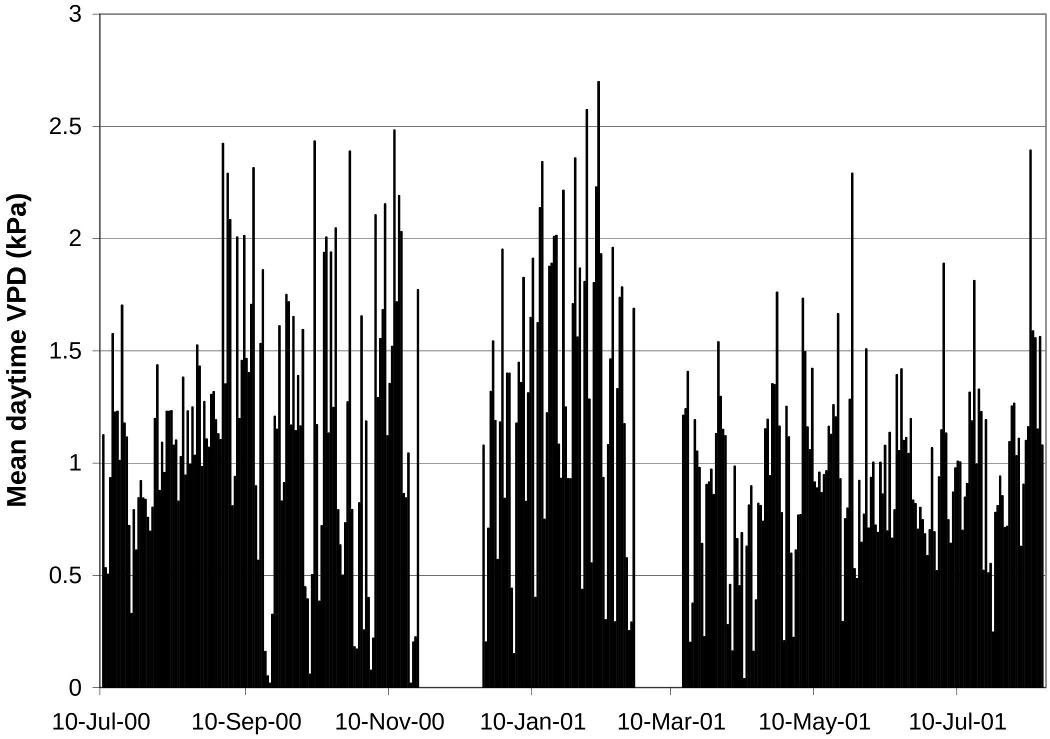

Figure 7. The annual pattern of mean daytime vapour pressure deficit recorded by a Hobo sensor at the Bushlands site A04c.

4.2 Forest stand description

The following stand descriptors were recorded in each of the 12 sites:

4.2.1 Allometric relation between DBH and Ws (stem + branch dry mass)

Figure 8 illustrates the relation between DBH and Ws for the combined Kwambonambi and Bushlands sites. We assume from this figure that the fitted curve adequately describes the trends displayed by both sets of data.

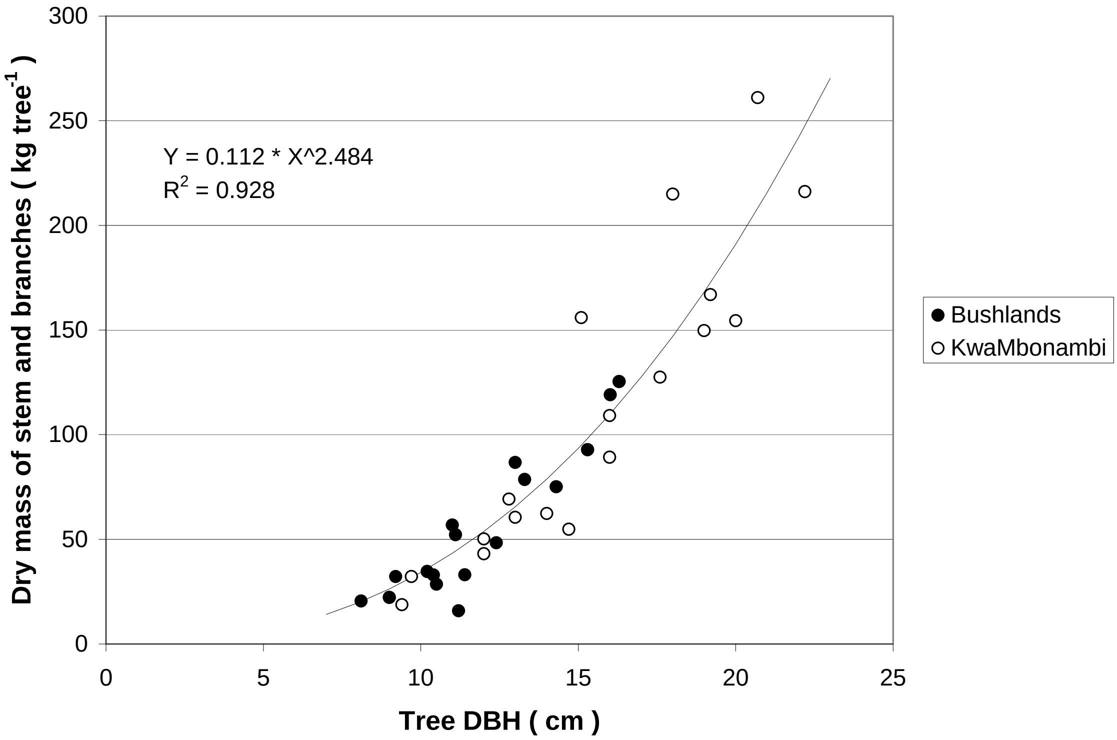

Figure 8. The relation between tree DBH and Ws for destructively sampled trees from Bushlands and Kwambonambi sites. The trend is defined by a non-linear regression fitted to the data.

4.2.2 Branch fraction and calculation of Ws

Tables 5 and 6 summarise the calculations leading to the estimation of Ws at the start and end of the sample period in each stand. Mean DBH and height of sampled trees were used to calculate stem volume, which was converted to stem mass. The additional biomass contributed by the branches was estimated from the biomass data recorded from destructively sampled trees. The site index and Ws annual increment calculated for each site are shown in Table 6.

Figure 9 illustrates the relationship between trunk dry mass and the combined mass of trunk and branches used in the calculations of Ws. 3-PG also requires parameter values that describe the relation between tree age and the fraction of Ws comprising branch mass. The same biomass data were used to illustrate this relationship (Figure 10).

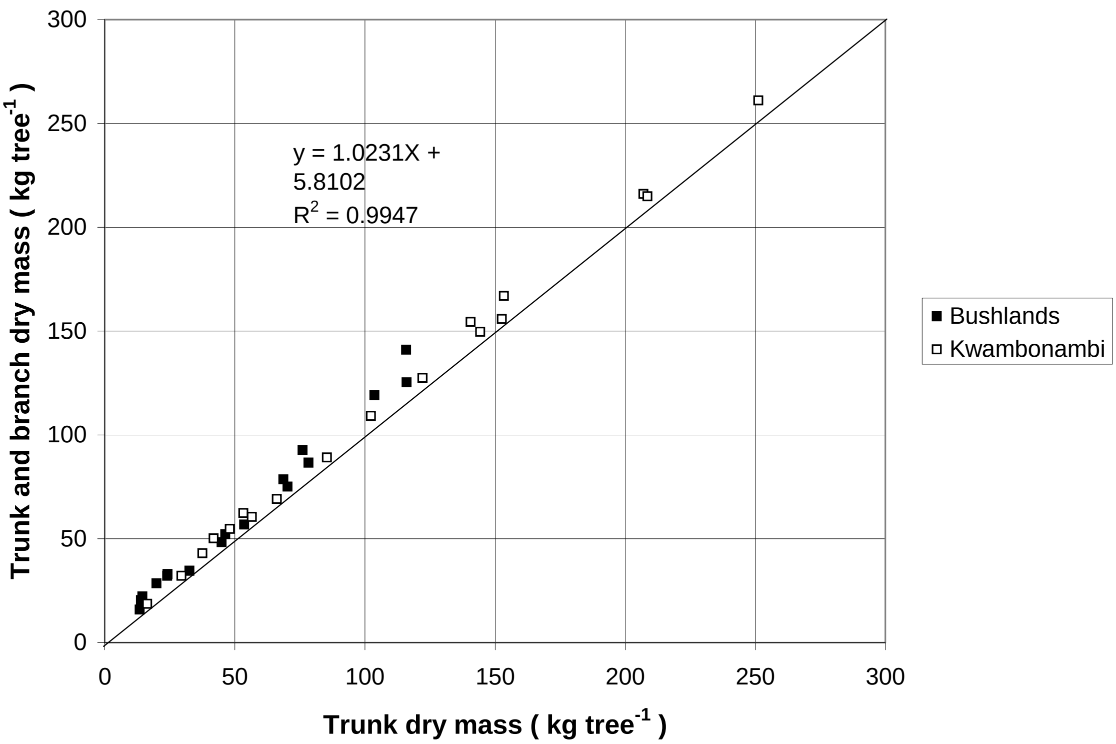

Figure 9. The relation between trunk dry mass and the combined mass of trunk and branches, based on the data from the destructively sampled trees.

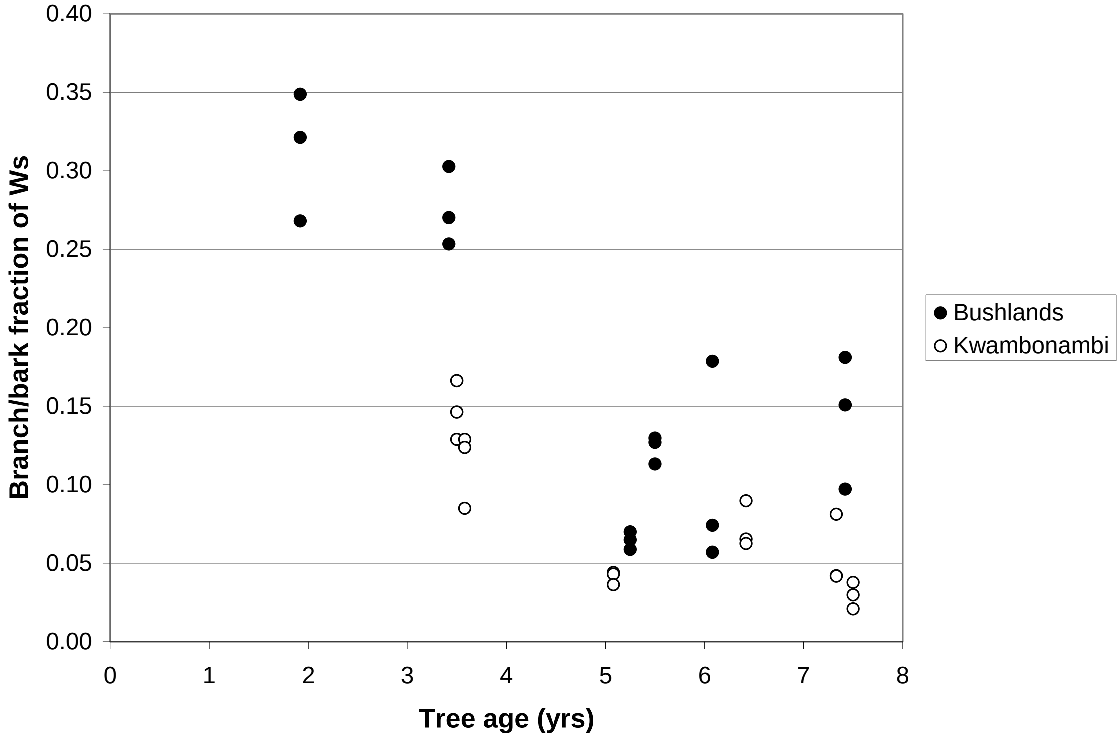

Figure 10. The relation between tree age and fraction of Ws consisting of branches and bark, as recorded in three sample trees at the Bushlands and Kwambonambi sites.

Table 5. A summary of measurements performed at the first enumeration survey at the study sites.

	Bushlands						**Kwambonambi**					
	Low site index			**High site index**			**Low site index**			**High site index**		
Stand age	**early**	**mid**	**late**	**early**	**mid**	**late**	**early**	**mid**	**late**	**early**	**mid**	**late**
Compartment No.	**A04c**	**B04**	**F05**	**A10b**	**A05a**	**A05c**	**NP23**	**RG20b**	**NH01**	**NA24b**	**NK25**	**NP20b**
1st enumeration date, 2000	**17 Aug**	**17 Aug**	**19 Sep**	**17 Aug**	**17 Aug**	**17 Aug**	**5 Jul**	**5 Jul**	**5 Jul**	**5 Jul**	**5 Jul**	**5 Jul**
SPH	1418	1143	1170	1330	1177	1220	1390	1098	1116	1316	1285	1211
% mortality	0	0	1.25	6.25	2.5	5	0	2.5	3.75	1.25	7.5	14.3
No. of trees measured	80	80	79	75	78	76	80	78	77	79	74	58
Mean DBH (cm)	10.1	12.8	13.2	10	14.7	14.1	11.8	15.8	16.2	11.4	15.5	17.5
Mean Height (m)	11.8	16.8	19.9	11.8	19	20.6	14	21.8	23.1	15.6	23.3	23.0
Mean stem vol. (m^3 $tree^{-1}$)	0.0353	0.0837	0.1078	0.0347	0.1291	0.1277	0.0585	0.1698	0.2136	0.0624	0.1847	0.2209
Mean stem mass (kg $tree^{-1}$)	17.65	41.85	53.90	17.35	64.55	63.85	29.25	84.90	106.80	31.20	92.35	110.45
Stem and branch mass (kg $tree^{-1}$)	23.87	48.63	60.96	23.56	71.85	71.14	35.74	92.67	115.08	37.73	100.29	118.81
W_s (t ha^{-1})	33.85	55.58	71.32	31.33	84.57	86.79	49.68	101.75	128.43	49.65	128.87	143.88

Table 6. A summary of measurements performed at the second enumeration survey at the study sites.

	Bushlands						Kwambonambi					
	Low site index			High site index			Low site index			High site index		
Stand age	**early**	**mid**	**late**	**early**	**mid**	**late**	**early**	**mid**	**late**	**early**	**mid**	**late**
Compartment. No.	**A04c**	**B04**	**F05**	**A10b**	**A05a**	**A05c**	**NP23**	**RG20b**	**NH01**	**NA24b**	**NK25**	**NP20b**
2nd enumeration date 2001	**1 Aug**	**1 Aug**	**Sep**	**1 Aug**	**1 Aug**	**Sep**	**1 Jul**	**1 Jul**	**1 Jul**	**1 Jul**	**1 Jul**	**1 Jul**
SPH	1418	1143	1170	1330	1177	1220	1389	1098	1116	1316	1285	1211
No. of trees measured	71	75	73	72	75	71	72	75	69	75	64	78
Mean DBH (cm)	11.1	13.3	13.8	11.7	15.1	14.4	13.3	16.7	16.2	12.3	16.3	19.4
Mean Height (m)	11.8	19.5	19.9	13.7	21.0	20.5	16.9	24.0	23.5	16.7	23.5	26.7
Mean stem volume (m^3 $tree^{-1}$)	0.0416	0.1083	0.1155	0.0541	0.1543	0.1314	0.0915	0.2073	0.2309	0.0794	0.2085	0.3373
Mean stem mass (kg $tree^{-1}$)	20.80	54.15	57.75	27.05	77.15	65.70	45.75	103.65	115.45	39.7	104.25	168.65
Stem and branch mass (kg $tree^{-1}$)	27.09	61.21	64.89	33.49	84.74	73.03	52.62	111.85	123.93	46.43	112.47	178.36
Ws (t ha^{-1})	38.41	69.96	75.92	44.54	99.74	89.10	73.09	122.81	138.31	61.10	144.52	215.99
Annual Ws growth increment (t ha^{-1})	4.56	14.38	4.60	13.21	15.17	2.31	23.41	21.06	9.88	11.45	15.65	72.11
SI 5 (m)	14.58	19.61	17.48	21.12	22.01	19.71	19.85	22.85	25.09	19.94	25.45	27.01

4.2.3 Leaf area index

4.2.3.1 Estimates based on destructive sampling

Tables 7 and 8 show the calculations relating the leaf mass of destructively sampled trees to the whole stand LAI. It is assumed that the mean foliage mass of the three sample trees (chosen to represent small, medium and large size classes of tree) adequately represented the stand. A specific leaf area measured in a sub-sample of leaves from each tree was used to convert foliage total dry mass to total leaf area per mean tree. The values of Wf in Table 7 were entered as the starting Wf in the simulations, while the values of Wf in Table 8 were used as a check of the end of year simulated Wf.

Table 7. A summary of leaf area index estimates based on destructive sampling at the start of the 12-month monitoring period.

	Bushlands (Low rainfall)						Kwambonambi (high rainfall)					
	Low site index			High site index			Low site index			High site index		
Stand age	**early**	**mid**	**late**	**early**	**mid**	**late**	**early**	**mid**	**late**	**early**	**mid**	**late**
Compt No.	**A04c**	**B04**	**F05**	**A10b**	**A05a**	**A05c**	**NP23**	**RG20b**	**NH01**	**NA24b**	**NK25**	**NP20b**
Tree 1 fresh leaf mass (kg)	5.23	3.17	2.00	4.75	3.43	1.83	2.36	3.00	3.00	2.80	1.80	7.00
Tree 2 fresh leaf mass (kg)	6.27	5.81	3.60	8.40	5.77	4.05	7.6	4.20	9.00	4.80	4.50	15.30
Tree 3 fresh leaf mass (kg)	4.60	6.86	4.75	7.05	9.27	7.10	11.7	13.00	10.55	8.90	8.00	10.29
Mean fresh leaf mass (kg)	5.37	5.28	3.45	6.73	6.16	4.33	7.22	6.73	7.52	5.50	4.77	10.86
Dry/fresh mass ratio	0.42	0.46	0.41	0.37	0.41	0.40	0.37	0.41	0.39	0.37	0.36	0.37
Mean dry leaf mass (kg)	2.26	2.43	1.41	2.49	2.53	1.73	2.67	2.76	2.93	2.04	1.72	4.02
SLA (m^2 kg^{-1} dry mass)	7.14						8.11					
Mean leaf area (m^2 $tree^{-1}$)	16.14	17.35	10.07	17.78	18.06	12.35	21.65	22.38	23.76	16.54	13.95	32.60
Tree density (SPH)	1418	1143	1170	1330	1177	1220	1390	1098	1116	1316	1285	1211
LAI (m^2 m^{-2})	2.29	1.98	1.18	2.36	2.13	1.51	3.01	2.46	2.65	2.18	1.79	3.95
Wf (t ha^{-1})	3.20	2.78	1.65	3.31	2.98	2.11	3.71	3.03	3.27	2.68	2.21	4.87

Table 8. A summary of leaf area index estimates based on destructive sampling at the end of the 12-month monitoring period.

	Bushlands (Low rainfall)						Kwambonambi (high rainfall)					
	Low site index			High site index			Low site index			High site index		
Stand age	**early**	**mid**	**late**	**early**	**mid**	**late**	**early**	**mid**	**late**	**early**	**mid**	**late**
Compartment No.	**A04c**	**B04**	**F05**	**A10b**	**A05a**	**A05c**	**NP23**	**RG20b**	**NH01**	**NA24b**	**NK25**	**NP20b**
Tree 1 fresh leaf mass (kg)	2.45	2.85	3.20	2.0	2.9	2.05	3.4	3.25	2.6	1.90	2.50	8.80
Tree 2 fresh leaf mass (kg)	4.65	5.10	5.30	5.9	6.1	4.25	4.9	9.1	5.45	3.70	7.10	13.30
Tree 3 fresh leaf mass (kg)	8.75	6.55	8.30	8.8	16.45	6.75	13.3	13.05	18.30	8.35	9.80	15.50
Mean fresh leaf mass (kg)	5.28	4.83	5.60	5.57	8.48	4.35	7.20	8.47	8.78	4.65	6.47	12.53
Dry/fresh mass ratio	0.471	0.454	0.479	0.427	0.447	0.467	0.419	0.420	0.431	0.418	0.374	0.398
Mean dry leaf mass (kg)	2.49	2.19	2.68	2.38	3.79	2.03	3.02	3.56	3.78	1.94	2.42	4.99
SLA (m^2 kg^{-1} dry mass)	6.37						7.70					
Mean leaf area (m^2 $tree^{-1}$)	15.86	13.95	17.07	15.16	24.14	12.93	23.25	27.41	29.11	14.94	18.63	38.42
Tree density (SPH)	1418	1143	1170	1330	1177	1220	1389	1098	1116	1316	1285	1211
LAI (m^2 m^{-2})	2.25	1.59	2.00	2.02	2.84	1.58	3.23	3.01	3.25	1.97	2.39	4.20
Wf (t ha^{-1})	3.53	2.50	3.14	3.17	4.46	2.48	4.19	3.91	4.22	2.55	3.11	6.04

4.2.3.2 Estimates based on canopy analyzer measurements

Figures 11 and 12 illustrate the corrected LAI estimates recorded at Bushlands and Kwambonambi, respectively. The Bushlands data in Figure 11 show most estimates of LAI to lie between 2 and 3.5, but with a declining trend over the 12-month sample period. The Kwambonambi data (Figure 12) show greater variation, which is largely due to the consistently higher LAI displayed by NP20b. Excluding this stand, LAI readings again mostly range between 2 and 3.5.

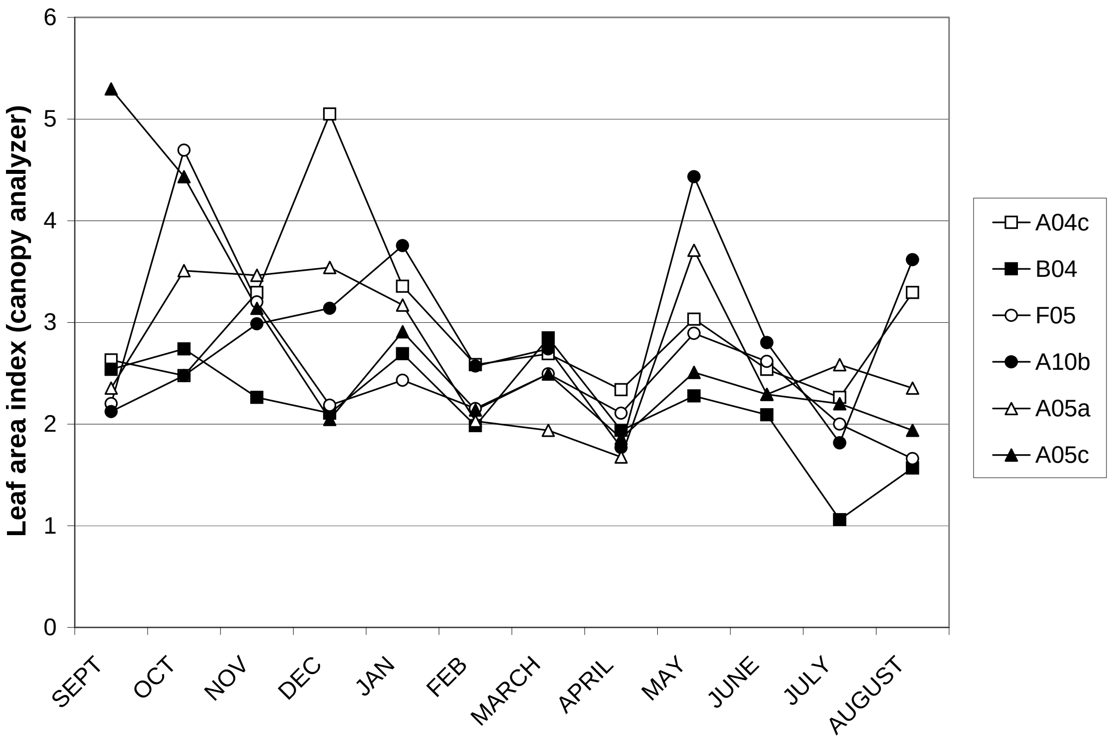

Figure 11. Monthly LAI recorded at the Bushlands sites with a canopy analyzer.

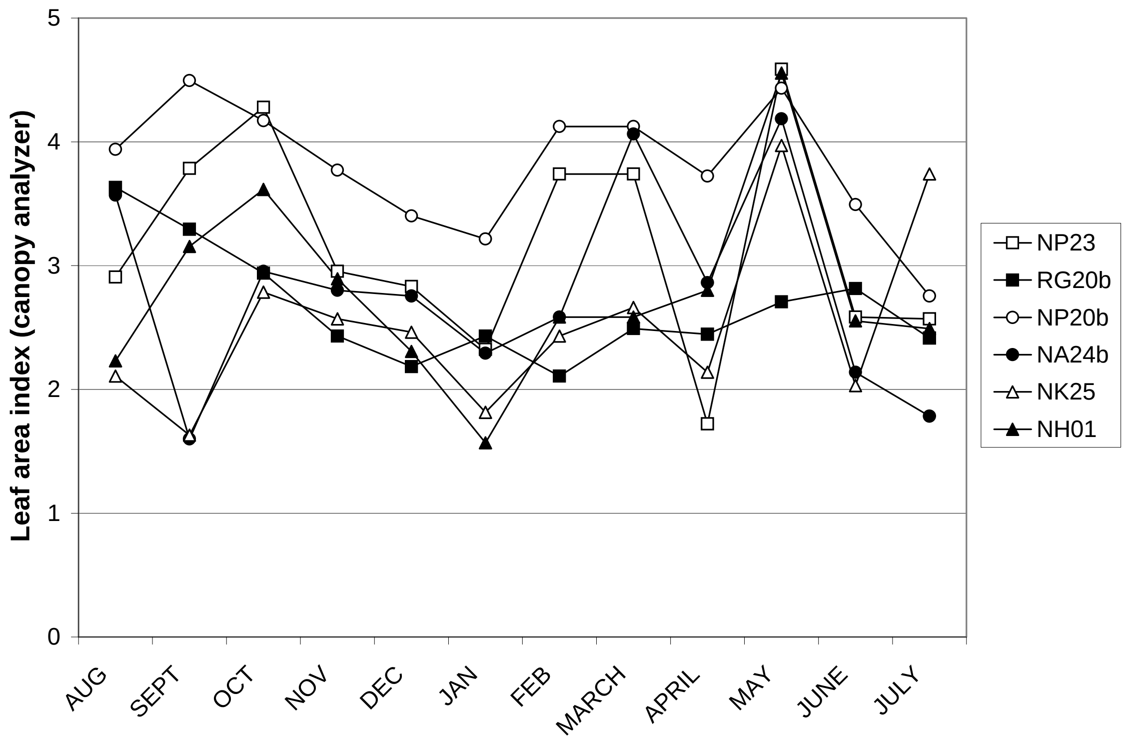

Figure 12. Monthly LAI recorded at the Kwambonambi sites with a canopy analyzer.

4.2.4 Specific leaf area

Table 9 summarises the specific leaf areas measured in foliage sub-samples. Since a single species parameter set was preferred for this study in order to reduce the number of parameters to be altered, an overall mean was used in the model simulations.

Table 9. A summary of specific leaf area (m^2 leaf area per kg dry mass) recorded for sample trees of different age at Bushlands and Kwambonambi.

	Bushlands (Low rainfall)						**Kwambonambi (high rainfall)**					
	Low site index			**High site index**			**Low site index**			**High site index**		
Stand age	**early**	**mid**	**late**	**early**	**mid**	**late**	**early**	**mid**	**late**	**early**	**mid**	**late**
Compt No.	**A04c**	**B04**	**F05**	**A10b**	**A05a**	**A05c**	**NP23**	**RG20b**	**NH01**	**NA24b**	**NK25**	**NP20b**
SLA (2000)	7.59	6.85	7.47	7.64	6.58	6.72	6.97	7.45	8.34	8.16	7.92	9.81
	7.14						8.11					
SLA (2001)	7.33	5.95	5.57	6.87	6.56	5.97	7.43	7.43	7.72	7.61	8.01	7.98
	6.38						7.70					
District mean	6.76						7.91					
Overall mean	7.34											

4.2.5 Wf (foliage dry mass)

Figure 13 shows the general relation between foliage dry mass and DBH recorded in 36 trees felled in 2001. This relationship is sufficiently well defined to permit useful estimates of Wf from the mean tree diameter of a stand.

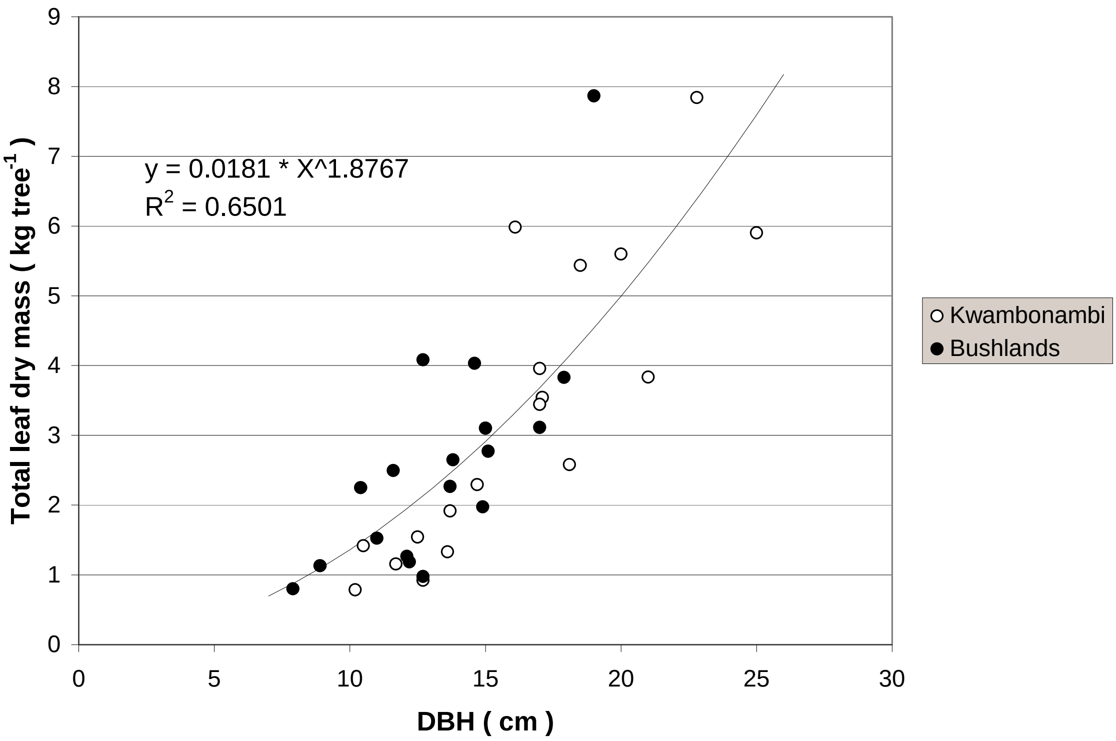

Figure 13. The relation between tree DBH and Wf measured from destructively sampled trees from Bushlands and Kwambonambi sites in 2001.

4.2.6 Sap flow.

Figure 14 illustrates the range of daily sap flow (l day^{-1}) recorded in single sample trees within NP20b, NP23, NK25, B04, F05 and A04c at different times of the year. Box and whisker plots illustrate the median and 25 and 75% percentiles, non-outlier maximum and minimum values, and outliers. These diagrams have been ranked in order of site productivity as defined by the observed annual growth increment. As expected, NP20b, NP23 and NK25 showed higher growth increments than BO4, F05 and A04c. Despite each box and whisker reflecting daily sap flows in only one sample tree, the diagrams reveal a clear difference between the two groups of sites. Median daily flows range from approximately 30 to 64 l day $^{-1}$ for the more productive sites, and from approximately 15 to 34 l day $^{-1}$ for the less productive group. Seasonal differences are not clearly expressed, owing the loss of some data sets due to equipment problems, and probable physiological variation among successive sample trees in a plot. These results nevertheless provide a very useful guide to the range of sap flow rate that 3-PG should predict.

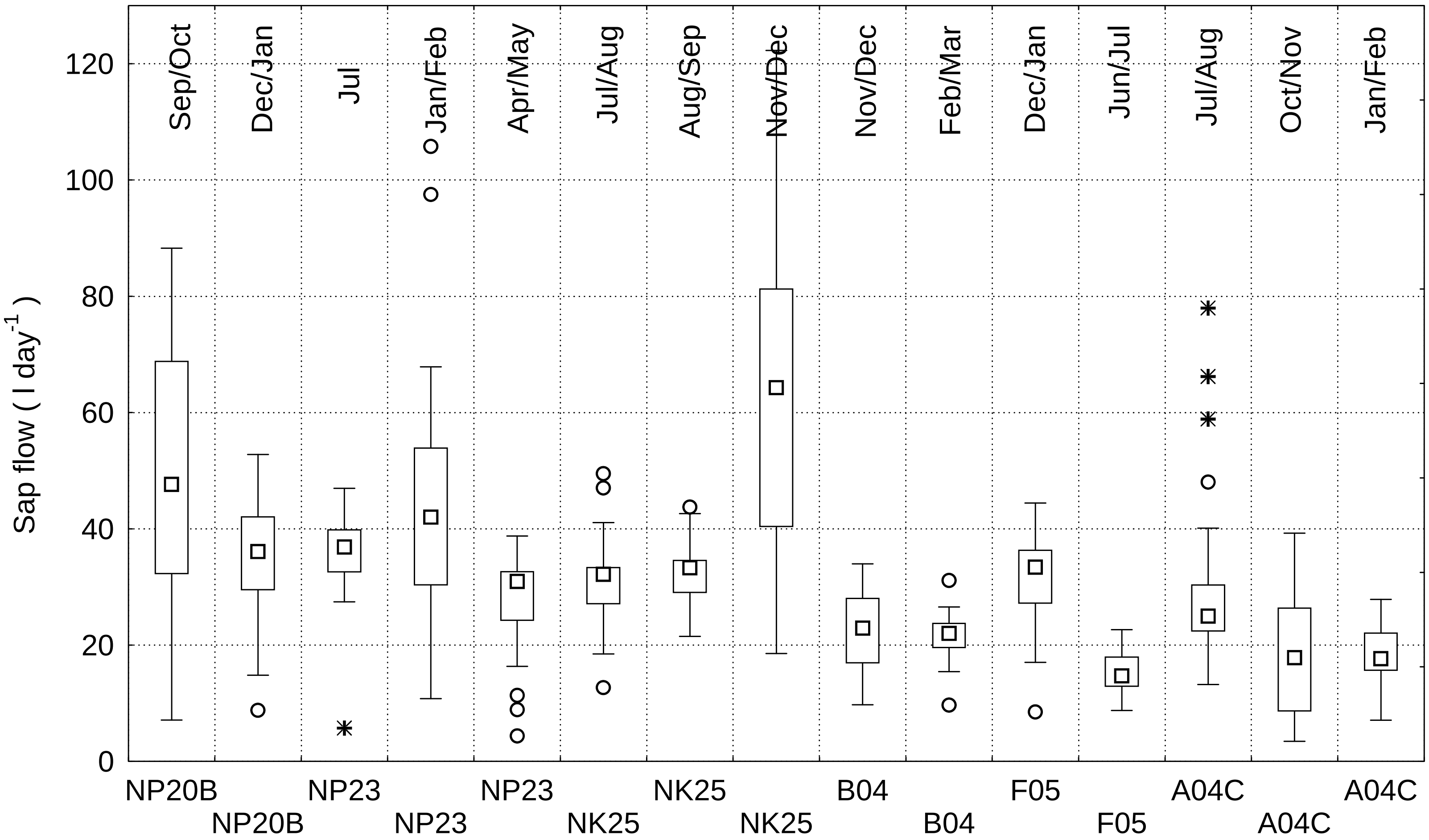

Figure 14. Variation in daily sap flow recorded at six sites at different times of the year.

4.2.7 Litterfall.

Figures 15 and 16 illustrate the trend in litterfall recorded at the Bushlands and Kwambonambi sites, respectively. Storms were found to have a marked effect in increasing the litter catch in traps, and the effects of a severe January storm are particularly clear in both Figures. Seasonal variation in litterfall was particularly evident at the Kwambonambi sites: lowest rates occurred during the summer months, but these gradually increased during the dry winter. A similar dry season increase is evident at the Bushlands sites.

3-PG does not make provision for month-by-month variation in litterfall rate, but rather assumes a constant rate through the year. A mean Wf for the Bushlands sites was estimated from Tables 7 and 8 to be 2.94. A mean annual litterfall rate of approximately 2.4 t ha^{-1} is equivalent to an annual leaf turnover rate of 0.82, and a monthly rate of 0.068. Similarly, a mean Wf for the Kwambonambi sites was estimated to be 3.55 t ha^{-1}. A mean annual litterfall rate of approximately 3 t ha^{-1} is equivalent to an annual turnover rate of 0.85, and a monthly rate of 0.071.

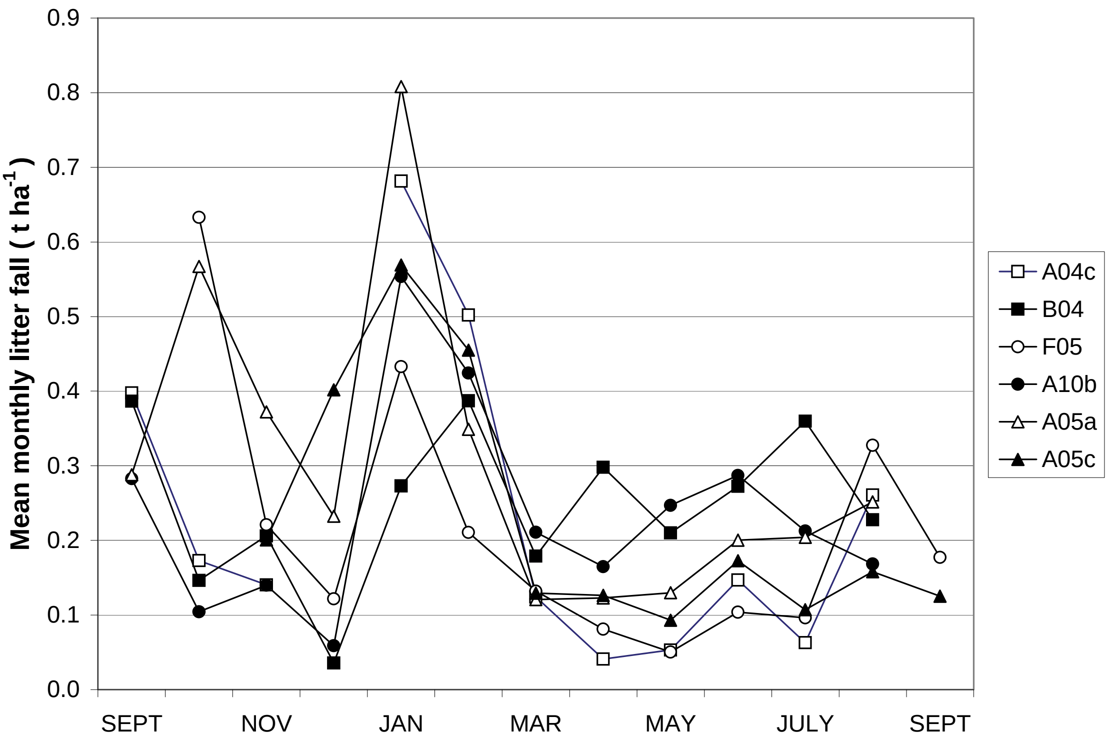

Figure 15. Monthly litterfall recorded at the Bushlands sites.

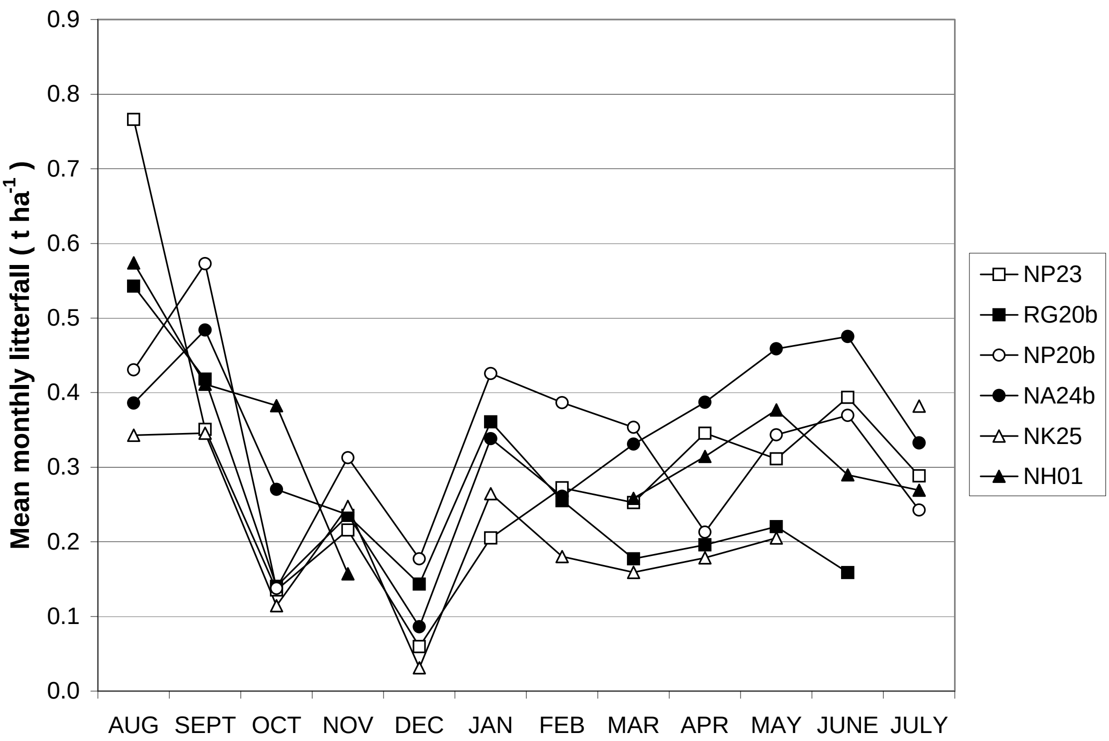

Figure 16. Monthly litterfall recorded at the Kwambonambi sites.

4.2.8 Pre-dawn xylem pressure potential

Table 10 summarises the pre-dawn XPP measurements recorded over the two winter periods. Comparison between Bushlands and Kwambonambi sites is difficult because of the limited sampling that took place at Kwambonambi. Nevertheless, the expected higher level of water stress at the drier Bushlands sites is apparent. Severe water stress was experienced by trees at the Bushlands sites B04, F05, A10b and A05c, while indications of stress are also evident at the Kwambonambi sites RG20b and NA24b.

Table 10. Pre-dawn xylem pressure potential readings (Bars) recorded at the Bushlands and Kwambonambi sites. Numbers in brackets indicate the number of leaves sampled.

	Bushlands (Low rainfall)						Kwambonambi (high rainfall)					
	Low site index			High site index			Low site index			High site index		
Stand age	**early**	**mid**	**late**	**early**	**mid**	**late**	**early**	**mid**	**late**	**early**	**mid**	**late**
Compartment No.	**A04c**	**B04**	**F05**	**A10b**	**A05a**	**A05c**	**NP23**	**RG20b**	**NH01**	**NA24b**	**NK25**	**NP20b**
Aug 2000	-6.7 (6)			-6.4 (5)	-7.7 (3)							
Sep 2000	-6.5 (5)	-5.8 (3)	-10.0 (3)	-11.0 (3)	-9.2 (3)							
May 2001	-8.9 (5)	-15.9 (5)	-15.8 (4)	-10.6 (4)	-7.0 (5)	-9.9 (4)						
Jun 2001	-10.4 (5)	-20.3 (4)	-16.2 (5)	-16.0 (5)	-11.3 (3)	-15.7 (5)	-10.1 (5)					-9.5 (4)
Jul 2001	-14.0 (5)	-12.4 (5)	-13.8 (5)	-13.2 (5)	-8.4 (5)	-14.0 (5)	-9.2 (5)		-9.2 (5)	-18.4 (5)	-5.8 (5)	-7.8 (5)
Aug 2001								-16.7 (6)				

4.3 3-PG parameter estimation strategy and simulation results

The ability of 3-PG to duplicate the observed range of annual growth increments recorded at the 12 sample sites was assessed using the standard Excel "point" version of 3-PG. 3-PG requires two sets of input parameters: a set of species parameters defines the physical and physiological characteristics of the species being simulated, while a set of site and initialisation parameters describes the principle soil and climate conditions, and starting biomass pertaining at each site. Our strategy was to develop a single set of species parameter values that applies to all sites, with variation in growth and ET among the sites largely accounted for by differences in site conditions and starting biomass. This was to minimize the amount of arbitrary changes to those species parameters for which field evidence is very difficult to obtain.

A set of default species parameter values applicable to *Eucalyptus globulus* provided a useful starting point. Those parameters for which we had field data were modified accordingly. With this preliminary parameter set, we checked to see whether 3-PG could duplicate the highest observed growth increments. Starting biomass of stems and branches (Ws) and foliage (Wf) were based on the results of the first biomass survey at each site. Starting Wr was estimated as being approximately 25% of total tree biomass (Shepherd, 1985). There were strong indications that both NP20b and NP23 had access to the water table. The stands were situated close to a lake, and measurements of pre-dawn xylem pressure potential indicated little water stress during the dry seasons (Table 10). The forest manager confirmed that the local water table commonly approaches to within 2 m of the surface, a depth considered easily within reach of *Eucalyptus* roots. The parameter MAXASW was experimentally increased until a point (1500 mm) where the soil water modifier remained close to one (no water stress) in every month of the year. It was quickly evident that 3-PG could still not simulate the high growth increments, despite both MAXASW and FR being set close to maximum. Simulated foliage mass (Wf) declined over most sites in response to the high rate of litterfall. Changes (kept within a realistic range) were made to two species parameters (Minimum fraction of NPP to roots; Canopy quantum efficiency; see Table 11) to increase above-ground growth, stabilize Wf and

Table 11. A summary of *Eucalyptus gXc* parameter values adopted in the simulations. These are based on default values for *E. globulus*, or on field data measured in this study. Choice of these values is discussed further in Appendix 2.

Standard 3-PG parameter values			
Meaning/comments	**Default**	***E. gXc***	**ID**
Allometric relationships & partitioning			
Foliage:stem partitioning ratio @ D=2 cm	1	1	1
Foliage:stem partitioning ratio @ D=20 cm	0.15	0.15	2
Constant in the stem mass v. diam. relationship	0.095	0.112	3
Power in the stem mass v. diam. relationship	2.4	2.484	4
Maximum fraction of NPP to roots	0.8	0.8	5
Minimum fraction of NPP to roots	0.25	0.2	6
Temperature modifier (fT)			
Minimum temperature for growth	2	5	7
Optimum temperature for growth	20	24	8
Maximum temperature for growth	32	36	9
Frost modifier (fFRost)			
Days production lost per frost day	1	1	10
Litterfall & root turnover			
Maximum litterfall rate	0.03	0.07	11
Litterfall rate at t = 0	0.001	0.001	12
Age at which litterfall rate has median value	24	24	13
Average monthly root turnover rate	0.015	0.015	14
Conductance			
Maximum canopy conductance	0.02	0.03	15
LAI for maximum canopy conductance	3.33	3.33	16
Defines stomatal response to VPD	0.05	0.05	17
Canopy boundary layer conductance	0.2	0.2	18
Fertility effects			
Value of 'm' when FR = 0	0	0.5	19
Value of 'fNutr' when FR = 0	1	0.3	20
Soil water modifier (fSW)			
Moisture ratio deficit for f_θ = 0.5	0.7	0.7	21
Power of moisture ratio deficit	9	9	22
Stem numbers			
Max. stem mass per tree @ 1000 trees/hectare	300	300	23
Age modifier (fAge)			
Maximum stand age used in age modifier	50	50	24
Power of relative age in function for fAge	4	4	25
Relative age to give fAge = 0.5	0.95	0.95	26
Canopy structure and processes			
Specific leaf area at age 0	4	7.6	27

Standard 3-PG parameter values			
Meaning/comments	**Default**	***E. gXc***	**ID**
Allometric relationships & partitioning			
Specific leaf area for mature leaves	4	7.6	28
Age at which specific leaf area = (SLA0+SLA1)/2	2.5	2.5	29
Extinction coefficient for absorption of PAR by canopy	0.5	0.45	30
Age at canopy cover	0	0	31
Proportion of intercepted rainfall evaporated from canopy	0.15	0.04	32
Canopy quantum efficiency	0.055	0.07	33
Branch and bark fraction (fracBB)			
Branch and bark fraction at age 0	0.15	0.3	34
Branch and bark fraction for mature stands	0.15	0.1	35
Age at which fracBB = (fracBB0+fracBB1)/2	1.5	3.5	36
Various			
Ratio NPP/GPP	0.47	0.47	37
Basic density	0.5	0.5	38
Conversion factors			
Intercept of net v. solar radiation relationship	-90	-90	
Slope of net v. solar radiation relationship	0.8	0.8	
Molecular weight of dry matter	24	24	
Conversion of solar radiation to PAR	2.3	2.3	

match the higher growth increments. These modifications were successful, and so this species parameter set was held constant for all subsequent simulations.

We then evaluated what 3-PG site parameter values were required to match the lowest growth increments. Particular attention was again given to maximum available soil moisture capacity (MAXASW) and the fertility rating (FR), which are easily demonstrated to have large effects on simulated growth and ET. Both these parameters are recognized amongst 3-PG modellers as being difficult to quantify. MAXASW may be very hard to estimate from soil pit information. Tree roots often extend deep into sub-soils in which variable proportions of rocks complicate the estimation of water holding capacity. Deep soil/subsoil profiles may also be difficult to excavate. This is particularly so in the loose, deep sandy soils of coastal Zululand.

It is also acknowledged among 3-PG modellers that assigning values of FR to sites remains a subjective process. No satisfactory index relating FR to foliar or soil nutrient status has yet been developed. The problem is once again magnified in sandy Zululand soils, where a very wide range of soil fertility may be encountered (Noble *et al*., 1991), and where nutrients may not be heavily concentrated in the surface horizons of such deep, coarse-textured and well-drained soils.

Both MAXASW and FR were reduced for the sites showing lowest annual growth (A05c; A04c; F05) until a reasonable match with observed data was obtained. Having defined the range of ASM and FR required to simulate the maximum and minimum growth increments, the final parameterization step was to estimate MAXASW and FR for the remaining intermediate sites. We took care to avoid assigning parameter values in a manner that merely produces the best fit to observed growth data. Values of both parameters were varied experimentally, but constrained by having to remain correlated to the observed growth increments at each site. Thus, in the sequence of sites from NP20b to A05c, FR declines consistently from 1.0 to 0.2, while MAXASW declines from 1500 to 150 mm. Table 12 shows the final choice of site and initialisation parameter values, while Figure 17 illustrates the match between simulated and observed growth increment achieved for the 12 sites. Eleven of the sites describe a well-defined trend (R^2 = 0.84) with a slope of 0.85. The 12th site (NP20b) exhibited an extremely high annual growth increment, with Ws exceeding 72 t ha^{-1}. Both diameter (1.9 cm) and height (3.7 m) annual increments are large in comparison to those expected from 7 year-old *E. grandis* trees managed for pulpwood and experiencing high site quality (DBH ~ 0.5 cm; Height ~ 1.8 m; Kassier and Kotze, 2000; Page 189). Herbert (1992) considers *E. grandis* MAI to vary from 4-35 t ha^{-1}. Assuming that MAI is similar to CAI for short-rotation, fast growing eucalypts in Zululand, and taking into account additional biomass due to branches, the maximum Ws is unlikely to exceed 40 t ha^{-1}.

Various explanations were considered. Due to an earlier plan to sample four sub-plots in each stand, the first survey at NP20b was based on 58 sample trees whereas the second survey was based on a larger sample of 78 trees. Both plots shared a common boundary on one side, so that nearly all of the trees measured in the first survey would have been re-measured in the second survey. There was no indication that the additional trees measured in the second survey were larger than the remaining trees. We believe that this altered sample size cannot account for the exceptionally large growth increment recorded at this site. The only conclusion we can draw is that the measured growth increment is real. A possible clue as to why growth rate should be so high comes from some sap flow data recorded at this site. Extremely fast heat pulse velocities were measured on clear days, suggests that xylem vessels may have been of very large diameter, offering low resistance to flow. If this is true, then the greater efficiency of water transport to the leaves is likely to have enhanced stomatal conductance, carbon assimilation and growth rate. Considering that the trees are believed to have easy access to shallow groundwater, that they would have experienced little water stress for most of their life, and that they display the highest site index and leaf area index, this appears to be a plausible hypothesis. In a study of transpiration patterns of *Eucalyptus* species along a steep rainfall gradient in a north Australian savanna, Eamus *et al.* (2000) reported evidence that the intensity of dry season water deficits exert control on tree water use during the wet season, possibly through an effect on xylem structure. Image analysis of sapwood samples from NP20b trees and from trees from other sites with no groundwater access are planned for the near future. The problem of NP20b emphasizes the need for more physiological information from forest stands to bring greater certainty to some of the “hard to measure” physiological parameters. The move towards clonal eucalypts in South Africa has revealed a high degree of physiological variation amongst even the most productive clones (Dye *et al*., 1997b), suggesting that default eucalypt parameter values may be inadequate when applied to selected genotypes.

The simulated monthly rate of transpiration was checked against observed sap flow data to assess their realism. Table 13 shows that highest monthly sap flow (expressed as a mean daily rate over the month) corresponds very well to the median daily sap flows depicted in Figure 14. It is clear, though, that the minimum monthly sap flow rates are nearly all lower than the observed lowest daily sap flow rates. We believe this discrepancy is due to the simple manner in which 3-PG calculates the availability of soil water to tree roots. Roots are considered to be able to completely exhaust available soil water in soil with a fixed water storage capacity. In reality, the availability of soil water is likely to be less clear cut, with the deepest (sinker) roots penetrating below the major water storage zone to tap yet deeper water reserves. Such dimorphic root systems (Jacobs, 1955; Kimber, 1974) have been described for several *Eucalyptus* species (Knight, 1999). Although root densities may be low in the deeper strata, slow rates of uptake are sufficient to keep the tree alive until the higher soil strata are again recharged by rainfall. 3-PG requires improvement in this area. An additional means by which trees are able to access soil water from below the rooting zone during dry periods has recently been described by Soares and Almeida (2001). They describe an upward flux of water from a deep water table towards a 2.5 m deep *E. grandis* rooting zone. This flux was close to 1 mm per day, and prevented the leaf stomata from closing down completely.

Table 14 shows the total yearly sap flow simulated for the 12 sites. The upper range accords with results obtained in a previous study, where continuous sap flow measurements in three clones indicated annual sap flows varying from 900 to 1400 mm (Dye *et al*., 1997b). The lower range of simulated annual sap flow at the Bushlands sites is believed to be unrealistically low, as a result of the likely access of deep soil water reserves during dry periods, as discussed above.

FR was empirically determined to range from 0.2 to 1.0. While we have no direct means of verifying that this range is realistic, we note that in a study of 19 Tasmanian forest plots, Landsberg (2000) found that best predictions of *E. globulus* MAI were obtained when FR was allowed to vary from 0.1 to 0.9 over a full range of site index.

Table 12. A summary of 3-PG site and initialisation parameter values used in the simulation of the 12 sample sites.

	Bushlands (Low rainfall)						Kwambonambi (high rainfall)					
	Low site index			High site index			Low site index			High site index		
Stand age	**early**	**mid**	**late**	**early**	**mid**	**late**	**early**	**mid**	**late**	**early**	**mid**	**late**
Compt No.	**A04c**	**B04**	**F05**	**A10b**	**A05a**	**A05c**	**NP23**	**RG20b**	**NH01**	**NA24b**	**NK25**	**NP20b**
Latitude (deg.)	-28	-28	-28	-28	-28	-28	-28	-28	-28	-28	-28	-28
Fertility rating	0.2	0.9	0.2	0.8	0.9	0.2	0.9	0.9	0.7	0.7	0.9	1.0
Soil class	Sa	Sa	Sa	Sa	Sa	Sa	Sa	Sa	Sa	Sa	Sa	Sa
Maximum ASW (mm)	150	300	150	300	300	150	1500	500	300	300	500	1500
Minimum ASW (mm)	0	0	0	0	0	0	0	0	0	0	0	0
Initial SW	10	150	10	100	150	10	1500	250	60	60	250	1500
Initial year	3	5	7	2	5	6	3	6	7	3	5	7
End year	4	6	8	3	6	7	4	7	8	4	6	8
Wf (t ha^{-1})	3.20	2.78	1.65	3.31	2.98	2.11	3.71	3.03	3.27	2.68	2.21	4.24
Wr (t ha^{-1})	9.26	14.59	18.24	8.66	21.89	22.22	13.35	26.20	32.93	13.08	32.77	37.03
Ws (t ha^{-1})	33.85	55.58	71.32	31.33	84.57	86.79	49.68	101.75	128.43	49.65	128.87	143.88
SPH	1418	1143	1170	1330	1177	1220	1390	1098	1116	1316	1285	1054

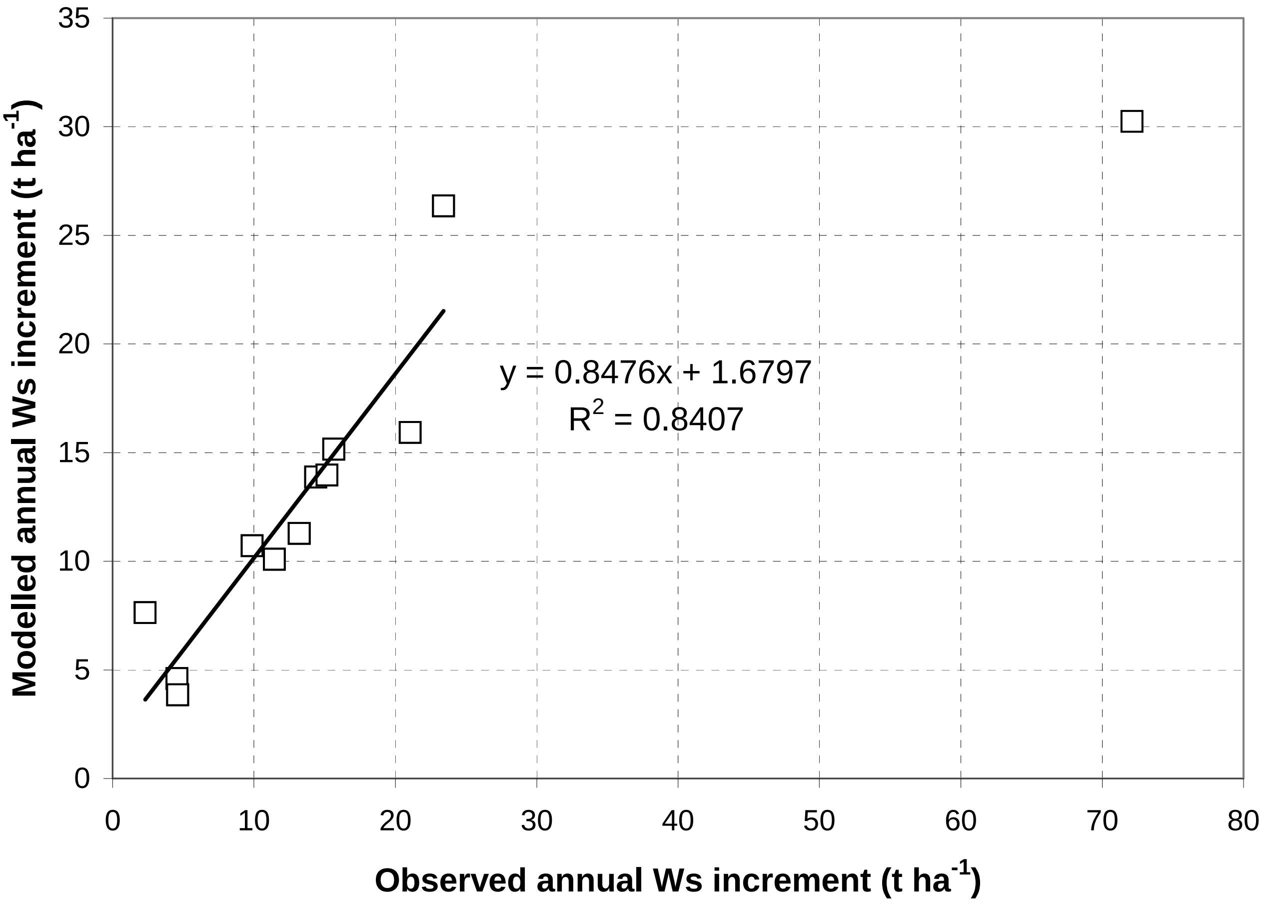

Figure 17. Comparison of simulated and observed annual Ws growth increment for the 12 study sites. The outlier data point was excluded from the regression analysis.

Table 13. Simulated monthly sap flow (expressed as a mean daily sap flow (litres day^{-1}) in each month) for six of the sample sites.

	A04c	B04	F05	NP23	NP20b	NK25
Jul	2.7	24.2	1.5	18.1	25.4	13.0
Aug	15.9	25.9	14.4	29.0	37.8	20.5
Sep	19.6	25.5	5.8	27.6	35.1	20.2
Oct	1.9	3.9	2.3	32.1	40.8	24.4
Nov	1.4	2.5	4.0	35.7	45.5	27.7
Dec	2.9	3.3	6.3	32.7	41.6	24.6
Jan	5.7	5.3	9.2	37.2	47.4	9.6
Feb	0.7	1.3	7.8	34.6	44.0	5.9
Mar	11.2	6.7	12.1	19.6	25.0	1.9
Apr	15.5	20.9	11.9	18.5	23.6	7.8
May	16.5	23.5	9.3	27.0	34.3	17.8
Jun	12.3	18.9	11.9	26.8	34.1	18.7
Max	**19.6**	**25.9**	**14.4**	**37.2**	**47.4**	**27.7**
Min	**0.7**	**1.3**	**2.3**	**18.1**	**23.6**	**1.9**

Table 14. Simulated annual sap flow (mm) at each of the 12 sites.

	Bushlands (Low rainfall)						Kwambonambi (high rainfall)					
	Low site index			High site index			Low site index			High site index		
Stand age	**early**	**mid**	**late**	**early**	**mid**	**late**	**early**	**mid**	**late**	**early**	**mid**	**late**
Compt No.	**A04c**	**B04**	**F05**	**A10b**	**A05a**	**A05c**	**NP23**	**RG20b**	**NH01**	**NA24b**	**NK25**	**NP20b**
Annual sap flow (mm)	450	555	339	553	552	335	1412	777	601	608	740	1423

The parameter estimation strategy described above is considered to be a practical one to follow at this early stage in our understanding and experience of 3-PG. A typical forestry estate includes a large number of forest compartments differing in species, tree age and site conditions. It would be impractical to attempt to define for each compartment such parameters as MAXASW and FR on the basis of field measurements. We suggest that a three-step procedure should be followed in parameterizing multi-compartment forestry estates.

- Follow the procedure adopted in this study to quickly obtain an initial parameter set for every compartment.
- Test model parameters against available whole-rotation growth and yield data. Growth trends over a number of years are a better test of model realism than one-year growth increments. Whole-rotation data are not always available, since species or clones are sometimes changed between one rotation and the next. A representative subset of compartments may still offer useful scope for testing and fine-tuning parameter values.
- Finally, apply the model operationally to predict current monthly growth and ET. This allows one the opportunity to take physiological measurements at significant times of the year. For instance, if the model predicts that a number of compartments are beginning to experience significant soil water deficits, this can be checked, both in the compartments concerned and a control group of “unstressed” compartments, by measuring pre-dawn XPP, or obtaining remote sensing imagery portraying spatial patterns of canopy temperature. This is the best means of fine-tuning parameter values and evaluating model realism.

5. REVIEW OF THE POTENTIAL USE OF SATELLITE REMOTE SENSING DATA FOR CHARACTERISING FORESTS

As mentioned in the review of literature and 3-PG software, two model versions of 3-PG were developed to take advantage of the availability of satellite remote sensing (RS) data, as well as other spatial data commonly available for GIS analyses. In circumstances where a wide variety of different forest stands is to be simulated, such spatial data have the potential to greatly increase the efficiency of the simulation.

Assessing the potential usefulness of satellite remote sensing data in 3-PG simulations of forest plantations was a key objective of this study. This chapter reviews some recent remote sensing literature as a means of assessing the potential and limitations of using RS data to characterise vegetation (with emphasis on forests).

5.1 Sources of satellite remote sensing data and their spatial resolution

The most commonly used satellite sensors for vegetation studies in South Africa are LANDSAT, SPOT and NOAA AVHRR. All three of the satellite systems are supported by the regular launch of new satellites that ensures updated technology and continuity of earth coverage over time. The last decade has seen particularly rapid increases in the number of launched satellites, as well as improvement in resolution and increases in the sensed bands. The planned launch of several new satellites will implement further improvements in the quality of RS data.

Various levels of spatial resolution have been useful in tracking spatial and temporal changes in vegetation. In South Africa, low-resolution satellite imagery (1000 m) obtained from the NOAA AVHRR sensor is available from the Agricultural Research Council. NOAA imagery received from the Satellite Applications Centre is regularly modified and analysed to calculate monthly NDVIs for South Africa.

Medium resolution imagery is available from NASA through the MODIS sensor on the TERRA satellite. The resolution is 250 m and several bands are available, covering the visible, infrared and thermal parts of the spectrum. These data are available free of charge from the MODIS website (http://www.modis.gcsf.gov), but does not yet cover a full year. In addition, there are a number of problems related to downloading the data. However, it is expected that once these data are readily available, they will prove to be an invaluable resource, permitting medium-resolution modelling of forest ecosystems.

LANDSAT imagery has been the mainstay for a large number of RS-based vegetation studies. The 30 m resolution, relative non-specificity of the bands and relatively low cost are especially suited to ecosystem-level monitoring and modelling, and many successful studies of this nature have been reported.

In the last two years, further high-resolution imagery has become commercially availably through the launch of satellites such as IKONOS, EROS and QUICKBIRD. The panchromatic bands on these satellites vary from 0.6 to 2 m and the multispectral bands for 1 to 4 m. Typical applications vary from town planning to disaster monitoring. The future use of these satellites or other similar satellites for vegetation studies is a possibility, although the price for imagery is prohibitively expensive at this time. Table 15 summarises resolution, pass-over frequency, imagery price and typical uses associated with the major satellite systems.

For research on global change in carbon and water cycles, and studying land surface-climate interactions, spatial resolution of up to 1000 m (low resolution) is sufficient. Many examples exist that illustrate the successful use of low resolution instruments like NOAA AVHRR data for monitoring vegetation change (Senay and Elliot, 2000) and modelling global change using various dynamic models (Coops *et al*., 1998; Birky, 2001; Coops *et al*., 2001). However, for developing and implementing plantation growth and water use models using remote sensing as inputs, medium-resolution satellite imagery is needed (Coops *et al*. 1997) to cope with the mix of species, age classes and structural diversity typically found on forestry estates. The price for LANDSAT imagery increased significantly following the increase in R/$ exchange rates at the end of 2001, making continued use of LANDSAT imagery as a tool for routine monitoring and modelling of ecosystems questionable, at least in the short term.

Table 15. Information on satellite sensors available for use in vegetation monitoring, in order of increasing spatial resolution.

Satellite	Resolution	Availability/ Price	Use
NOAA AVHRR	1000 m	NDVI data for SA obtainable at minimal service fee	Ecological modelling/Vegetation monitoring/Ocean monitoring
SPOT Vegetation	1000 m	Available for purchase; imagery older than 3 months available free from the internet	Ecological modelling/Vegetation monitoring/
MODIS	250 m	Free from the Internet	Ecological modelling/Vegetation monitoring
LANDSAT	30 m	R0.74/ha (LANDSAT 5; 1997 price) R1.14/ha (LANDSAT 5; 2002 price#)	Ecological modelling/Vegetation monitoring
SPOT	20 m	R1.45/ha	Ecological modelling/Vegetation monitoring
IKONOS	1.0 m panchromatic	Upwards of R20/ha, depending on specifications	Town/regional planning

- # LANDSAT imagery increased considerably following an increase in the R/$ exchange rate at the end of 2001.

5.2 Land use categorisation and forest species discrimination

Numerous examples are reported in the literature of the use of satellite remote sensing data to determine areas under various land cover categories. Thompson (1997) successfully used LANDSAT TM imagery to determine land use classification across the whole of South Africa, and was able to discriminate between *Eucalyptus*, pine and wattle plantations.

It is possible to use medium to low resolution satellite sensors, such as SPOT, LANDSAT TM and LANDSAT MSS, for broad scale discrimination of vegetation types, such as coniferous versus broadleaved forests (Lillesand and Kiefer, 1994). In a number of other studies, attempts have been made to use such satellite data to identify forests to the species level, with varying degrees of success (Lillesand and Kiefer, 1985). Most success has been obtained with airborne sensors, especially with the introduction of hyperspectral instruments with high resolution (Martin *et al*. 1998). Martin *et al*. (1998) used an airborne method to distinguish between different species in a mixed species forest in the eastern United States. The high spectral resolution of the new generation of multispectral instruments allows one to use a number of full spectrum analyses techniques (Martin *et al*. 1998). These authors used the AVIRIS instrument to identify species by using the difference in foliar chemistry (lignin, N) between the species as criteria. In other studies, digital videography (airborne) has been used successfully to discriminate vegetation into broad classes, for instance for habitat identification (Coops and Catling, 1997) and by species (Everitt *et al*. 1986).

Locally, Rowlinson *et al.* (1999) used various forms of remote sensing data to identify alien vegetation in riparian zones, using visual identification techniques based upon differences in roughness. LANDSAT TM imagery was only partly successful in identifying the alien vegetation, but was the most cost-effective. Videography proved to be the most successful, but was also the most expensive source of data.

5.3 Forest structural attributes

5.3.1 Canopy attributes

Much work has centred on seeking correlations between various plant canopy attributes and a variety of vegetation indices. A vegetation index is defined as a mathematical combination of channels or bands that indicates the presence or condition of green vegetation (Lillesand and Kiefer, 1994). The most commonly used vegetation indices utilize the information contained in red and near infrared reflectances; either as differences, or as ratios (Teillet *et al*. 1997; Baret and Guyot, 1991). Vegetation indices are routinely used to determine green biomass, green leaf area, LAI, standing biomass, percent ground cover, amount of photosynthetically active vegetation, photosynthesis activity and productivity (Baret and Guyot, 1991).

The simplest vegetation index is called “vegetation index” (VI) and is calculated as follows:

$$VI = \alpha_{nir} - \alpha_{red} \tag{7}$$

where α_{nir} and α_{red} are surface reflectances of the near infrared band and the red band (Lillesand and Kiefer, 1994). The most commonly used vegetation index used in ecological research on forest ecosystems is the normalized difference vegetation index (NDVI) (Goward *et al*. 1985; Huete *et al*. 1997; Teillet *et al*. 1997; Coops and Waring, 2001c). NDVI takes into account red and near infrared reflectance and is defined as:

$$NDVI = \frac{\alpha_{nir} - \alpha_{red}}{\alpha_{nir} + \alpha_{red}} \tag{8}$$

where α_{nir} and α_{red} are surface reflectances of the near infrared band and the red band, respectively (Baret and Guyot, 1991). This index has been used extensively and shows a linear or near linear relationship between NDVI and the amount of photosynthetically active radiation absorbed by the vegetation (Coops and Waring, 2001c). Absorbed PAR (fPAR in Figure 2) is an important input parameter in 3-PG. Despite the longstanding use of this vegetation index in vegetation studies, the theoretical basis of the relationship between NDVI and canopy properties has not yet been fully explained (Coops and Waring, 2001c). In spite of this lack of clarity, many examples are available of where NDVI has proven useful in monitoring changes in temporal and spatial dynamics in natural vegetation (Coops *et al*. 1995; Coops *et al*. 1998; Senay and Elliot, 2000).

The use of NDVI has been criticized, based on the following points (Carlson and Ripley, 1997):

- Interference from the atmosphere – there may be differences between the NDVI measured at the ground level and that measured from space due to interference from atmospheric aerosols.
- The problem of saturation of the relationship between NDVI and LAI above a threshold LAI of 2-3.
- Interference from the soil – reflectance from the soil could interfere with NDVI values from one image to the next.

The interference of aerosols in application of multi-temporal imagery to change detection is of particular concern. If atmospheric conditions differ among the images, a form of atmospheric correction may be necessary. Song *et al*. (2001) suggested several atmospheric correction algorithms developed specifically for LANDSAT TM, all of which improved data analysis. As an alternative, vegetation indices that account for the influence of aerosols have been developed, such as AFRI (Karnieli *et al*. 2001). Under clear conditions, AFRI produced values that were almost identical to that of NDVI. Under the presence of smoke or other aerosols, AFRI have the ability to penetrate the layer of aerosol. The measurements for determining this vegetation index, however, are based on field spectrometer measurements mounted on an aerial platform and are, as such, not readily accessible.

The phenomenon of saturation of NDVI above a certain LAI (2-4) is well known, but is not restricted to NDVI (Baret and Guyot, 1991). It is also the case with the perpendicular vegetation index (PVI) and the transformed soil vegetation index (TSAVI), and in all cases the relationship can be fitted to an exponential equation. The last two vegetation indices were developed to take account the interference of soil.

It has been found that NDVI is influenced by soil brightness (Baret and Guyot, 1991), a problem that is especially prevalent when LAI is low. TSAVI, SAVI and PVI have been found to strongly reduce the noise inherent in reflectance of low LAI (<2-3) areas (Baret and Guyot, 1991). SAVI derived from NDVI, with the introduction of a correction factor, while TSAVI introduces angles within the red and near infrared reflectance relationship. Various versions of SAVI have been developed, differing slightly depending on the effects of wet and dry soils (Major *et al*. 1990; Baret and Guyot, 1991). All showed improved reduction of background soil-brightness effects.

In addition, fractional vegetation cover and LAI may not be totally independent, which may influence the relationship between LAI and NDVI determined from space (Carlson and Ripley, 1997). In order to account for these criticisms, several authors have suggested and tested alternative vegetation indices, or attempted to improve NDVI by introducing correction factors (Carlson and Ripley, 1997).

Nemani *et al.* (1993) developed a modified NDVI, which uses mid-IR in addition to the near-IR and Red. This vegetation index was developed to increase the small range in LAI where NDVI is effective. It takes the form:

$$NDVI_C = \frac{\alpha_{nir} - \alpha_{red}}{\alpha_{nir} + \alpha_{red}} * \left(1 - \frac{\alpha_{mir} - \alpha_{mir\,\min}}{\alpha_{mir\,\max} - \alpha_{mir\,\min}}\right) \quad (9)$$

where α_{nir} and α_{red} are surface reflectances of the near infrared band and the red band, respectively. α_{mir} represents the mid-IR band, while α_{mirmin} and α_{mirmax} represent the mid-IR digital numbers from completely open and completely closed canopy (Nemani *et al*. 1993). It was found that NDVIc improved the relationship between NDVI and LAI by changing the regression relationship and the slope of the relationship. This relationship resulted from the correction of outsized NDVI values obtained under open canopies (Nemani *et al*. 1993; Lucas *et al*. 2000).

Tree structural information can also be obtained from hyperspectral instruments. Lucas *et al*. (2000) suggested that a combination of red and near-IR reflectances in narrow bandwidths can be used to obtain LAI to an accuracy of 0.94%.

The close relationship between LAI and NDVI has been shown for several forest ecosystems (Baret and Guyot, 1991; Fassnacht *et al*., 1997; Coops *et al*., 1998). The temporal variation in NDVI presumably reflects the changes in LAI over time. Both seasonal (Coops *et al*. 1995) and longer-term changes (Senay and Elliot, 2000) have been found.

Limburner *et al.* (2000) investigated the use of LANDSAT imagery to determine specific leaf area (SLA) in a mixed species tropical forest using various vegetation indices. Specific leaf area is directly correlated with net photosynthesis, LAI, aboveground NPP, leaf nitrogen content and leaf water content, showing the importance of this variable in ecological function. Red, near Infrared and mid infrared reflectances showed good correlation with SLA. Thus SARVI2, NDVI and RVI also showed good correlations with SLA.

The close relationship between fPAR, LAI and the Normalized Difference Vegetation Index (NDVI) has been shown for several forest ecosystems, both theoretically and empirically (Baret and Guyot, 1991; Fassnacht *et al*., 1997; Coops *et al*., 1998). The relationship allows for the direct estimation of fPAR from satellite imagery. Remote sensing can also be used to estimate the foliage biomass of the standing crop at various stages in the simulation, or merely to categorise land uses in the way it is used in Pnet and BIOME-BGC.

5.3.2 Tree height, diameter at breast height and volume

There are various examples of forest inventory techniques based on LANDSAT or SPOT remote sensing data (Cohen and Spies, 1992; Coops *et al*. 1999a`; Lefsky *et al*. 2001) and in combination with additional data sources (Poso *et al*. 1999). This technique has been used successfully in Finland and Germany for forest inventory purposes of large areas of natural forest (Katch and Vogt, 1999). These authors quote Finish results that reflect insignificant differences between forest inventory data obtained with LANDSAT and that from ground-truthing, while in Germany, accuracies of 96-99% for timber volume from satellite have been obtained in natural forest stands (Katch and Vogt, 1999). Intuitively, the spatial resolution of 20 m and 30 m for SPOT and LANDSAT respectively seems too coarse for getting information that would satisfy statistical error ranges for stand level information in commercial plantation forestry. In addition, Hunsacker *et al*. (1998) revealed that information on forest structure could be obtained from SPOT, but not LANDSAT images, citing the difference in resolution as the main problem. Generally low R-squared values were obtained, but when LANDSAT data were integrated with ancillary GIS data, an R^2 of 0.8 was obtained in some cases. The difference in results obtained with the latter study as opposed to that obtained in Finland and Germany probably relates to the level of accuracy and the spatial resolution required. A factor that influences the relationship with tree and stand characteristics is the time of the year that the image is taken. Another obvious limitation of satellite imagery is the availability of cloud-free imagery.

A novel method for obtaining tree heights was employed by Puhr and Donoghue (2000), who found an R^2 value of 0.77 between the combination of LANDSAT TM bands 1, 3 and 5, and tree height of upland conifer plantations in Britain. This relationship was, however, indirect, since the bands picked up the reflectance from the understory more than that from the trees themselves. The relationship was negative and non-linear, suggesting that tree canopy development played a role. This meant that the relationship only held for stands with an open canopy, and is probably dependant on uniform understory and the same type of understory across the whole of the area studied. This means that this technique is probably not suited to South African conditions, where active weed control is practiced and weed species are not uniformly distributed through stands and plantations. This technique may, however, be useful from the point of view of determining the progress of weeding as a management activity.

Good results have been obtained when multi-temporal LANDSAT images have been used (Lefsky *et al*. 2001). These authors used an image consisting of a layered stack of six images of the same scene from different months regressed against tree parameters (height, basal area, crown diameter). Results obtained were generally better than that of single date LANDSAT TM scenes. The authors suggest that this technique of combining images to reduce seasonal variability may have application in the northern hemisphere forests where previously only single data LANDSAT imagery was used for forest inventory purposes.

The availability of the new generation of high-resolution satellites, such as IKONOS, EROS and Quickbird, with a resolution of between 1 and 4 m opens the door to using these satellites for forest inventory at higher resolution. IKONOS has a panchromatic resolution of 1 m, and a multispectral resolution of 4 m. The extraction of tree structural attributes is dependant on a combination of different bands and it is thus the multispectral sensor that is of interest. While none of these satellites have yet been used for this purpose, theoretically, it should be possible to use them in the same way as LANDSAT and SPOT for obtaining tree heights, basal areas, stand density and stand areas. Currently, imagery is extremely expensive (IKONOS), but it is expected that the cost may drop with the introduction of yet newer satellites such as EROS (available locally from September 2001) and Quickbird (launched in 2001). EROS, LANDSAT and SPOT imagery is archived and distributed by the Satellite Applications Centre (SAC) in Pretoria, while IKONOS can be ordered through SAC, but is not archived in South Africa.

5.4 Vegetation health

5.4.1 Foliage chemistry

Determining foliage nutrient status and chemical composition is essential for understanding the factors limiting growth of forest stands (Martin and Aber, 1997), and is therefore relevant to models of forest growth. However, it is also one of the more difficult and time-consuming measurements to take, due mainly to the spatial heterogeneity (vertically and on a landscape basis) in forest plantations. The importance of foliar nutrient status, especially N, in forest functioning has been highlighted by Martin and Aber (1997). N status is directly associated with photosynthetic capacity of the foliage (Field and Mooney, 1986). As such, it is also related to water use of forests, although the relationships are more equivocal than those between N and photosynthesis rate. Prediction of foliage nutrient status using remote sensing would increase measurement efficiency considerably.

Several attempts are ongoing to predict foliage nutrient status, in particular N, using remote sensing data. The basis of the technique has been developed by among others, Aber *et al.* (1995), Aber and Federer (1992), Matson *et al*. (1994), Martin and Aber (1997) and Kokaly and Clark (1999). Kokaly and Clark (1999) discuss many of the potential pitfalls of using remote sensing to determine and predict foliar nutrient and chemical content, but come to the conclusion that it will be possible to use remote sensing for this purpose. Both airborne and lately, satellite-based sensors, have been employed. However, because of the requirement for narrow bands (characteristic of hyperspectral instruments), the well known multispectral satellites, such as SPOT and LANDSAT cannot be used successfully for the determination of foliar chemistry and nutritional content.

The aforementioned studies clearly demonstrate the potential usefulness of remote sensing data for estimating foliar chemistry (N, lignin, starch). The airborne sensor AVIRIS (Airborne Visible/Infrared Imaging Spectrometer) has a long history of use to determine foliage N. Martin and Aber (1997) showed that with appropriate calibration equations N and lignin in mixed coniferous and deciduous forests could be predicted to a useful accuracy (r^2 = 0.87 and 0.77, respectively). The calibration equations were then used to predict N levels across study areas for input into a spatially explicit ecosystem model (PnET; Aber and Federer, 1992). The model has been developed as a point model, but has been modified to use spatially explicit data especially for this exercise (Martin and Aber, 1997). Although validation of the model prediction has to date not been carried out, the results obtained demonstrate the potential for using spatially explicit, remotely sensed estimates of N and lignin as inputs into spatial models of forest growth and functioning.

The EO-1 satellite, launched in 2001, carries the experimental sensor Hyperion (Hyperion website, 2002). It is essentially a hyperspectral sensor with much the same spectral characteristics as AVIRIS. However, due to the general robustness of airborne sensors in terms of footprint and resolution, and the relatively low resolution of Hyperion (30 m), the spatial characteristics of the latter sensor are not as high as that of AVIRIS. Despite this disadvantage, it is still expected that Hyperion will be able to provide invaluable information on the chemical composition of foliage in forests. The temporal regularity of the satellite overpasses (1-2 times a day) is especially useful from the point of view of temporal changes in nutrient and chemical dynamics and thus functioning of ecosystems.

No serious development is underway to determine techniques and methodologies for determining other nutrients (P, Ca, S, K and micronutrients) and chemical components (cellulose etc,). In many cases technological barriers prevents to development of appropriate technologies.

5.4.2 Vegetation stress

Measuring vegetation stress has been of particular interest to forest and remote sensing scientists, particularly due to the immediate effect that stress has on the functioning and growth of trees. Vegetation stress can be the result of a number of factors, most notably lack of soil water, nutrient imbalances and deficiencies, and insect damage. Water stress is especially prevalent in South Africa and its recognition in remote sensing imagery is of particular interest to the South African forest industry.

Vegetation stress is defined as any disturbance that adversely influences growth (Jackson, 1986). Water stress is defined in its simplest form as not enough water to the plants, or a water potential that is too negative (Salisbury and Ross, 1985). Numerous studies have been conducted to determine the onset and progression of water stress in plants using remote sensing (Jackson, 1986; Danson *et al*., 1992; Moran *et al*., 1994; Ustin *et al*., 1998). The techniques used are based on (a) the visible to shortwave infrared bands (SWIR), (b) thermal infrared and (c) radar (Ceccato *et al*. 2001). The three techniques measure different manifestations of stress. The SWIR technique provides information on vegetation biophysical parameters such as the chlorophyll content, leaf area index and the vegetation water content. The thermal infrared technique uses the premise that the thermal signature of plant material changes as the rate of evapotranspiration changes. As the latent heat component of the energy balance declines with closing stomata and reduced evaporation, sensible heat increases, causing the plant canopy to warm. Radar provides information on the dielectric constant, which could be related to vegetation water content. It is clear that each technique measures different aspects of the manifestation of water stress in plants, as well as different stages in the progression of water stress in plants. The ideal is to detect water stress at a stage where visible signs are not yet present.

A number of studies have been aimed at characterizing the relationship between vegetation indices and vegetation moisture content, with marginal degrees of success (Ceccato *et al*. 2001). Others assumed proportionality between chlorophyll content and the moisture content of foliage. A moderate degree of success has been noted with this technique, depending on the species involved (Ceccato *et al*. 2001). This is because the relationship can be influenced by various factors (e.g. phenological status of the plant, nutrient deficiency, plant disease) causing a divergence between chlorophyll content and water content. Changes in water content are therefore not directly related to the chlorophyll concentration for all types of vegetation. Low and medium resolution satellite data do not effectively discriminate between different vegetation types (mixed pixels), and are thus not effective in determining the water content of a given type of vegetation. It is clear that indicators of water content must be independent of species, and preferably related to absolute water content. It is clear that indirect measurement of water content using remote sensing methods is problematic. Ceccato *et al*. (2001) investigated various aspects of direct measurement of water content and conclude that water content (represented by Equivalent Water Thickness) can be extracted using leaf reflectance. They recommend that a combination of SWIR and near infrared reflectances be used to extract information on water content from remote sensing.

Thermal remote sensing has been used infrequently in studies to determine the extent of water stress in vegetation. The thermal band aboard LANDSAT 5 has a resolution of 120 m (LANDSAT 5 website, 2001), which makes its use in forestry and agricultural application questionable. It passes over South Africa during night-time, making georeferencing virtually impossible. It also passes over South Africa again during mid morning, when background reflection from the ground makes discrimination of the reflectance patterns from the vegetation relatively difficult. Thus, while theoretically the thermal band could be useful from the point of view of detecting changes in temperature due to water stress, the low resolution and overpass times inhibit the use of this band for this purpose. Thermal remote sensing using airborne systems has much greater potential, due to greater flexibility in timing flights, as well as improved resolution.

5.5 Evapotranspiration

Actual evaporation is a critical parameter in determining regional water balance. This has been determined as a residual from water balance equations, from estimation of potential evaporation, and from field measurements using meteorological equipment. The increasing accessibility of remote sensing data has seen its application in determining actual evaporation (Bastiaanssen *et al*., 1999; Granger, 2000).

Kite and Droogers (2000) compared eight different methods for determining evaporation and transpiration. These included using field measurement, hydrological models and remote sensing techniques. They found that some of the remote sensing techniques used were relatively successful, provided that high resolution LANDSAT data is used rather than AVHRR. However, data availability proved to be a problem.

5.6 Soil moisture

A number of attempts have been made to gauge soil moisture content using remote sensing. These have been hampered by technological barriers such as the impenetrability of soil, interference from the vegetation, and interference from the atmosphere. Until recently, the only remote sensing technology that has been partially successful in gaining information remotely is radar. However, the radar is only successful in measuring soil moisture within the first few centimetres of soil, and thus cannot describe the soil moisture content of deeper soil layers commonly within the vegetation rooting zones.

McVicar and Jupp (2002) reported a novel method for determining moisture availability in the Murray-Darling basin in SE Australia using remote sensing and meteorological data. They combined AVHRR and meteorological data to determine the Normalized Difference Temperature Index (NDTI). They found that surface temperature minus air temperature, percentage vegetation cover (from the AVHRR data) and net radiation explained 85% of the variation in the NDTI, and that these three covariates can thus be used to estimate NDTI spatially, using a network of meteorological stations. NDTI is then used to calculate changes in moisture availability, using per-pixel variation in the AVHRR data to spatially interpolate the moisture availability. This method is exceptional for its independence from spatial interpolation of rainfall to determine regional water balance dynamics and for its use of remote sensing data to determine only vegetation cover rather than attempting to determine water availability through vegetation indices (i.e. energy balance methods).

With the advent of hyperspectral instruments, the measurement of soil moisture became possible through airborne remote sensing. Coops *et al*. (1998) used the Compact Airborne Spectrographic Imager (CASI) in eucalypt forests in south-eastern Australia, and were able to identify a relationship between one CASI channel and soil moisture to a few centimetres below the soil surface.

5.7 Image quality considerations

From time to time, imagery required for a particular date and area may be unavailable or of inferior quality. This can arise because of unexpected deterioration in the quality of the signal received, such as occurred with NOAA 7. Unexpected problems may also arise following the launch of new satellites such as LANDSAT 7. The receiving station at SAC has not been able to archive any imagery since inception. Image quality is more commonly compromised by factors unrelated to technology, such as interference from clouds or aerosols.

5.7.1 Clouds

The presence of significant cloud for a particular location and time may render imagery useless (Cahalan *et al*., 2001). This is a perpetual problem during periods of rainfall, which in most cases coincides with the season of active growth of vegetation. An image does not need to be completely cloudless in order to be of value. If clouds are confined to areas not coinciding with the area of interest, it may be possible to exclude the overcast area from calculations. It may also be possible to interpolate if a time series of imagery is used. However, the presence of scattered clouds over most of the image renders that image useless, especially if it needs to be transformed, for example in the calculation of NDVI. It is not only the area obscured by clouds that is affected; shadows produced by clouds can render large areas useless for image analysis purposes (Cahalan *et al.,* 2001). This is due to the changes in reflectance that are produced when a cloud shadow is cast over the earth; shadows reflect little light (Lillesand and Kiefer, 1994).

5.7.2 Aerosols

When comparing and using satellite imagery from different dates in terms of digital numbers, it is necessary to correct for differences in atmospheric conditions. Several options are available for correcting raw images for atmospheric effects. Vegetation indices such as AFRI (Karnieli *et al*. 2001) have been developed to take account of the atmospheric effect such as haze and smoke, while also correcting for soil influences.

Another method has been suggested by Chavez (1988). Here the effect of atmospheric scattering is suppressed by using a dark object subtraction technique. The images were normalized by comparing the mean pixel values (mean radiance) for seemingly unchanging objects (e.g. deep water and sand) across images.

For airborne remote sensing measurements, Running *et al*. (1986) suggested a simple procedure where a radiometer below the clouds (100 m above the target site) was used to correct the images produced with an aircraft-mounted thematic mapper similar in spectral and radiometric characteristics to the thematic mapper aboard LANDSAT 5. Atmospheric correction increased the slope of the LAI: vegetation index regression, thus improving the sensor sensitivity to LAI.

5.7.3 Shadows

Shadows influence image interpretation in both negative and positive ways (Lillesand and Kiefer, 1994). Shadows reflect little light; hence little information can be gleaned on the vegetation in the affected area. However, the shape and dimensions of shadows can impart some information on the shape and dimensions of objects such as trees and topographical features.

6. THE APPLICATION OF SPATIAL VERSIONS OF 3-PG

6.1 Can RS vegetation indices predict stand LAI?

3-PG SPATIAL permits the use of remotely sensed data to predict the LAI of forest stands on a given image. The strength of the relationship between four RS vegetation indices (VI) and measured LAI was investigated by Mthembu (2001) during this project. Landsat 7 imagery was acquired from the Satellite Application Centre (SAC). The data were recorded on the 17 September 2000 between 12:00 and 13:00 hours GMT at a flying height of 1000000 m above ground level across a swath width of 1000000 m. The 17 September 2000 was the closest day of the satellite pass to the first assessment of LAI and tree leaf areas at the start of the 12-month monitoring period. The other satellite passes before or after this period of field work coincided with cloud cover, thus potentially introducing an error to the analysis. A total of 100 flight lines provided full coverage of the study area. The flight lines were in a north-south direction and timed as close as possible to midday to minimize the effect of canopy shadow. The imagery was geometrically, radiometrically and atmospherically corrected. The images were co-registered with a digital terrain model by the SAC.

The Landsat 7 bands used in this project were the red, near-infrared and mid-infrared bands. These are the most useful for vegetation discrimination and VI calculations. In the ERDAS Imagine Software, these bands are allocated to numerical bands and the colours red, green and blue assigned to them. The red band normally represents number 1 (red), NIR by 2 (green) and MIR by 3 (blue). This combination generally shows the greatest differences among plantation species, different tree ages and different levels of plant stress. The remotely sensed imagery was interpreted using unsupervised, semi-supervised and supervised classification techniques in ERDAS-Imagine (Image processing package). This step produced areas under afforestation for the effective VI determination. The imagery was further manipulated through different vegetation indices, to produce a spatial map depicting LAI values throughout the study sites. Four vegetation indices were calculated (NDVI, NDVIc, RVI and NRVI. NDVI and NDVIc are defined by equations 8 and 9, respectively. The RVI is based on the ratio of red to near infrared reflectances (Richardson and Wiegand, 1977) while the NRVI is a modification of the RVI by Baret and Guyot (1991) and defined as:

$$NRVI = RVI-1/RVI+1 \quad (10)$$

Table 16 shows for each site the calculated numeric values for each of the vegetation indices, together with the two ground-based estimates of LAI. Table 17 summarises the correlations among vegetation indices and LAI estimates, while table 18 describes regression statistics.

Table 16. Calculated numeric values for each of the vegetation indices, together with two ground-based estimates of LAI.

Study area	Site	Age (years)	NDVI	NDVIc	NRVI	RVI	LAI Destructive Sampling	LAI-2000
Bushlands	A05C	7	187	137	219	7	2.45	2.95
	F05	6	121	159	219	8	2.9	3.12
	B04	5	199	138	224	7	1.08	1.85
	A05A	5	216	169	227	7	1.64	2.35
	A04C	3	213	153	224	7	1.11	1.68
	A10B	2.5	220	176	232	10	1.2	1.68
Kwambonambi	NP20B	7	170	148	230	5	2.63	2.78
	NH01	7	187	145	227	8	2.24	2.42
	RG20B	6	171	126	219	7	1.81	1.98
	NK25	5	202	164	232	10	1.58	1.88
	NP23	3	111	152	213	10	2.52	2.85
	NA24B	3	203	152	227	8	1.82	1.99

Table 17. Correlations (r) among four vegetation indices and two estimates of LAI calculated for data from all 12 Kwambonambi and Bushlands stands.

	NDVI	NDVIC	NRVI	RVI	Destructive sampling	LiCor-2000
NDVI	1					
NDVIC	0.24	1				
NRVI	0.73	0.504	1			
RVI	-0.107	0.504	-0.002	1		
Destructive sampling	-0.783	-0.189	-0.442	-0.147	1	
LiCor-2000	-0.745	-0.146	-0.520	-0.199	0.942	1

Table 18. Linear regression equations relating vegetation indices at all 12 sites to LAI estimates based on destructive sampling.

Vegetation index	Constant	Coefficient	Significance	R^2	Sample size (n)
NDVI	4.45	-0.0139	0.003*	0.61	12
NDVIc	3.179	-0.00834	0.556*	0.039	12
NRVI	12.395	-0.0467	0.151*	0.195	12
RVI	2.388	-0.0604	0.647*	0.022	12

Note: * indicates significance at 5% confidence level

The graphic model creator allows the user to place images, functions, tables, links etc. on the Model Maker page using the Tool Palette. To produce an image of best estimates of LAI values, the NDVI- LAI regression equation was entered into MODEL MAKER in ERDAS Imagine using the NDVI image (Figures 18 and 19) as an input into the model. This image was then converted to a GRID in ArcInfo and then displayed in ArcView by classifying the LAI values into predetermined classes. Values below 2 and greater than 5 were excluded as these are beyond the range of the data from the test sites.

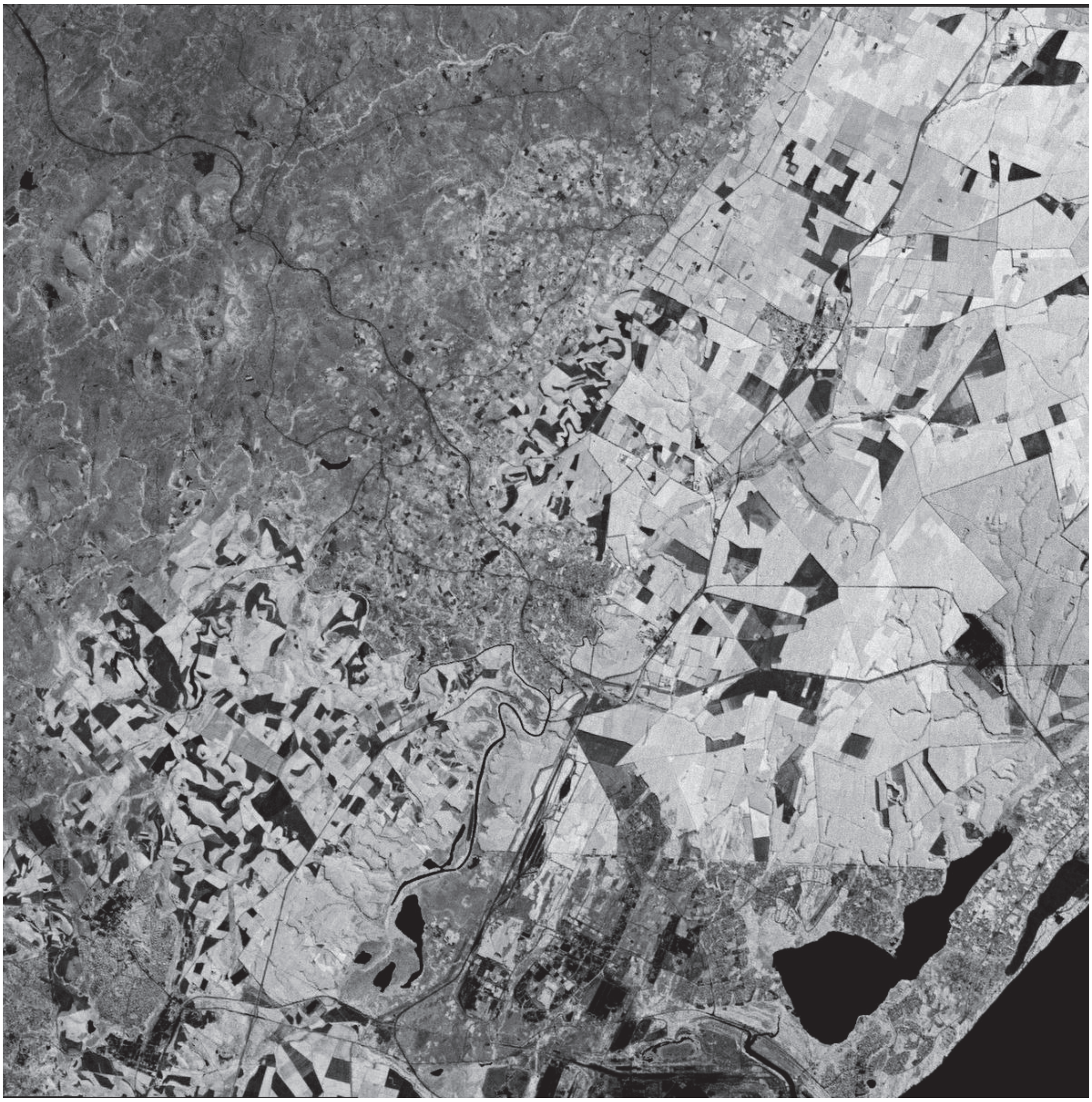

Figure 18. NDVI image of the LANDSAT data of the Kwambonambi district. The lighter areas indicate high NDVI.

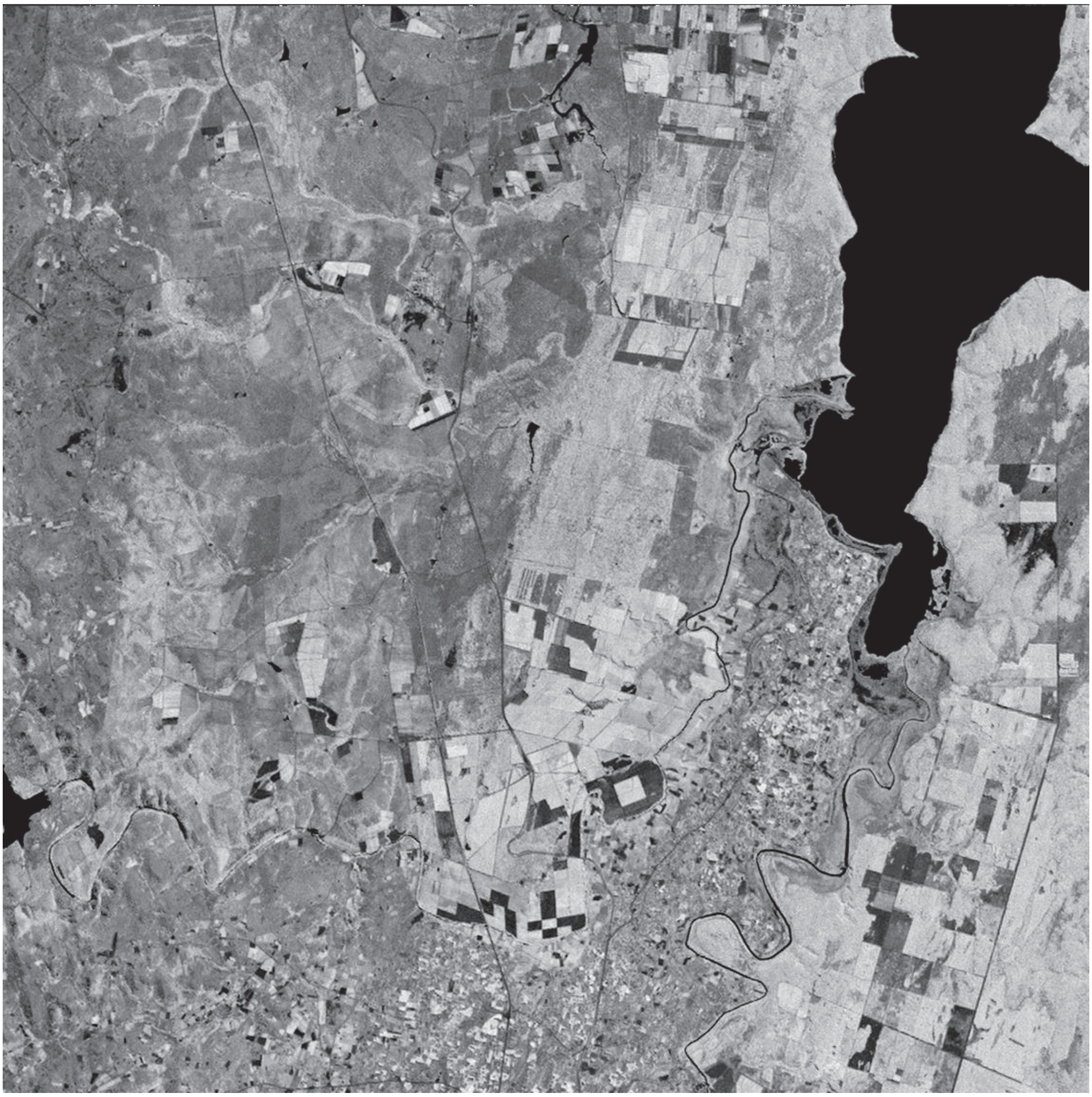

Figure 19. NDVI image of the LANDSAT data of the Bushlands district.

Table 16 shows that the LAI estimates based on destructive sampling and LiCor-2000 measurements show a high degree of correlation. However, the four vegetation indices show a disappointingly poor correlation to both ground-based LAI estimates, with the best shown by the NDVI index and the destructive harvesting LAI estimate. We conclude from these results that the use of LAI estimates based on the NDVI will be of limited value in initialising and verifying LAI in forestry compartments, given the sensitivity of both growth and transpiration to this canopy attribute. The close correlation between LAI estimates based on canopy analyser measurements and destructive sampling of trees suggests that ground-based measurements with the canopy analyzer are currently the most reliable estimates of forest LAI. We therefore decided to run the 3-PG SPATIAL version of the model without any input of satellite data (see Figure 2).

6.2 Application of 3-PG SPATIAL to the Kwambonambi and Bushlands districts

Spatial simulations were performed for two areas depicted in Figures 20 and 21. These were based on long-term averages of the climatic inputs, and were therefore expected to define long-term trends in productivity. The spatial version of 3-PG (referred to hereafter as 3-PGs) was provided by Dr. Nicholas Coops (CSIRO, Australia). Two slightly different versions, both compiled in C++, are available for use in Windows and Unix environments, respectively. The Windows version of the model was used in this study. In both versions, 3-PGs can be run with or without remote sensing data. In light of the poor LAI-VI correlations described above, we ran 3-PGs without remote sensing data input.

3-PGs requires spatial coverages of available soil water capacity, soil fertility, maximum temperature, minimum temperature and rainfall. Development of these coverages is outlined in the following sections.

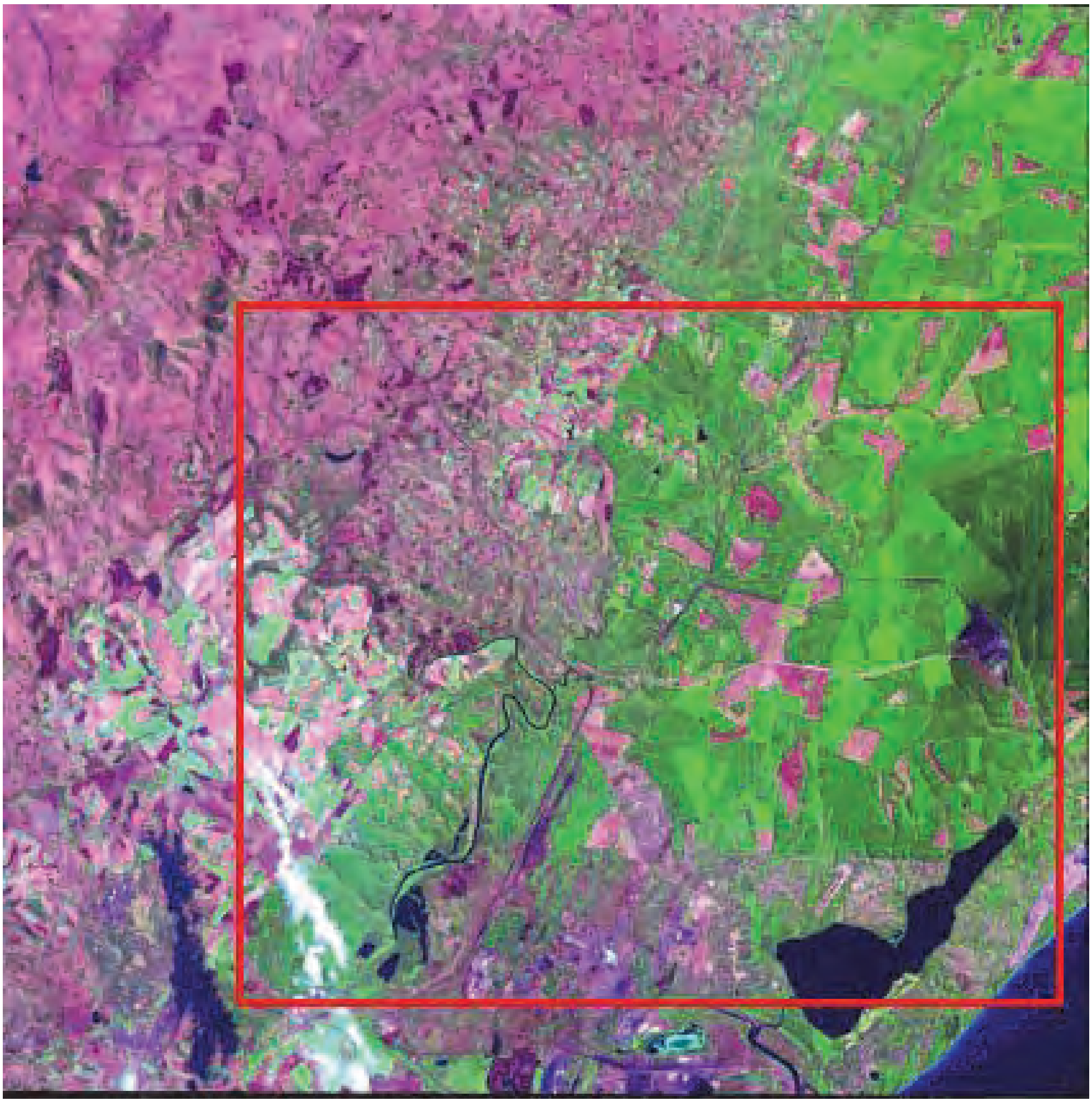

Figure 20. False-colour image of the Kwambonambi district, based on July 2000 LANDSAT data.

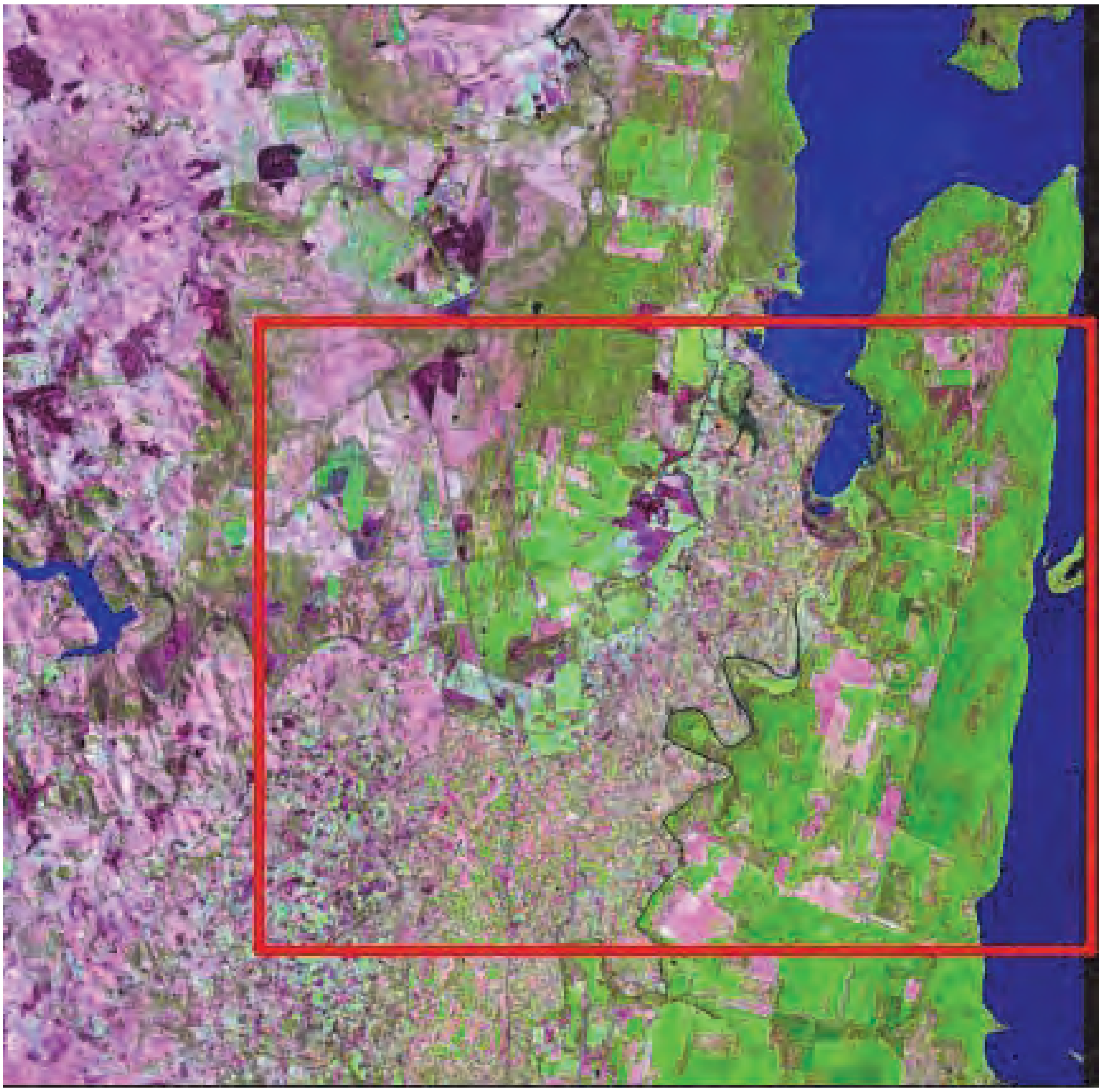

Figure 21. False-colour image of the Bushlands district, based on July 2000 LANDSAT data.

6.3 Available soil water capacity and soil fertility

An estimate of the maximum available soil water capacity is required for each soil type, but is widely acknowledged as being very difficult to estimate from standard soil descriptions (See Landsberg and Coops, 1999). We have based our estimations on soil depth, soil texture and the limited available information on tree water use. The spatial distribution of soil types was obtained from 1:250,000 soil maps, which were obtained from the Institute for Soil, Climate and Water (Agricultural Research Council, Pretoria). Figure 22 illustrates the data applicable to the Bushlands district. Information on soil texture and estimated available soil water for the various soil types in the study areas were obtained from Dr. Colin Smith (Institute for Commercial Forestry Research, Pietermaritzburg). The estimated maximum available soil water for the different soil groups is reflected in Table 18. Topographical and geological maps were used to assess the likely distribution of shallow ground water. Additional indications of groundwater availability at several of the study sites were described earlier, and used to delimit regions of freely available soil water.

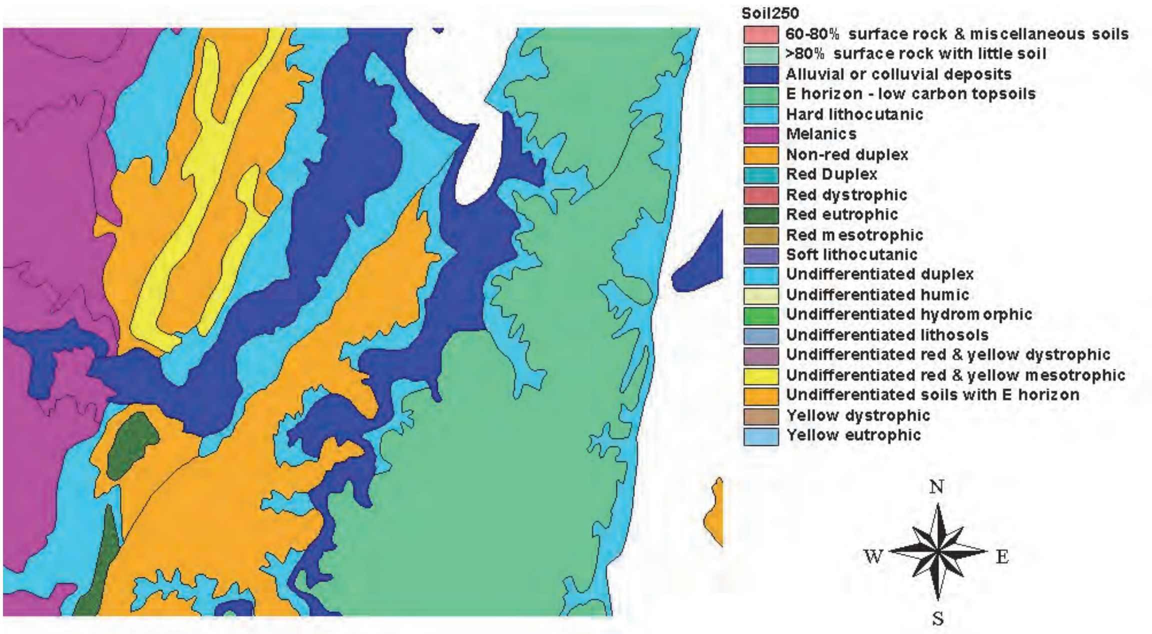

Figure 22. A map of soil categories applicable to the Bushlands area.

In earlier simulations with the point model, the SI obtained at each site was used as an index of soil fertility. This approach is supported by the high coefficient of determination that was found by Noble *et al*. (1991) when comparing SI to organic C for *Eucalyptus* stands in the Mtunzini area of Zululand. Organic C was also a very important variable for the prediction of *E. grandis* SI for the Mpumalanga area (Louw, 1997). We assumed that organic C content in Zululand coastal soils is the most useful predictor of soil fertility, and estimated it for each soil type on the basis of expert knowledge and information obtained from forestry companies.

Table 19: Estimated MAXASW and soil fertility index for the soils in the Bushlands and Kwambonambi districts.

Soil category	MAXASW (mm)	Soil Fertility index
Alluvial or Colluvial deposits	1500	0.95
E Horizon - low carbon top-soils	300	0.7
Soft lithocutanic	300	0.7
Red Duplex	300	0.85
Red dystrophic	300	0.9
Undifferentiated duplex	300	0.85
Undifferentiated Soils with an E horizon	150	0.2
Melanics	500	0.9

6.4 Maximum temperature, minimum temperature, rainfall and solar radiation

3-PGs requires monthly estimates of total rainfall, minimum and maximum temperature and total incoming solar radiation. Zululand is a frost-free area and no spatial coverage of frost incidence was required. For obtaining spatial coverages of climate information, a procedure similar to that of Coops *et al*. (1997) and Coops *et al*. (1998) was used. Mean monthly estimates of temperature and precipitation were obtained using the ANUSPLIN package (Hutchinson, 1999). We modelled the precipitation and temperature data for the whole of north-eastern KwaZulu-Natal, in order to keep edge-related errors associated with modelling of small areas to a minimum. The coverages required for the two areas of interest were then clipped from the larger modelled surface. Because the study area is flat and relatively small, it was assumed that the spatial variation in solar radiation would be relatively low. Thus, instead of using a spatial coverage, the monthly values from the climate stations, reported in Tables 3 and 4 were used as single value entries.

6.5 Results

3-PG was run to simulate final yields of stem and branch mass after a rotation period of eight years. The modelled spatial patterns of end-of-rotation Ws for both the Kwambonambi and Bushlands areas are shown in Figures 23 and 24, respectively. Yields are reasonably realistic when compared to final Ws measurements in the late-rotation stands (Table 6). There is a high degree of similarity between the simulated spatial pattern of rotation-end Ws (Figure 24) and the pattern of soil types in Figure 22, confirming that soil characteristics such as soil fertility index and ASW capacity are important determinants of forest yields in the Zululand region. The soils data used in these simulations are adequate for describing regional patterns of tree growth and yield, but need to be replaced with compartment-scale soils data in simulations of tree growth at the compartment scale.

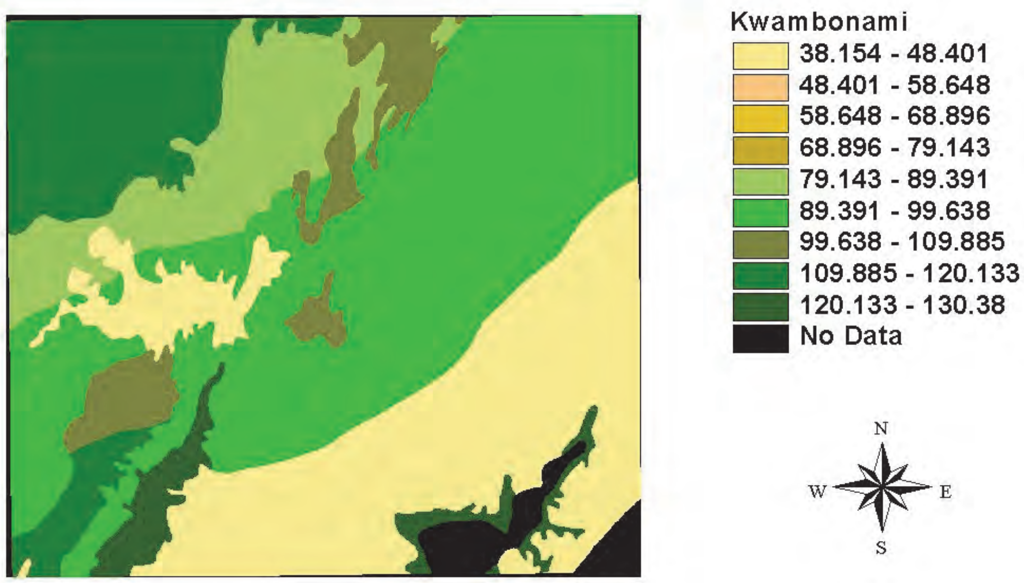

Figure 23. The pattern of final Ws (t ha^{-1}) simulated for the Kwambonambi district.

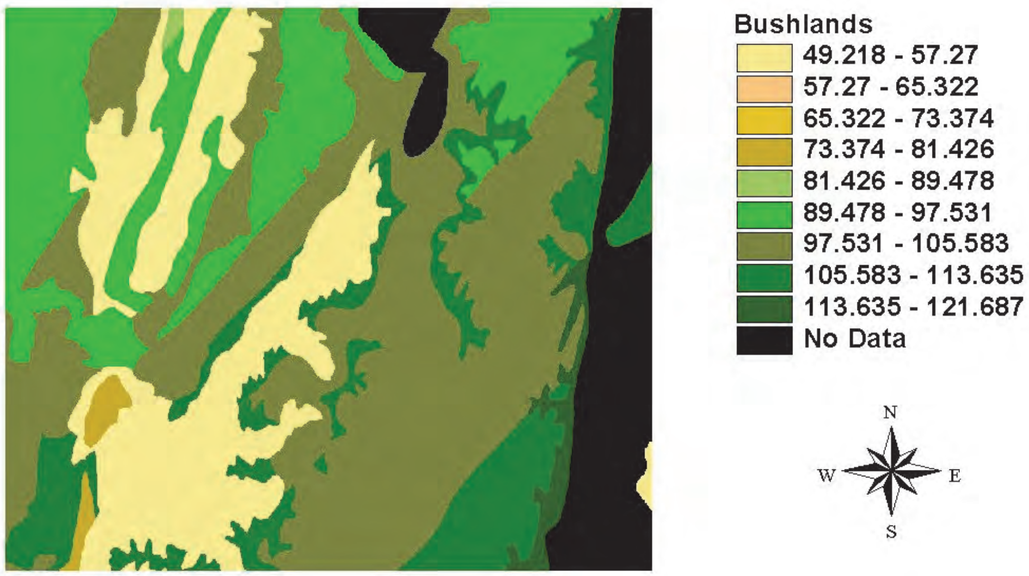

Figure 24. The pattern of final Ws (t ha^{-1}) simulated for the Bushlands district.

7. CONCLUSIONS AND RECOMMENDATIONS

The purpose of this project was to assess the practicality of linking a process-based model (3-PG) with remote-sensing data in a GIS environment to provide a practical means of predicting the growth and water use in heterogeneous compartments comprising forestry estates. The following main conclusions and recommendations arose from this project:

- A one-year field study of critical structural and physiological features of trees in 12 *Eucalyptus* stands representing a wide range of age and site quality was sufficient to produce a 3-PG parameterisation that yielded realistic and useful predictions of growth and water use. A practical procedure allowing further refinement of model parameters during real-time simulations of forest compartments is recommended and briefly described.

- This study has identified several areas in which the 3-PG model requires improvement.
    a. Soil water uptake during dry conditions. Sap flow data indicate that transpiration rates by trees during periods of low soil water content are higher than expected. This is believed to result from difficulty in adequately defining the rooting zone of the trees. While most roots are commonly restricted to a well-defined depth of soil, a feature of many *Eucalyptus* species is their ability to send relatively few sinker roots to very great depths in order to access further soil/subsoil water reserves (Knight, 1999). This supply is sufficient to prevent excessive water stress in the trees, which may lead to long-lasting physiological damage.
    b. Physiological changes brought about by continuous access to ground water. Exceptionally high growth and sap flow rates were recorded in a stand of trees known to have continuous access to a shallow water table. Such conditions are believed to be capable of altering some of the physiological characteristics of the trees (e.g. canopy conductance,

leaf dynamics, wood density) that are assumed in the model to be invariant for the species.

c. The need to quantify a soil fertility index. This remains a problem to all 3-PG modellers.
d. The need to estimate the maximum storage capacity for soil available water. The timing and intensity of water stress has a large effect on temporal patterns of growth and water use, and is very sensitive to the capacity of a soil to store soil water. Direct field measurement of this capacity is extremely difficult, and impractical in studies of large numbers of stands. Techniques to monitor xylem water potential of trees are becoming available, and offer a practical means of determining the onset of stress. This information is useful in gauging whether the assumed soil water storage capacity at a site is reasonably correct, too high or too low.
e. Detailed physiological studies on the major forest species are required to investigate such physiologically important features as carbon allocation patterns, canopy conductances, leaf dynamics and rooting patterns. Such “hard to measure” features are simulated on the basis of data obtained overseas for different species. Local data are required to improve the physiological foundation of 3-PG simulations in South Africa.

- The potential usefulness of remote-sensing data in spatial applications of 3-PG is unquestioned. However, a range of limitations (principally image resolution, cost and poor correlation to forest structural characteristics) prevents significant use of current satellite-derived data for operational use on forestry estates. Recent developments in hyperspectral remote sensing from aircraft appear to show better prospects for characterising forest stands and providing some of the spatial data required in forestry models (Coops, pers. comm.). LIDAR has also been shown to exhibit great potential in characterising forest plantations, especially structural attributes required for growth assessments. This is an active research field, and developments need to be monitored closely.

- Efforts should also be directed towards developing practical and low-cost ground-based methodologies for providing some of the critical physiological and structural inputs required by the model. Monitoring xylem water potential to detect water stress has already been mentioned. Such instruments as dendrometers and canopy analysers can provide valuable and low cost information on tree growth, standing biomass and leaf area index.

- There are insufficient sources of weather data in many forestry regions on which to base 3-PG simulations. Rainfall and ambient humidity data are particularly scarce, yet important inputs required by 3-PG. Automatic weather stations offer the best prospect for cost-effective, long-term collection of high quality weather data.

- This project represents an important step in the development and evaluation of process-based models for the South African forestry industry. It followed several earlier studies in South Africa that demonstrated the potential usefulness of 3-PG on a limited selection of *Eucalyptus* and pine stands. It is now to be followed by a three-year Innovation Fund project in which parameter values for all major forestry species will be developed for the entire national forestry estate, and where the eventual goal will be the development of model products suited for use by both small-scale growers and forestry companies. Experience gained in this project will significantly enhance the chance of success of the new project.

- There appear to be good prospects for spatial modelling of forest compartments in a GIS environment, based on field measurements of weather, site characteristics and forest attributes. Similar treatment of alternative land use crops could generate estimates of changes in ET brought about through afforestation, leading to estimates of streamflow reduction.

- There is no obvious reason why the 3-PG/remote sensing data/GIS approach to predicting growth and water use by forests cannot be broadened to include all land use options in a given catchment. A variety of crop-specific models are readily available, and GIS skills are becoming more available in many agricultural, forestry and hydrological organizations. A significant limitation remains in accessing cost-effective remote-sensing imagery, and also determining how it may best be analysed to provide the necessary spatial input into models.

This project was planned to make a significant contribution towards building research skills in a number of younger researchers. Mr Sibusiso Mthembu in particular was earmarked for intensive training in remote sensing and GIS modelling. This project contributed to the costs of his MSc degree in the Centre for Environment and Development, University of Natal, and he benefited considerably from interactions with Bekee Megown. With his departure, the main skills transfer effort was re-directed to Shayne Jacobs. Following a sudden loss of remote sensing skills in the CSIR, the project supported a one-week visit by Shayne to Pretoria in order to receive training within the CSIR remote-sensing group. The project also funded a one-week visit to the project team by Nicholas Coops from the CSIRO in Australia. Cindy Pretorius from the Pretoria remote-sensing group was invited to the Durban office during this visit, to gain experience from Dr Coops in using remote-sensing data for spatial application of 3-PG. This project supported her costs in this regard. David Drew, and two CSIR interns (Darren Naidoo and Frank Venter) gained valuable experience in various ecophysiological techniques during the course of this project. David Drew has drawn on this experience in planning his MSc degree in the University of Natal.

8. REFERENCES

ABER, J.D., BOLSTER, K.L., NEWMAN, S.D., Soulia, M. and MARTIN, M.E. 1995. Analysis of forest foliage II. Measurement of carbon fraction and nitrogen content by end-member analysis. Journal of Near Infrared Spectroscopy 2, 15-23.

ABER, J.D. and C.A. FEDERER. 1992. A generalized, lumped-parameter model of photosynthesis, evapotranspiration and net primary production in temperate and boreal forest ecosystems. Oecologia 92, 463-474.

ALMEIDA, A. 2000. *Eucalyptus* plantations in Brazil: Data from Aracruz Celulose S.A. and proposed analysis using 3-PG. In: 3-PG 2000: A workshop on the forest model 3-PG. New developments in calibration, performance, spatial inputs and practical applications. August 2000. K.J. Williams (ed). Forest Ecosystem Research and Assessment Technical Papers 00-18, 82-85.

BARET. F., and GUYOT, G. 1991. Potentials and limits of Vegetation Indices for LAI and APAR assessment. Remote Sensing of the Environment 35, 161-173.

BASTIAANSSEN, W.G.M., MOLDEN, D.J., THIRUVENGADACHARI, S., SMIT, A.A.M.F.R., MUTUWATTE, L., and JAYASINGHE, G. 1999. Remote sensing and hydrologic models for performance assessment in Sirsa irrigation circle, India. Research Report 27. International Water Management Institute. Colombo, Sri Lanka. 1-29.

BATTAGLIA, M., CHERRY, M.L., BEADLE, C.L., SANDS, P.J. and HINGSTON, A. 1998. Prediction of leaf area index in eucalypt plantations: effects of water stress and temperature. Tree Physiology 18, 521-528.

BIRKY, A.K. 2001. NDVI and a simple model of deciduous forest seasonal dynamics. Ecological Modelling 143: 43-58.

BREDENKAMP, B.V. 2000. Volume and mass of logs and standing trees. South African Forestry Handbook, Owen DL (ed.), Southern African Institute of Forestry, Pretoria, pp 170.

CAHALAN, R.F., OREOPOULOS, L., WEN, G., MARSHAK, A., TSAY, S.-C. and DEFELICE, T. 2001. Cloud characterization and clear-sky correction from LANDSAT-7. Remote Sensing of Environment 78, 83– 98.

CARLSON, T.N. and RIPLEY, D.A. 1997. On the relation between NDVI, fractional vegetation cover, and leaf area index. Remote Sensing of the Environment 62, 241-252.

CECCATO, P., FLASSE, S., TARANTOLA, S., JACQUEMOUD, S. and GREGOIRE J.-M. 2001. Detecting vegetation leaf water content using reflectance in the optical domain. Remote Sensing of Environment 77, 22-33.

CHAVEZ, P.S. 1988. An improved dark-object subtraction technique for atmospheric scattering correction of multi-spectral data. Remote Sensing of the Environment 39, 1289-1294.

CLUTTER, J.L. and JONES, E.P. 1980. Prediction of growth after thinning in old-field slash pine plantations. US Department of Agriculture, Service Research Paper 217, p1-8.

COHEN, W.B. and SPIES, T.A. 1992. Estimating structural attributes of Douglas-fir/western hemlock forest stands from Landsat and SPOT imagery. Remote Sensing of the Environment 41, 1-17.

COOPS, N.C. 1999a. Improvement in predicting stand growth of *Pinus radiata* (D. Don) across landscapes using NOAA AVHRR and LANDSAT MSS imagery combined with a forest growth process model (3-PGs). Photogrammetric Engineering & Remote Sensing 65, 1149-1156.

COOPS, N.C. 1999b. Linking multi-resolution satellite-derived estimates of canopy photosynthetic capacity and meteorological data to assess forest productivity in a *Pinus radiata* (D. Don) stand. Photogrammetric Engineering and Remote Sensing 65, 1149-1156.

COOPS, N. and CATLING, P.C. 1997. Predicting the Complexity of Habitat in Forests From Airborne Videography for Wildlife Management, International Journal of Remote Sensing 18, 2677 – 2682.

COOPS, N.C. and WARING, R.H. 2001a. Assessing forest growth across Southwestern Oregon under a range of current and future global change scenarios using a process model, 3-PG. Global Change Biology 7*, 15-29.*

COOPS, N.C. and WARING, R.H. 2001b. The use of multi-scale remote sensing imagery to derive regional estimates of forest growth capacity using 3-PGs*.* Remote Sensing of Environment 75*, 324-334.*

COOPS, N.C. and WARING, R.H. 2001c. Estimating forest productivity in the eastern Siskiyou Mountains of southwestern Oregon using a satellite driven process model, 3-PGs. Canadian Journal of Forest Research 31, 143-154.

COOPS, N.C., AUSTIN, M.P. and RYAN, P.R. 1995. Global vegetation datasets utilizing remotely sensed data: Applications to eucalypt forests. Proceedings of IFA ’95. Ballarat, April 17-21.

COOPS, N.C., WARING, R.H. and LANDSBERG, J.J. 1998. Assessing forest productivity in Australia and New Zealand using a physiologically-based model driven with average monthly weather data and satellite-derived estimates of canopy photosynthetic capacity. Forest Ecology and Management 104, 113-127.

COOPS, N.C., WARING, R.H., BROWN, S. and RUNNING, S. 2001. Comparisons of predictions of net primary production and seasonal patterns in water use derived with two forest growth models in Southwestern Oregon. Ecological Modelling 142, 61 – 81.

DANSON, F,M., STEVEN, M.D., MALTHUS, T.J. and CLARK, J.A. 1992. High-spectral resolution data for determining leaf water content. Journal of Remote Sensing 13: 461-470.

DUNLAP, F. 1912. The specific heat of wood. USDA Forest Service Bulletin No. 110. 28pp.

DU PLESSIS, M. 1996. Tree volume and taper equation for *Eucalyptus grandis (Eucalyptus camuldulensis GXC*). Internal report. HL&H Mining Timber, Tree Improvement Centre, White River.

DYE, P.J. 1998. An improved general model of water use and canopy conductance of *Eucalyptus grandis* trees. CSIR Report, ENV-P-I 98116.

DYE, P.J. 2000. Water use efficiency in South African *Eucalyptus* plantations: a review. Southern African Forestry Journal 189, 17-26.

DYE, P.J. 2001. Modelling growth and water use in four *Pinus patula* stands with the 3-PG process-based model. Southern African Forestry Journal 191, 53-63.

DYE, P.J. and OLBRICH, B.W. 1992. Estimating transpiration from 6-year-old *Eucalyptus grandis* trees: development of a canopy conductance model and comparison with independent sap flux measurements. Plant, Cell and Environment, 16: 45-53.

DYE, P.J., POULTER, A.G., SOKO, S. and MAPHANGA, D. 1997a. The determination of the relationship between transpiration rate and declining available water for *Eucalyptus grandis*. Water Research Commission Report No. 441/1/97. 101 pp.

DYE, P.J., SOKO, S. and MAPHANGA, D. 1997b. Intra-annual variation in water use efficiency of three clones in kwaMbonambi, Zululand. CSIR Report ENV/P/C 97048.

DYE, P.J. and VERSFELD, D.B. 1991. Rainfall interception by *Eucalyptus grandis* canopies: a proposed modelling procedure for use in catchment water balance simulations. CSIR Report FOR-DEA 369.

EAMUS, D., O'GRADY, A.P. and HUTLEY, L. 2000. Dry season conditions determine wet season water use in the wet-dry tropical savannas of northern Australia. Tree Physiology 20, 1219 – 1226.

ECONOMICS ADVISORY COMMITTEE, 1991. An economic analysis of the S.A. forestry industry: 1990 to 1992. Unpublished report to the Forestry Council.

EVERITT, J. H., ESCOBAR, D. E., BLAZQUEZ, C. H., HUSSEY, M. R., and Nixon, P. R. 1986. Evaluation of mid-infrared (1.45 - 2.0 mm) with a black and white infrared video camera. Photogrammetric Engineering and Remote Sensing 52, 1655-60.

FASSNACHT, K.S., GOWER, S.T., MACKENZIE, M.D., NORDHEIM, E.V. and LILLESAND, T.M. 1997. Estimating the leaf area index of north central Wisconsin forests using the LANDSAT Thematic Mapper. Remote Sensing of the Environment 61, 229-245.

FIELD, C.B., and MOONEY, H.A. 1986. The photosynthesis-nitrogen relationship in wild plants. In On the economy of plant form and function (Ed.) T.J. Givinish, pp. 25-56, Cambridge University Press, Cambridge.

GOWARD, S.N., TUCKER, C.J., and DYE, D.G. 1985. North American vegetation patterns observed with the NOAA-7 advanced very high resolution radiometer. Vegetatio 64, 3–14.

GRANGER, R.J. 2000. Satellite-derived estimates of evapotranspiration in the Gediz basin. Journal of Hydrology 229, 70–76

GUSH, M.B. 1999. A verification of the 3-PG forest growth and water use model for *Eucalyptus grandis*. CSIR Report ENV-P-I 98216.

GUSH, M.B., SCOTT, D.F., JEWITT, G.P.W., SCHULZE, R.E., HALLOWES, L.A. and GORGENS, A.H.M. 2001. Estimation of streamflow reductions resulting from commercial afforestation in South Africa. Proceedings of the 10th South African National Hydrology Symposium. 26-28 September, 2001. Pietermaritzburg.

HERBERT, M.A. 1992. Nutrition of Eucalypts in South Africa. ICFR Bulletin Series 27/92, Pietermaritzburg, South Africa.

HUBER, B. and SCHMIDT, E. 1937. Eine kompensationsmethode zur thermoelektrischen messung langsamer saftstrome. Die Berliner Deutsche Botanische Geselschaft 55, 514-529.

HUETE, A.R., LIU, H.Q., BATCHILY, K. and VAN LEEUWEN, W. 1997. A comparison of vegetation indices over a global set of TM images for EOS-MODIS. Remote Sensing of the Environment 59, 440-451.

HUNSAKER, C.T., RICH, A.C. and FITES-KAUFMANN, J. 1998. Integrated strategy for measuring vegetation structure using remote sensing technologies, Chapter 7. Workshop proceedings and proposed action. South Lake Tahoe, California, June 1998.

HUTCHINSON, M.F. 1999 *ANUSPLIN product information* under “CRES commercial packages” online @ http://cres.anu.edu.au/software/anusplin

JACKSON, R.D. 1986. Remote sensing of biotic and abiotic plant stress. Annual Review of Phytopathology 24: 265-287.

JACOBS, M.R. 1955. Growth habits of the eucalypts. Commonwealth Government Printer, Canberra, Australia.

JEWITT, G.P.W. and SCHULZE, R.E. 1993. Verification of the ACRU model using a Decision Support System developed for forest hydrology applications. *Proceedings, 6th South African National Hydrological Symposium, University of Natal, Pietermaritzburg, Department of Agricultural Engineering*. 715-724.

KARNIELI, A., KAUFMAN, Y.-J., REMER, L. and WALD, A. 2001. AFRI - aerosol free vegetation index. Remote Sensing of Environment 77, 20-21.

KASSIER, H.W. and KOTZE, H. 2000. Growth modelling and yield tables. In: South African Forestry Handbook 2000, Vol. 1, 175-189. The Southern African Institute of Forestry. V & R Printers, Pretoria.

KATCH, C. and VOGT, H. 1999. Remote sensing from space – present and future applications in forestry, nature conservation and landscape management. South African Forestry Journal 185, 14-26.

KEENAN, R., HAFNER, S. and ROPPOLA, A. 2000. 3PG-SPATIAL local, regional and national studies. In: 3-PG 2000: A workshop on the forest model 3-PG. New developments in calibration, performance, spatial inputs and practical applications. August 2000. K.J. Williams (ed). Forest Ecosystem Research and Assessment Technical Papers 00-18, 70 - 81.

KELLIHER, F.M., LEUNING, R., RAUPACH, M.R. and SCHULZE, E.-D. 1995. Maximum conductances for evaporation from global vegetation types. Agricultural and Forest Meteorology, 73: 1-16.

KIMBER, P.C. 1974. The root system of Jarrah (*Eucalyptus marginata*). Research Paper No. 10, Forests Department of Western Australia, Perth, 5pp.

KITE, G. and DROOGERS, P. 2000. Comparing evapotranspiration estimates from satellites, hydrological models and field data. Journal of Hydrology 229, 3-1.

KNIGHT, J.H. 1999. Root distributions and water uptake patterns in Eucalypts and other species. In: The Ways Trees Use Water . J.J. Landsberg (Ed.). Water and Salinity Issues in Agroforestry No 5: RIRDC Publication No. 99/37, Australia.

KOKALI, R.F. and CLARK, R. N. 1999. Spectroscopic determination of leaf biochemistry using band-depth analysis of absorption features and stepwise linear regression. Remote Sensing of the Environment 67, 267-287.

KUMAR, M. and MONTEITH, J.L., 1982. Remote sensing of plant growth. In (Eds.) Smith, H., Plants and the Daylight Spectrum, Academic Press, London, pp. 133–144.

LANDSBERG, J.J. 1997. Calibration, performance and further development of the forest productivity model 3-PG. Unpublished report.

LANDSBERG, J.J. 2000. The soil fertility question. . In: 3-PG 2000: A workshop on the forest model 3-PG. New developments in calibration, performance, spatial inputs and practical applications. August 2000. K.J. Williams (ed). Forest Ecosystem Research and Assessment Technical Papers 00-18, 86-89.

LANDSBERG, J.J. and COOPS, N.C. 1999. Modelling forest productivity across large areas and for long periods. Natural Resource Modelling 12, 1-28.

LANDSBERG, J.J. and GOWER, S.T. 1997. *Applications of Physiological Ecology to Forest Management*. Academic Press, San Diego.

LANDSBERG, J.J. and WARING, R.H. 1997. A generalised model of forest productivity using simplified concepts of radiation-use efficiency, carbon balance and partitioning. Forest Ecology and Management 95, 209-228.

LEFSKY, M.A., COHEN, W.B. and SPIES, T.A. 2001. An evaluation of alternate remote sensing products for forest inventory, monitoring, and mapping of Douglas-fir forests in western Oregon. Canadian Journal Forestry Research 31, 78–87

LILLESAND, T.M. and KIEFER, R.W. 1994. Remote Sensing and Image Interpretation. John Wiley and Sons.

LIMBURGER, L., BEGGS, P.J. and JACOBSEN, C.R. 2000. Estimation of canopy-average surface-specific leaf area using LANDSAT TM data. Photogrammatic Engineering and Remote Sensing 66, 183-191.

LOUW, J. 1997. A site-growth study of *Eucalyptus grandi*s in the Mpumalanga Escarpment Area. Southern African Forestry Journal, No. 180: 1-14.

LUCAS, N.S., CURREN, P.J., PLUMMER, S.E. and DANSON, F.M. 2000. Estimating the stem carbon production of a coniferous forest using an ecosystem simulation model driven by the remotely sensed red edge. International Journal of Remote Sensing 21, 619-631.

MAJOR, D.J., BARET, F. and GUYOT, G. 1990. A ratio vegetation index adjusted for soil brightness. International Journal of Remote Sensing 11, 727-740.

MALAN, F.S., MALE, J.R. and VENTER, J.S.M. 1994. Relationships between the properties of eucalypt wood and some chemical, pulp and paper properties. Paper Southern Africa,

MALHERBE, H.L.W. 1968. Afforestation and Water Supplies in South Africa. Report of an Interdepartmental Committee, Department of Foerstry, Pretoria, South Africa.

MARSHALL, D.C. 1958. Measurement of sap flow in conifers by heat transport. Plant Physiology 33, 385-396.

MARTIN, M.E. and J.D. ABER. 1997. Estimation of forest canopy lignin and nitrogen concentration and ecosystem processes by high spectral resolution remote sensing. Ecological Applications 7, 431-443.

MARTIN, M.E., NEWMAN, S.D., ABER, J.D. and CONGALTON, R.G. 1998. Determining Forest Species Composition Using High Spectral Resolution Remote Sensing Data, Remote Sensing of the Environment 65, 249-254. 1998.

MATSON, P.A., JOHNSON, L.F., MILLER, J.R., BILLOW, C.R. and PU, R. 1994. Seasonal changes in canopy chemistry across the Oregon Transect: patterns and spectral measurement with remote sensing, Ecological Applications 4, 280-298.

MCVICAR, T.R. and JUPP, D.L.B. 2002. Using covariates to spatially interpolate moisture availability in the Murray-Darling basin. A novel use of remotely sensed data. Remote Sensing of the Environment 79, 199-212.

MORAN, M.S., CLARKE T.R., INOUE Y. and VIDAL, A. 1994. Estimating crop water deficits using the relation between surface-air temperature and spectral vegetation index. Remote Sensing of the Environment 49: 246-263.

MORRIS, J. 2000. Further development of the 3-PG forest growth model and application to young eucalypt plantations in Victoria. In: 3-PG 2000: A workshop on the forest model 3-PG. New developments in calibration, performance, spatial inputs and practical applications. August 2000. K.J. Williams (ed). Forest Ecosystem Research and Assessment Technical Papers 00-18, 138-154.

MTHEMBU, S.L. 2001. Estimating leaf area index (LAI) of gum tree (Eucalyptus grandis X camaldulensis) using remote sensing imagery and LiCor-2000. Dissertation submitted in partial fulfilment of a Master degree in Environment and Development, Centre for Environment and Development, University of Natal, Pietermaritzburg.

NÄNNI, U.W. 1970. Trees, water and perspective. South African Forestry Journal 75, 9-17.

NEMANI, R.L., PIERCE, J., RUNNING. S., and BAND, L. 1993. Forest ecosystem processes at the watershed scale: sensitivity to remotely-sensed leaf area index estimates. International Journal of Remote Sensing 14(13), 2519-2534.

NOBLE, A.D., DONKIN, M.J. and SMITH, C.W. 1991. The importance of soil properties as indicators of site quality for *Eucalyptus grandis* on the Zululand coastal plain. IUFRO, Symposium on Intensive Forestry: The role of Eucalypts. 2-6 September 1991. Proceedings, Volume I, 433-443.

OLBRICH, B.W. 1991. Verification of the heat pulse velocity technique for estimating sap flow in *Eucalyptus grandis*. Canadian Journal of Forest Research 21, 836-841.

POSO, S., WANG, G. and TUOMINEN, S. 1999. Weighting alternative estimates when using multi-source auxiliary data for forest inventory. Silva Fennica 33, 41-50.

PUHR, C.B. and DONOGHUE, D. 2000. Remote sensing of upland conifer plantations using LANDSAT TM data: a case study from Galloway, south-west Scotland, International Journal of Remote Sensing 21, 633-646.

RICHARDSON, A.J. and WIEGAND, C.L. 1977. Distinguishing vegetation from soil background information. Photogramm. Eng. Remote Sensing, 43: 1541 – 1552.

ROWLINSON, L.C., SUMMERTON, M. and AHMED, F. 1999. Comparison of remote sensing data sources and techniques for identifying and classifying alien invasive vegetation in riparian zones. Water SA 25, 497-500.

RUNNING, S.W., PETERSEN, D.L., SPANNER, M.A. and TEUBER, K.B. 1986. Remote sensing of coniferous forest leaf area. Ecology 67, 273-276.

SALISBURY, F. B., and ROSS, C. W. 1985. Plant Physiology. Wadsworth. Publishers, California, USA, pp. 548

SANDS, P.J. 2000. 3-PGpjs – a user-friendly interface to 3-PG, the Landsberg and Waring model of forest productivity. Technical Report No. 29, CRC for Sustainable Production Forestry, Hobart, Australia.

SANDS, P.J. and LANDSBERG, J.J. 2001. Parameterisation of 3-PG for plantation grown *Eucalyptus globulus*. Forest Ecology and Management, in press.

SCHULZE, R.E. and GEORGE, W.J. 1987. A dynamic, process-based, user-orientated model of forest effects on water yield. Hydrological Processes 1, 293-307.

SCOTT, D.F., LE MAITRE, D.C. and FAIRBANKS, D.H.K. 1998. Forestry and streamflow reduction in South Africa: a reference system for assessing extent and distribution. Water SA 24, 187-199.

SCOTT, D.F. and SMITH, R.E. 1997. Preliminary empirical models to predict reductions in total and low flows resulting from afforestation. Water SA , 23, 135-140.

SELLERS, P.J. 1985. Canopy reflectance, photosynthesis and transpiration. International Journal of Remote Sensing 68, 1335–1372.

SELLERS, P.J. 1987. Canopy reflectance, photosynthesis, and transpiration 2. The role of biophysics in the linearity of their interdependence. Remote Sensing of the Environment 21, 143–183.

SENAY, G.B. and ELLLIOT, R.L. 2000. Combining AVHRR-NDVI and landuse data to describe temporal and spatial dynamics of vegetation. Forest Ecology and Management 128, 83-91.

SHEPHERD, K.R. 1985. Carbon balance, carbon partitioning and yield of forest crops. In: Landsberg, J.J. and Parsons, W. (eds). Research for Forest Management. CSIRO, Melbourne. Pp 36-51.

SOARES, J.V. and ALMEIDA, A.C. 2001. Modeling the water balance and soil water fluxes in a fast growing *Eucalyptus* plantation in Brazil. Journal of Hydrology 253, 130-147.

SONG, C., WOODCOCK, C.E., SETO, K.C., LENNEY, M.P. and MACOMBER, S.A. 2001. Classification and Change Detection Using LANDSAT TM Data: When and How to Correct Atmospheric Effects? Remote Sensing of the Environment 75,230-244.

SPECHT, R.L. 1972. Water use by perennial evergreen plant communities in Australia and Papua New Guinea. Australian Journal of Botany 20, 273-299.

SPECHT, R.L. and SPECHT, A. 1989. Canopy structure in *Eucalyptus*-dominated communities in Australia along climatic gradients. Acta Oecologia, Oecologia Plantarum 10, 191-213.

SWANSON, R.H. 1974. Velocity distribution patterns in ascending xylem sap during transpiration. In: Flow – its measurement and control in science and industry. Ed. R.B. Dowell. Instrument Society of America, Pittsburgh. Pp 1425-1430.

SWANSON, R.H. AND WHITFIELD, D.W.A. 1981. A numerical analysis of heat pulse velocity theory and practice. Journal of Experimental Botany 32, 221-239.

TEILLET, P.M., HORLER, D.N.H. and O'NEILL, N.T. 1997. Calibration, Validation, and Quality Assurance in Remote Sensing: A New Paradigm. Canadian Journal of Remote Sensing 23, 401-414.

THOMPSON, M.W. 1997. CSIR/ARC National Land Cover Database Project. CSIR Report ENV/P/C 97081, Pretoria, South Africa.

TICKLE, P., COOPS, N.C. and HAFNER, S. 2000. Assessing forest productivity across a native eucalypt forest using a process model, 3-PG SPATIAL. Forest Ecology and Management 152, 1-17.

TICKLE, P.K., COOPS, N.C., HAFNER, S.D., THE BAGO SCIENCE TEAM. 2001a. Assessing forest productivity at local scales across a native eucalypt forest using the spatial model, 3PG-SPATIAL. Forest Ecology and Management 152: 275-291.

TICKLE, P.K., COOPS, N.C., HAFNER, S.D. 2001b. Comparison of a forest process model (3-PG-SPATIAL) with growth and yield models to predict growth at Bago state forest, NSW. Australian Forestry 64(2), 111-222.

USTIN, S.L., ROBERTS, D.A., PINZON, D.A., JACQUEMOUD, S., GARDNER, M., SCHEER, G., CASTANEDA, C.M. and PALACIOS-ORUETA, A. 1998. Estimating canopy water content of chaparral shrubs using optical methods. Remote Sensing of the Environment 65: 280-291.

VAN DER ZEL, D.W. 1995. Accomplishments and dynamics of the South African Afforestation Permit System. South African Forestry Journal 172, 49-58.

VERSFELD, D.B. 1994. The forest industry and management for water conservation. Forestry Handbook. The South African Institute of Forestry. pp 657-674.

WARING, R.H. 2000. A process model analysis of environmental limitations on the growth of Sitka spruce plantations in Great Britain. Forestry 73, 65-79.

WARING, R.H., LANDSBERG, J.J. and WILLIAMS, M. 1998. Net primary production of forests: a constant fraction of gross primary production? Tree Physiology, 18: 129-134.

WHITE, J.D., COOPS, N.C. and SCOTT, N.A. 2000. Predicting broad-scale forest and scrub biomass for New Zealand: Investigating the application of a physiologically based model. Ecological Modelling 131, 175-190.

Appendix 1. Comments on choice of 3-PG parameter values (identified by number)

1 & 2. Foliage:stem partitioning ratio @ D = 2 and 20 cm (1; 0.15) No information is available for GXC clones, so default values applicable to *Eucalyptus globulus* were used in simulations.

3 & 4. Constant and power in the stem mass vs diameter relationship (0.112; 2.484). These were derived from the function fitted to actual data shown in Figure 8.

5 & 6. Maximum and minimum fraction of NPP allocated to roots (0.8; 0.20) We changed the minimum fraction from 0.25 to 0.20 as part of the strategy to force more allocation to above-ground parts.

7, 8 and 9. Minimum, optimum and maximum temperature for growth (5; 24; 36) These are based on estimates for *E. grandis* reported by Morris (2000).

10. Days production lost per frost day (1) This value has no influence on the simulations since no frost was experienced at any of the sites.

11. Maximum litterfall fraction per month (0.07) This value of 0.07 is much higher than the default value of 0.02, but is based on the field data depicted in Figures 15 and 16. Such a high litterfall rate may be a consequence of rapid height growth and a relatively low leaf area that are characteristic of the GXC clones.

12. Litterfall rate at T = 0 (0.001)

13 Age at which litterfall rate has median value (24). Both parameters 12 and 13 have little influence on the simulations, since most trees were aged three or more years.

14. Average monthly root turnover rate (0.15). This value has no influence on growth simulation, but merely serves to keep the root mass within realistic bounds.

15. Maximum canopy conductance. 0.02 m s^{-1} is the default value recommended for *Eucalyptus globulus*. Higher values of *Eucalyptus* canopy conductance have been reported (Morris, 2000; Dye, 1998), and a value of 0.03 was found to be necessary to ensure a realistic annual ET.

16. LAI for maximum canopy conductance (3.33). This default value is based on work reported by Kelliher *et al*. (1995).

17. Defines stomatal response to VPD (0.05). Similar in several species of tree, value based on a study of *Eucalyptus grandis* in Sabie, South Africa (Dye and Olbrich, 1992)

18 Canopy boundary layer conductance (0.2 m s^{-1}). The boundary layer conductance of well-ventilated forest stands is known to be considerably higher than canopy conductance, and so ET is relatively insensitive to this parameter value. The default value is accepted for this parameter.

19 & 20 Values of m and fNutr when FR = 0. These were set to 0.5 and 0.3 respectively, in the process of fitting 3-PG to the low growth increment sites.

21 & 22 Soil water modifier parameters (0.7, 9) These two parameters describe the availability of soil water to plant roots for four soil texture classes. The soils in this study were all assumed to be sands.

23 Max stem mass per tree @ 1000 trees/hectare (300). This parameter controls the onset of self-thinning in forest stands. Negligible self-thinning occurred in the stands in this study, because of relatively wide espacement and short rotation lengths. The default value of 300 ensured that no self thinning occurred during simulations.

24, 25 and 26 Age modifier parameters. These were set to their default values, which ensured that negligible physiological decline was simulated in these short-rotation stands.

27, 28 & 29 Specific leaf area. A mean SLA of 7.3 was recorded in the sample stands (Table 9). As there was no evidence of any link between tree age and SLA, we assumed that SLA remained constant over all stands.

30 Extinction coefficient for absorption of PAR by canopy (0.45). A default value of 0.5 is believed to apply to many different types of forests (Landsberg and Gower, 1997). Morris (2000) reported that a value of 0.45 fitted *Eucalyptus grandis* data at Shepparton in Australia, and this value has been used in this study.

31 Age at canopy cover. This parameter is not invoked during simulations as every stand was characterised by a closed canopy.

32 Proportion of intercepted rainfall evaporated from the canopy (0.04). The value used is based on experimental data from a South African *Eucalyptus* plantation (Dye and Versfeld, 1991).

33 Canopy quantum efficiency (0.07). Landsberg considers this parameter to vary from 0.4 to 0.7 for *Eucalyptus* stands: a default value of 0.055 is recommended for *E. globulus*. In a calibration study involving a wide range of research plot data in Western Australia and Tasmania, Landsberg (1997) commented that a value for this parameter of 0.07 was not unrealistic. We found that a value of 0.07 was necessary to ensure that 3-PG could generate enough stem and foliage to match observed growth increments.

34 Branch and bark fraction at age 0 (0.3). Based on data shown in Figure 10.

35 Branch and bark fraction for mature stands (0.1). Based on data shown in Figure 10.

36 Age at which BBF is intermediate (3.5) Based on data shown in Figure 10.

37 Ratio NPP/GPP (0.47). This value is believed to be relatively constant over a broad range of tree species (Waring *et al.*, 1998).

38 Wood basic density (0.5). This estimate of wood basic density is based on data reported by Malan *et al*. (1994).

Appendix 2. Availability of LANDSAT 5 and 7 imagery from United States Geological Survey and Satellite Applications Centre.

Availability of LANDSAT 5 and 7 imagery with a 5 or less cloudcover (USGS notation) from Satellite Applications Centre (SAC) and United States Geological Survey (USGS) archives for the period November 2000 to July 2001. The two areas of interest are on separate LANDSAT 7 images, with Bushlands on the edge of the Kwambonambi image. However, there is considerable overlap between the two images, which allows for easier access. The asterisk (*) refers to dates when the two areas of interest fall on the same image.

Satellite	Source	Date	Area Covered	Cloud Cover	Usability	Path	Row
LANDSAT 5	USGS	Not avaliable	-	-	-	-	-
LANDSAT 7	USGS	2000/11/12	Kwambo	1	Not Usable	167	80
	USGS	2000/12/14	Kwambo	2	Not Usable	167	80
	USGS	2000/12/30	Kwambo	5	Not Usable	167	80
	USGS	2001/02/16	Kwambo	1	?	167	80
	USGS	2001/03/20	Kwambo	0	Usable	167	80
	USGS	2001/05/07	Kwambo	0	Usable	167	80
	USGS	2000/11/12	Bushlands	2	Not Usable	167	79
	USGS	2000/12/14	Bushlands	4	Not Usable	167	79
	USGS	2000/12/30	Bushlands	3	Not Usable	167	79
	USGS	2001/02/16	Bushlands	5	Not Usable	167	79

Satellite	Source	Date	Area Covered	Cloud Cover	Usability	Path	Row
	USGS	2001/03/20	Bushlands	0	Usable	167	79
	USGS	2001/05/07	Bushlands	0	Usable	167	79
LANDSAT 7	SAC	Not available	-	-	-	-	-
LANDSAT 5	SAC	2000/12/06	Bushlands	5	Not Usable	167	79
	SAC	**2001/01/23***	**Bushlands**	**2**	**Usable**	**167**	**79**
	SAC	2001/02/08	Bushlands	3	Usable	167	79
	SAC	**2001/05/15**	**Bushlands**	**0**	**Usable**	**167**	**79**
	SAC	2001/06/16	Bushlands	0	Usable	167	79
	SAC	2000/12/06	Kwambo	4	Not Usable	167	80
	SAC	**2001/01/23***	**Kwambo**	**2**	**Usable**	**167**	**80**
	SAC	2001/02/08	Kwambo	9	Not Usable	167	80
	SAC	**2001/05/15**	**Kwambo**	**0**	**Usable**	**167**	**80**
	SAC	2001/06/16	Kwambo	0	Usable	167	80